Ammonia-oxidizing archaea and complete ammonia-oxidizing bacteria in a municipal wastewater treatment plant

by

Emilie Spasov

A thesis
presented to the University of Waterloo
in fulfillment of the
thesis requirement for the degree of
Master of Science
in
Biology

Waterloo, Ontario, Canada, 2018

Author's declaration

I hereby declare that I am the sole author of this thesis. This is a true copy of the thesis, including any required final revisions, as accepted by my examiners.
I understand that my thesis may be made electronically available to the public.

Statement of contributions

Chapter 2
Marco Quattrociocchi, from the Aucoin lab in the Faculty of Engineering, performed the described NMR analysis.

Chapter 3
Laura Sauder collected the 2010 RBC samples, and also assisted, along with Josh Neufeld, with collecting the 2016 samples.

Metagenomic sequencing was performed at The Centre for Applied Genomics, in Toronto.

Jackson Tsuji processed the metagenomic sequencing data through the described ATLAS pipeline for both the individual assemblies and co-assemblies. He also performed the dereplication of bins using dRep and read mapping to comammox bins.

Abstract

High levels of ammonia in aquatic environments can lead to eutrophication, oxygen depletion, and toxicity to aquatic animals. An important goal of municipal wastewater treatment plants (WWTPs) is to remove ammonia from human waste before the treated effluent is released into receiving waters. Nitrification, the oxidation of ammonia to nitrate via nitrite, is a process that removes ammonia, and it is mediated solely by microorganisms. Historically it was thought that the two enzymatic steps of nitrification were carried out by distinct groups of microorganisms. The first step, aerobic ammonia oxidation, was long-known to be carried out by ammonia-oxidizing bacteria (AOB), and more recently the ammonia-oxidizing archaea (AOA) were discovered as contributors to the same process. The second step, nitrite oxidation, is carried out by nitrite-oxidizing bacteria (NOB), which are phylogenetically distinct from the AOB. However, certain species of *Nitrospira* are now recognized as being capable of catalyzing both steps of nitrification in the process of complete ammonia oxidation (comammox).

Due to the importance of nitrifiers to the functionality of WWTPs, this research aimed to better understand microorganisms and processes associated with ammonia oxidation within the tertiary treatment system biofilm of a municipal WWTP. The Guelph WWTP has four trains of rotating biological contactors (RBCs) that are each composed of eight individual RBC stages. As water flows from RBC 1 to 8, the ammonia concentration decreases due to the activity of ammonia oxidizers. Because of relatively low ammonia concentrations entering the RBCs, compared to secondary treatment aeration basins, and their fixed-film design, these RBCs present a valuable opportunity to study novel nitrifiers, such as the AOA and comammox bacteria.

The group I.1b AOA representative *Candidatus* Nitrosocosmicus exaquare was previously enriched from the RBCs. Initial enrichment cultivation and genome analysis data indicated that ammonia oxidation by this archaeon was stimulated by the addition of organic carbon sources, such as pyruvate and succinate. For other AOA, pyruvate stimulation is likely a result of hydrogen peroxide detoxification, not mixotrophy. Conversely, *Ca.* N.

exaquare may already be capable of detoxifying hydrogen peroxide without pyruvate because it possesses a gene for catalase. Additionally, it possesses dicarboxylate transporters. This suggests that *Ca*. N. exaquare may be able to use pyruvate and succinate mixotrophically. To test this hypothesis, incubation experiments without organic carbon, and with organic carbon sources or catalase were established. Both succinate and pyruvate did not consistently or significantly stimulate ammonia oxidation over controls with repeated incubations. Catalase was also not stimulatory to nitrite production, indicating that *Ca.* N. exaquare does not require exogenous catalase, and the pyruvate may be used instead as a carbon source. Evidence for mixotrophy was inconclusive, and further work with a pure culture of *Ca.* N. exaquare, and experiments with labelled organic carbon, would help determine if this AOA species is capable of mixotrophy.

Due to their recent discovery, comammox bacteria had not previously been reported in the Guelph WWTP, and little is known about their abundances in WWTPs. Using a combination of metagenomics and quantitative PCR, the abundance and diversity of comammox bacteria in the RBCs were explored over two sampling years. Taxonomic profiling of all microorganisms revealed that *Nitrospira* spp. dominated the RBC microbial community. Functional profiling indicated that comammox-associated *Nitrospira* represented the most abundant group of ammonia-oxidizing microorganisms. The diversity of comammox bacteria was also high, with multiple populations present. A cluster of comammox *Nitrospira* was also phylogenetically distinct from cultivated comammox species and these taxa represent ideal targets for future cultivation efforts. Genetic evidence that RBC *Nitrospira* are capable of complete ammonia oxidation includes *Nitrospira* metagenome assembled genomes that contain genes for both ammonia oxidation (e.g. *amoA*) and nitrite oxidation (e.g. *nxrB*). The results indicate that comammox bacteria co-exist with AOA and AOB, as well as with strict nitrite-oxidizing *Nitrospira*. The ammonia oxidizers displayed distinct patterns in relative abundance. In 2010 samples, AOA-associated *amoA* and 16S rRNA genes were higher in abundance in RBC 8 than RBC 1, but the opposite pattern was observed for 2016 samples. The relative abundance of AOB *amoA* genes was lower for 2016 samples than 2010 samples, suggesting a change in the environmental

conditions of the RBCs. The relative abundance patterns of comammox *Nitrospira amoA* genes were consistent across the two years. This study indicated that the environmental factors that govern AOA, AOB, and comammox bacteria differ, suggesting that these groups occupy distinct niches within this wastewater biofilm environment.

This thesis research is an important step towards understanding the nitrifying microorganisms in the Guelph RBCs. Although *Ca.* N. exaquare possesses the ability to deal with hydrogen peroxide stress, this research did not conclusively address organic carbon stimulation and assimilation. This thesis work showed that comammox bacteria were the dominant ammonia oxidizers in the Guelph RBCs, and this is the first study showing that comammox bacteria can be the dominant nitrifiers in a WWTP. This research paves the way for future studies on the microbial ecology of nitrification in engineered and aquatic environments.

Acknowledgements

I would like to thank all those who supported me through this degree. Thank you to my supervisor Josh Neufeld for your support, enthusiasm, and guidance throughout my program, and for your unwavering determination to support my research with adequate funding and laboratory resources. Thank you to my committee members Barb Butler, Andrew Doxey, and Laura Hug for your insight and advice.

Thank you to my collaborators, without whom this work would not have been possible. A huge thank you to Laura Sauder for entrusting me with the AOA cultures and for troubleshooting advice. She set the stage for all the subsequent research in the Guelph RBCs and many of the protocols in this thesis are based on her work. Thanks also to Laura and Josh for assisting with RBC sample collection. Another huge thank you goes to Jackson Tsuji for assistance with the metagenomic sequencing data analysis, from performing preliminary hidden Markov model (HMM) analyses to the many attempts at running ATLAS, helping me run analyses, and for insightful conversations about the results. Thank you to Wayne Parker from the Faculty of Engineering for assisting with securing funds for sequencing, as well as providing an engineer's perspective on the WWTP. Thank you to Marc Aucoin in the Faculty of Engineering for facilitating NMR analysis, and to Marco Quattrociocchi for performing the NMR analyses. Also thank you to Daniel Richard and Andrew Doxey for assisting with analysis of an earlier RBC sample that first showed evidence for comammox bacteria. Thank you to Sergio Pereira from TCAG for the advice on sequencing options. Thanks also to the Guelph WWTP operators who helped with sampling and data requests.

A heartfelt thank you goes out to my labmates in the Neufeld lab for advice, helpful lab meeting feedback, and for all the laughs and wonderful artwork. Each of you has helped me in so many ways. I especially want to thank Katja Engel for the wonderful training and mentorship, and for troubleshooting assistance. Thank you also to Lee Bergstrand and again to Jackson for all the Bash and R help.

Thank you to the Canadian Society of Microbiologists for providing me with the opportunity to present my research and thank you to the Faculties of Science and Engineering

and the Natural Sciences and Engineering Council of Canada (NSERC) for funding this research.

Finally, I want to thank my family and friends for their ongoing support, especially my parents, sisters, and Ken for always being there. I could not have done this without you.

Table of Contents

List of Figures

List of Tables

List of Abbreviations

3HP/4HB	3-hydroxypropionate/4-hydroxybutyrate
AMO	Ammonia monooxygenase
AmoA	Ammonia monooxygenase subunit A protein
amoA	Ammonia monooxygenase gene subunit a
amoB	Ammonia monooxygenase gene subunit B
amoC	Ammonia monooxygenase gene subunit C
Anammox	Anaerobic ammonia oxidation
ANI	Average nucleotide identity
AOA	Ammonia-oxidizing archaea
AOB	Ammonia-oxidizing bacteria
AOP	Ammonia-oxidizing prokaryotes
ATU	Allylthiourea
CARD-FISH	Catalyzed reporter deposition fluorescence *in situ* hybridization
ccm	Cytochrome *c* biosynthesis gene
Comammox	Complete ammonia oxidation
cyc	Cytochrome c554 gene
cyn	Cyanate hydratase gene
ddhB	Dimethylsulfide dehydrogenase subunit beta gene
DNA-SIP	DNA stable isotope probing
dNTP	Deoxynucleotide triphosphate
DSS	4,4-dimethyl-4-silapentane-1-sulfonic acid
fdh	Formate dehydrogenase gene
GeneFISH	Gene fluorescence *in situ* hybridization
hao	Hydroxylamine oxidoreductase gene
HAO	Hydroxylamine oxidoreductase/hydroxylamine dehydrogenase
HMM	Hidden Markov model
HOPE	Hierarchical oligonucleotide primer extension

hyb, hyd	Group 3[Ni-Fe] sulfur-reducing hydrogenase gene
hyp	Hydrogenase accessory protein gene
K_m	Half saturation constant
MAG	Metagenome assembled genome
NADH	Nicotinamide adenine dinucleotide hydride
ND	Not detected
NE	Northeast
Ngm	*Nitrososphaera gargensis* media
NH_3	Ammonia
NH_3-N	Ammonia-nitrogen
NH_4^+	Ammonium
NH_4Cl	Ammonium chloride
NMR	Nuclear magnetic resonance
NO	Nitric oxide
NOB	Nitrite-oxidizing bacteria
NW	Northwest
nxr	Nitrite oxidoreductase gene
nxrA	Nitrite oxidoreductase subunit A gene
nxrB	Nitrite oxidoreductase subunit B gene
OPA	Orthophthaldialdehyde
ORF	Open reading frame
OTU	Operational taxonomic unit
PCR	Polymerase chain reaction
pmo	Particulate methane monooxygenase gene
PTIO	2-phenyl- 4,4,5,5-tetramethylimidazoline-1-oxyl 3-oxide
QC	Quality control
qPCR	Quantitative PCR
RBC	Rotating biological contactor
ROS	Reactive oxygen species

rpoB	RNA polymerase subunit beta gene
rRNA	Ribosomal RNA
rTCA	Reverse tricarboxylic acid cycle
SD	Standard deviation
SE	Southeast
SIP	Stable isotope probing
SW	Southwest
TC	Total community
TCA	Tricarboxylic acid
TCAG	The Centre for Applied Genomics
ure	Urease gene
WWTP	Wastewater treatment plant

"One sometimes finds what one is not looking for."

–Sir Alexander Fleming

Chapter 1: Introduction and literature review

1.1 Nitrifiers in wastewater treatment plants

1.1.1 Nitrification and nitrifiers

Nitrogen is a necessary nutrient for life, as it is needed for the synthesis of nucleic acids and proteins. Microorganisms are responsible for the conversion of dinitrogen into ammonia, which can be assimilated into biomass by plants and other microorganisms (Figure 1.1). Ammonia can be further oxidized to nitrite and nitrate by other microorganisms, and these compounds can also be assimilated by some organisms. These assimilatory forms of nitrogen are often growth-limiting nutrients, which means that the bacteria and archaea that reduce dinitrogen to ammonia (nitrogen fixers) and those that oxidize ammonia (nitrifiers) largely control the amount of assimilatory forms of nitrogen available to other organisms.

Nitrification is composed of two aerobic respiratory steps: ammonia oxidation and nitrite oxidation (Figure 1.1, step 2). For over 100 years, ammonia oxidation was thought to be performed only by chemolithoautotrophic bacteria (ammonia-oxidizing bacteria, AOB). These bacteria belong to the phylum *Proteobacteria*, with most species belonging to the class *Betaproteobacteria*, and others belonging to the class *Gammaproteobacteria* (Purkhold *et al.*, 2000). First predicted by marine metagenomics (Treusch *et al.*, 2005; Venter *et al.*, 2004), and demonstrated by a pure culture isolated from a marine aquarium (Könneke *et al.*, 2005), members of the *Thaumarchaeota* can also oxidize ammonia (ammonia-oxidizing archaea, AOA). Anaerobic ammonia oxidation (anammox) is carried out by several bacterial genera associated with the *Planctomycetes* (Strous *et al.*, 1999). The second step of nitrification, nitrite oxidation, is performed by distinct microorganisms, collectively known as nitrite-oxidizing bacteria (NOB). These are taxonomically very diverse, belonging to four different phyla (*Proteobacteria*, *Nitrospinae*, *Nitrospirae*, and *Chloroflexi*) (Daims *et al.*, 2016).

Although the two steps of aerobic nitrification, ammonia oxidation and nitrite oxidation, were historically thought be carried out by separate microorganisms, theoretical predictions indicated that these two steps should be carried out by individual microorganisms

capable of complete ammonia oxidation (comammox) (Costa *et al.*, 2006). Comammox bacteria were predicted to have high growth yields and low growth rates. In addition, they were predicted to be competitive nitrifiers in biofilm habitats where ammonia mass transfer is low. A decade after the prediction of comammox, bacteria of the genus *Nitrospira* that can carry out both ammonia and nitrite oxidation were reported by two research groups simultaneously. These cultures were isolated from the biofilm of a hot-water pipe from a deep exploration well (Daims *et al.*, 2015) and the trickling filter of an aquaculture system (van Kessel *et al.*, 2015).

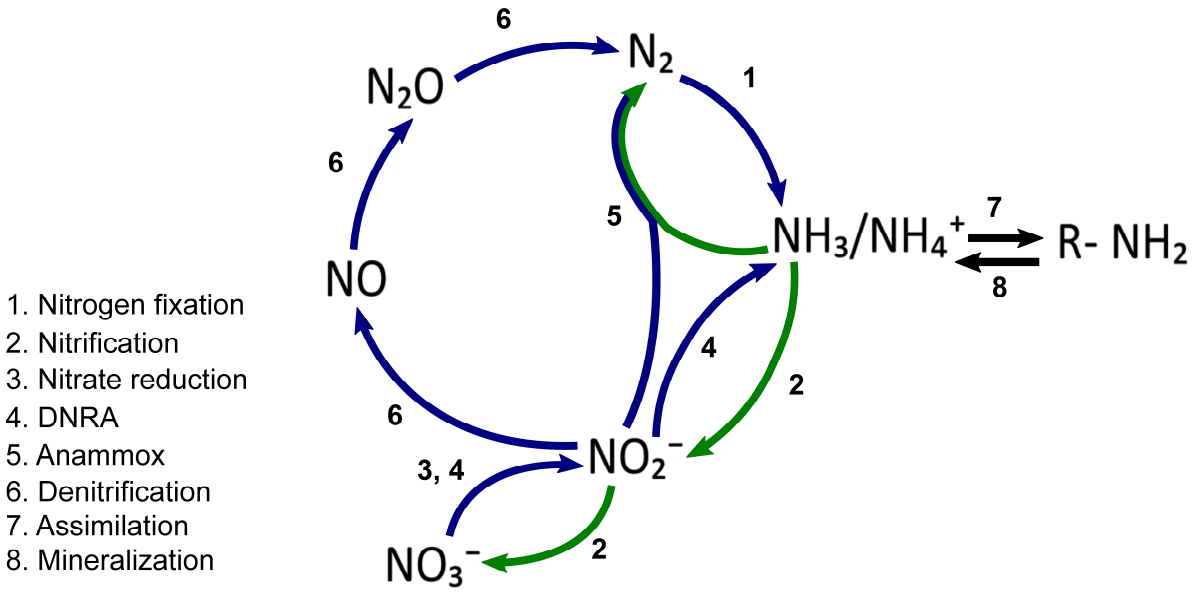

Figure 1.1 The nitrogen cycle, modified from Stein and Klotz (2016). Oxidation reactions are shown with green arrows, reduction reactions are shown with blue arrows, and neutral reactions are shown with black arrows. DNRA is dissimilatory nitrite reduction to ammonia, anammox is anaerobic ammonia oxidation. R-NH_2 indicates an organic nitrogen containing molecule. Ammonia oxidation is the first step of nitrification. Complete ammonia oxidation (comammox) involves both steps of nitrification.

Engineered systems such as wastewater treatment plants (WWTPs) are designed to promote nitrification, in order to reduce ammonia concentrations. Wastewater influent contains high levels of ammonia and must be treated before being released into waterways. High levels of ammonia in effluent can be toxic to fish and lead to eutrophication. Nitrite is also of concern if it leaks into receiving waters, as high levels can be toxic to fish (Lewis and Morris, 1986) and inhibit bacterial growth (Yarbrough *et al.*, 1980). Therefore, nitrification is an important process in wastewater treatment. The product of nitrification, nitrate, is another important cause of eutrophication, but in wastewater effluents it is preferential to ammonia because it is less toxic than ammonia and nitrite. Species of AOA, AOB, NOB, and more recently comammox bacteria, have been found in WWTPs, and their abundances and diversity have been the focus of studies on nitrifiers in WWTPs (e.g. Park *et al.*, 2006; Wells *et al.*, 2009; Daims *et al.*, 2001; Pjevac *et al.*, 2017). Compared to AOB, relatively few studies of AOA in WWTPs have been published, and fewer still have been published on comammox bacteria, given their more recent discovery. Therefore, the specific roles of these ammonia oxidizing groups in WWTPs remain uncertain.

1.1.2 Ammonia-oxidizing archaea

The AOA can be found in many diverse environments, including hot springs (Hatzenpichler *et al.*, 2008), soil (Tourna *et al.*, 2011), marine (Qin *et al.*, 2014), and freshwater environments (French *et al.*, 2012), in addition to WWTPs (Li *et al.*, 2016; Sauder *et al.*, 2017). The AOA can be classified into five main clusters, based on phylogeny of the *amoA* gene (ammonia monooxygenase) (Pester *et al.*, 2012). The main groups are Group I.1a, also called the "marine group", which includes such AOA as *Nitrosopumilus maritimus* (Könneke *et al.*, 2005) and *Nitrosoarchaeum limnia* (Blainey *et al.*, 2011), and Group I.1b, also called the "soil group", which includes such AOA as *Nitrososphaera viennensis* (Tourna *et al.*, 2011) and *Nitrososphaera gargensis* (Hatzenpichler *et al.*, 2008), among others. All cultivated AOA are thus far considered chemolithoautotrophs because they gain energy from ammonia oxidation and fix carbon dioxide (Walker *et al.*, 2010; Könneke *et al.*, 2014). They

use a modified 3-hydroxypropionate/4-hydroxybutyrate (3HP/4HB) pathway for carbon fixation, which is more efficient than the Calvin-Benson cycle used by the AOB (Könneke *et al.*, 2014).

Both AOA and AOB have genes for ammonia monooxygenase, but their mechanisms for ammonia oxidation differ. The exact pathway for ammonia oxidation in the AOA has not been fully identified. For AOB, ammonia is converted to hydroxylamine by the enzyme ammonia monooxygenase (AMO). The long held view was that subsequently, the enzyme hydroxylamine oxidoreductase (HAO, also known as hydroxylamine dehydrogenase) converts hydroxylamine to nitrite (Arp and Stein, 2003). However, a new model was recently proposed, due to the discovery that nitric oxide is the product of HAO, instead of nitrite (Caranto and Lancaster, 2017). Under this model there is a third enzyme that converts nitric oxide to nitrite, but this enzyme is yet to be properly identified. The AOA differ in this pathway because they do not have genes for HAO (Walker *et al.*, 2010). There are two proposed pathways for ammonia oxidation in AOA. One involves an as-yet-unidentified HAO containing copper, which converts hydroxylamine to nitrite. The other predicts nitroxyl, and not hydroxylamine, as being the product of AMO, followed by subsequent oxidation of nitroxyl to nitrite by a putative nitroxyl oxidoreductase (Stahl and de la Torre, 2012). The first proposed pathway is supported by the recent work of Kozlowski *et al.* (2016), who showed that nitric oxide (NO) is an important intermediate in AOA ammonia oxidation, and is proposed to facilitate oxidation of hydroxylamine to nitrite. This is also supported by the finding of the production of hydroxylamine as an intermediate of the ammonia oxidation process in AOA (Vajrala *et al.*, 2013). However, the required enzyme for this reaction has not been isolated, and therefore the exact ammonia oxidation pathway in AOA remains unknown. Even more recently another pathway for AOA ammonia oxidation has been proposed, which is similar to the pathway proposed by Caranto and Lancaster (2017) for AOB, though the enzymes required for the conversion of hydroxylamine to nitric oxide, and subsequent conversion to nitrite, are unknown (Lehtovirta-Morley, 2018).

Previously, the AOA were considered to have a much higher affinity for ammonia than AOB (Martens-Habbena *et al.*, 2009). The high affinity of AOA for ammonia confers an advantage to the AOA when ammonia levels are low. This could explain the dominance of AOA in low ammonia environments, such as oligotrophic waters (Martens-Habbena *et al.*, 2009). However, the reported affinities of AOA for ammonia vary depending on species, with K_m NH_3 values from around 3 nM for *Nitrosopumilus maritimus* (Martens-Habbena *et al.*, 2009) to 4.4 µM for *Candidatus* Nitrosotenuis uzonensis (Kits *et al.*, 2017). In comparison, the reported K_m NH_3 values for AOB range from 6 to 11 µM (Lehtovirta-Morley, 2018; Kits *et al.*, 2017; Prosser and Nicol, 2012). However, reported K_m values (0.3 to 4.0 µM NH_3) for oligotrophic AOB are in the same range as those of some AOA, complicating this view of niche partitioning based on ammonia affinity (Kits *et al.*, 2017).

All aerobic ammonia-oxidizing microorganisms possess ammonia monooxygenase genes (i.e., *amoC*, *amoA*, *amoB*), which together encode the AMO enzyme. Portions of the *amoA* and 16S rRNA genes are commonly targeted by PCR to screen for ammonia oxidizers. The AMO enzyme is responsible for the first step in the oxidation of ammonia, but, just as the overall pathways for ammonia oxidation differ in AOA and AOB, the AMO enzymes differ. In fact, the *amo* genes in all autotrophic ammonia oxidizers are phylogenetically distinct (Daims *et al.*, 2015). Primer sets for bacterial *amoA* do not bind to archaeal *amoA*, which helps explain why the AOA were only discovered a little over a decade ago (Könneke *et al.*, 2005).

1.1.3 Ammonia-oxidizing archaea in wastewater treatment plants

The AOA in WWTPs were first detected via PCR in a survey of municipal WWTPs (Park *et al.*, 2006). Most of these AOA belonged to the *Thaumarchaeota* Group I.1b, and since then this group has been found in many WWTPs around the world (Zhang *et al.*, 2011; Gao *et al.*, 2013, 2014). Subsequent studies also reported AOA in WWTPs, but most found that AOB were numerically dominant over AOA in both municipal and industrial WWTPs (Gao *et al.*, 2013, 2014; Zhang *et al.*, 2011; Wang *et al.*, 2014). For example, a one-year

study of a municipal WWTP found that AOB were dominant over AOA, as detected by qPCR quantification of their *amoA* genes (Wells *et al.*, 2009). More recently, AOB have again been found to outnumber AOA in municipal WWTPs (Fan *et al.*, 2017), WWTP effluent (Huo *et al.*, 2017), a constructed wetland treating wastewater (Pelissari *et al.*, 2017), and nitrifying bioreactors (Gao *et al.*, 2016). In contrast, a few studies have found that AOA can be dominant over AOB (Limpiyakorn *et al.*, 2011; Ding *et al.*, 2015; Bai *et al.*, 2012; Sauder *et al.*, 2012, 2017), or at least at equal abundance (Sonthiphand and Limpiyakorn, 2011; Limpiyakorn *et al.*, 2011; Reddy *et al.*, 2014). The AOA tend to be numerically dominant over AOB in systems that have low ammonia levels, such as in tertiary wastewater treatment systems (Sauder *et al.*, 2012), or in municipal WWTPs that have lower influent levels of ammonia (Limpiyakorn *et al.*, 2011). Higher AOA numbers are proposed to be due to the high affinity of AOA for ammonia (Sonthiphand and Limpiyakorn, 2011). The AOA have also been suggested to be more numerically dominant in municipal WWTPs rather than industrial WWTPs due to their sensitivity to the higher levels of toxic compounds in the industrial WWTPs (Bai *et al.*, 2012).

Very little is known about the relative contributions of AOA to nitrification in WWTPs. A study by Mussmann *et al.* (2011) showed that AOA did not assimilate labelled bicarbonate, indicating they were not coupling ammonia oxidation to autotrophy. Therefore, it was not clear how much the AOA contributed to ammonia oxidation. Recently the activity of AOA from WWTPs has been reported by several research groups. Compounds that differentially inhibit AOA and AOB ammonia oxidation can be used to determine their contributions to ammonia oxidation. AOB ammonia-oxidizing activity can be inhibited by allylthiourea (ATU) (Martens-Habbena *et al.*, 2015; Shen *et al.*, 2013), while AOA activity can be inhibited by 2-phenyl- 4,4,5,5-tetramethylimidazoline-1-oxyl 3-oxide (PTIO) (Martens-Habbena *et al.*, 2015; Shen *et al.*, 2013). In two different fixed film wastewater treatment systems, a nitrifying trickling filter and a moving bed bioreactor, AOA *amoA* genes outnumbered AOB *amoA* genes. Ammonia oxidation was also reduced when either the inhibitors ATU or PTIO were used, indicating that both AOA and AOB contributed to

ammonia oxidation in these systems (Roy *et al.*, 2017). In biofilm samples from RBCs, a different type of fixed film system, inhibition of ammonia oxidation occurred upon incubation with PTIO, indicating that AOA contributed to ammonia oxidation. But experiments measuring incorporation of labelled bicarbonate indicated that these AOA do not fix inorganic carbon, as no cells were labelled, and so it is unclear whether these AOA assimilate a different carbon source, or use an alternative metabolism (Sauder *et al.*, 2017). The use of ATU and PTIO also revealed that both AOA and AOB contribute to ammonia oxidation in a lab scale nitrifying reactor in which AOA *amoA* genes outnumbered those of AOB (Srithep *et al.*, 2018). In that study, both the AOA and AOB incorporated labelled bicarbonate, indicating that they could both be coupling autotrophy with ammonia oxidation, though the authors note that cross-feeding could have occurred in this stable isotope probing (SIP) experiment. A SIP experiment on activated sludge from a full-scale WWTP also found that both AOA and AOB assimilate labelled inorganic carbon, though more AOB assimilated the labelled carbon than AOA, despite the fact that AOA slightly outnumbered AOB (Pan *et al.*, 2018). These experiments indicate that among different wastewater treatment environments, AOA can contribute to ammonia oxidation and are autotrophs, but more studies are needed to determine how much they contribute to this process and how consistently. Furthermore, comammox bacteria must also now be considered in these types of experiments, as they could be contributors to ammonia oxidation as well.

Two AOA enrichment cultures from WWTPs have been reported, but neither have been grown in pure culture. The first, *Candidatus* Nitrosotenuis cloacae, was enriched from activated sludge of a full-scale WWTP (Li *et al.*, 2016). It is adapted to low salinity and encodes genes for flagella. A representative of group I.1b, *Candidatus* Nitrosocosmicus exaquare, has been cultivated from the RBCs of a municipal WWTP (Sauder *et al.*, 2017). This AOA culture is stimulated by various organic carbon sources including dicarboxylic acids and encodes genes for dicarboxylate transporters, indicating that it has the potential for utilizing alternative carbon sources. Both cultures demonstrated active ammonia oxidation

and inorganic carbon assimilation, demonstrating that AOA from WWTPs are capable of autotrophic ammonia oxidation.

1.1.4 Ammonia-oxidizing archaea and organic carbon sources

Because AOA were initially considered to be autotrophic, it is expected that their growth would not be stimulated by organic carbon. However, several studies have shown that different AOA species are stimulated by various forms of organic carbon (Tourna *et al.*, 2011; Qin *et al.*, 2014), suggesting that AOA may in fact be mixotrophic. A study by Mussmann *et al.* (2011) showed that AOA did not incorporate labelled inorganic carbon, suggesting that some AOA might be capable of assimilating organic carbon. The closely related AOA strains studied by Lehtovirta-Morley *et al.* (2014) showed different growth stimulation and inhibition patterns in response to various organic carbon sources studied. Based on these studies, it is not clear whether AOA are strict chemolithoautotrophs or mixotrophs.

A recent study by Kim *et al.* (2016) showed that growth stimulation of AOA due to alpha-keto acids (such as pyruvate) was not due to mixotrophy, but rather detoxification of reactive oxygen species (ROS). Via a decarboxylation reaction, alpha-keto acids react non-enzymatically with hydrogen peroxide, converting it to water. Additions of both catalase and alpha-keto acids protected tested AOA from oxidative stress (Kim *et al.*, 2016). No hydrogen peroxide was detected when catalase or pyruvate was added, demonstrating that pyruvate acts as a ROS detoxification agent, and not as an organic carbon source for mixotrophy. Protection from ROS was further demonstrated in two other AOA strains by Qin *et al.* (2017).

1.1.5 Complete ammonia-oxidizing (comammox) bacteria

A decade after the prediction of comammox, bacteria of the genus *Nitrospira* that were capable of carrying out both the ammonia and nitrite oxidation steps of nitrification were reported by two research groups. An enrichment culture of *Candidatus* Nitrospira inopinata was obtained from the biofilm of a hot water pipe from a deep exploration well

(Daims *et al.*, 2015). To obtain this enrichment culture, a biofilm sample was incubated in mineral media containing ammonium, and a series of subcultivations over four years led to an enrichment coculture of *Nitrospira* and a betaproteobacterium. The enrichment culture of *Candidatus* Nitrospira nitrosa and *Candidatus* Nitrospira nitrificans was enriched from the trickling filter of an aquaculture system (van Kessel *et al.*, 2015). Biofilm from the filter was used to inoculate a bioreactor operating under hypoxic conditions, and the medium contained low concentrations of ammonia, nitrite, and nitrate. After 12 months, a coculture containing *Nitrospira* and anammox bacteria was obtained. Both the hot water pipe and the trickling filter provided a surface for attached growth, and were relatively oligotrophic, consistent with the predicted niche of comammox bacteria (Costa *et al.*, 2006). Since the initial discovery of these comammox bacterial species, *Ca.* N. inopinata has been isolated in pure culture, facilitating study of its growth kinetics (Kits *et al.*, 2017). Additionally, an enrichment culture from a lab scale biological nutrient removal reactor containing comammox strain UW-LDO-01 was classified as *Ca.* N. nitrosa (Camejo *et al.*, 2017). Before these discoveries, comammox *amoA* had been classified as the particulate methane monooxygenase (*pmo*) gene of *Crenothrix polyspora* (Daims *et al.*, 2015; van Kessel *et al.*, 2015). The bacterial *pmo* and *amo* genes are homologs (Holmes *et al.*, 1995), and so the stretches of sequence similarity between these two genes could explain why the comammox *amoA* gene was not previously properly classified.

Prior to the discovery of comammox bacteria, all *Nitrospira* species were considered nitrite oxidizers. The genus *Nitrospira* is quite diverse, consisting of at least six lineages (Lebedeva *et al.*, 2011; Daims *et al.*, 2001), as well as species not yet assigned to a lineage (Daims *et al.*, 2016). The comammox bacteria discovered so far belong to *Nitrospira* lineage II (Daims *et al.*, 2015; van Kessel *et al.*, 2015) (Figure 1.2), a widely spread lineage found in many diverse environments, such as marine, freshwater, soil, geothermal, and engineered environments (Daims *et al.*, 2001, 2016).

In addition to nitrite oxidoreductase (*nxr*), comammox bacterial genomes encode genes for ammonia oxidation, including *amo* and hydroxylamine oxidoreductase (*hao*). The

amo genes of comammox bacteria are phylogenetically distinct from those of AOA and AOB (van Kessel *et al.*, 2015; Daims *et al.*, 2015; Pinto *et al.*, 2015). Based on phylogenetic analysis of *amoA* genes affiliated with lineage II *Nitrospira*, Daims *et al.* (2015) identified two distinct clades of comammox bacteria: clades A and B. All existing cultivated species of comammox *Nitrospira* belong to clade A (Figure 1.3). Among all *Nitrospira*, only comammox bacteria encode genes for ammonia oxidation, and therefore identification of comammox bacteria can be established through phylogenetic analysis of the *amoA* gene (Palomo *et al.*, 2018; Pjevac *et al.*, 2017; Fowler *et al.*, 2018). However, within *Nitrospira* lineage II itself, the comammox bacteria do not form a monophyletic group. This is demonstrated by the phylogeny of *Nitrospira* according to 16S rRNA genes, concatenated ribosomal proteins, and *nxr* genes (Daims *et al.*, 2015; van Kessel *et al.*, 2015; Pinto *et al.*, 2015; Palomo *et al.*, 2018).

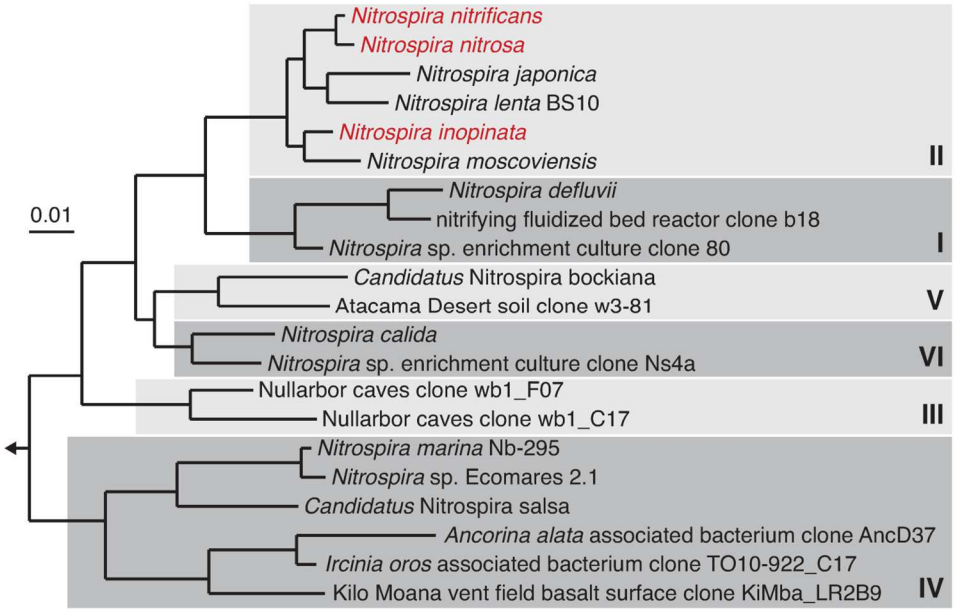

Figure 1.2 Phylogeny of *Nitrospira*, based on 16S rRNA genes (from Lawson and Lücker, 2018). Lineages of *Nitrospira* are shown with roman numerals. Comammox *Nitrospira* are shown in red.

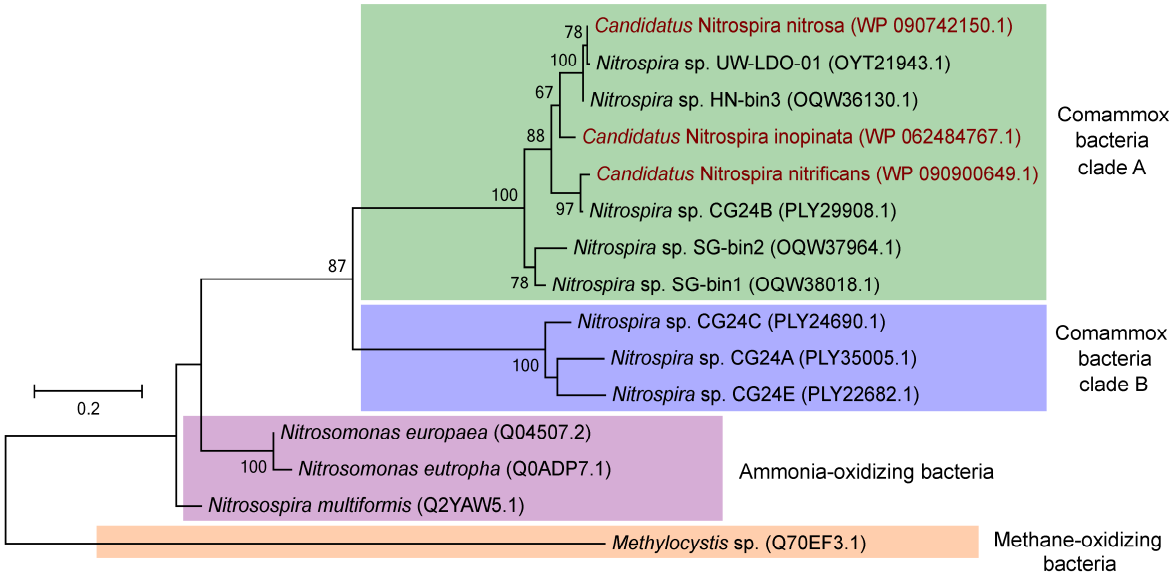

Figure 1.3 Phylogeny of comammox *Nitrospira* AmoA. Analysis of AmoA amino acid sequences was inferred using maximum likelihood analysis based on the Le Gascuel evolutionary model (Le and Gascuel, 2008). The model was chosen using the "Find Best Protein Model" tool in Mega7. Amino acid sequences were used to build an alignment using Muscle (Edgar, 2004). Comammox bacteria sequences selected are from metagenomic and cultivation studies. Cultivated species of comammox bacteria are shown in red. A *Methylocystis* sp. PmoA sequence was used as an outgroup. The tree is drawn to scale, with branch lengths measured in the number of substitutions per site. A total of 500 bootstrap replicates were used, and values over 60% are shown. Phylogenetic analysis was performed with MEGA7 (Kumar *et al.*, 2016).

Because the *amoA* genes of comammox bacteria are more closely related to those of betaproteobacterial AOB than AOA, and are restricted to only a subset of the *Nitrospira* genus, it appears the genetic capacity for ammonia oxidation was acquired horizontally by *Nitrospira* from one or more AOB donors (Daims *et al.*, 2015). Indeed, evidence for lateral gene transfer includes the presence of putative transposase genes just upstream of the

amoCAB genes of *Ca.* N. inopinata. Both clades of comammox bacteria share genomic features in the region containing the *amo* genes. This is exemplified by the presence of genes for cytochrome *c* biosynthesis (*ccm*) near the *amo* and *hao* genes in comammox bacteria. In AOB, these genes are not located near *amo* and *hao* (van Kessel *et al.*, 2015; Daims *et al.*, 2015; Palomo *et al.*, 2018). This suggests that both comammox clades have a common ancestry for ammonia oxidation (Palomo *et al.*, 2018).

A comparative genomic study of comammox *Nitrospira* and other related nitrifiers predicted that the ancestor of comammox bacteria acquired *amo* genes from a betaproteobacterium (Palomo *et al.*, 2018). The ancestor of *Ca.* N. inopinata did not have *amo* genes and a separate transfer event between an *amo*-containing *Nitrospira* and the ancestor of *Ca.* N. inopinata was predicted to have occurred after this initial transfer event. The two comammox clades diverged after the initial transfer event, likely because of niche adaptation. Evidence for this divergence is the faster evolution rate of comammox clade B ammonia-oxidizing proteins compared to clade A. The ancestor of comammox *Nitrospira* acquired *hao* genes from a betaproteobacterium as well. Following a loss of *hao* genes by some clade A members, another transfer of *hao* genes likely occurred from a comammox clade B member to these clade A members. The comammox bacteria do not form a monophyletic group within *Nitrospira*, possibly because some *Nitrospira* species, located between the comammox clades on a ribosomal protein phylogenetic tree, lost ammonia oxidation genes due to the selective advantage of an increased growth rate under certain environmental conditions (Palomo *et al.*, 2018). Bacteria capable of complete ammonia oxidation have a high growth yield and a low growth rate, which is beneficial in environments with low substrate concentrations, but not as competitive in environments with higher substrate concentrations (Costa *et al.*, 2006). Loss of ammonia oxidation genes would create a shorter metabolic pathway for nitrification (compared to complete ammonia oxidation) and would increase the growth rate of these bacteria, which could be preferable in some environments (Costa *et al.*, 2006).

Acquisition of ammonia oxidation genes means that comammox *Nitrospira* can oxidize ammonia, whereas other *Nitrospira* cannot. This process of complete ammonia oxidation yields more energy than either ammonia oxidation or nitrite oxidation do on their own (Daims *et al.*, 2015). All *Nitrospira* are considered chemolithoautotrophs (Daims *et al.*, 2015, 2016), and comammox *Nitrospira* require ammonia as an inorganic electron and energy source (Daims *et al.*, 2015; van Kessel *et al.*, 2015). Unlike the strict nitrite-oxidizing *Nitrospira*, comammox bacteria cannot grow solely on nitrite, due to the lack of genes encoding assimilatory nitrite reductase, as well as a lack of nitrite transporters (Palomo *et al.*, 2018; Daims *et al.*, 2015; van Kessel *et al.*, 2015). Carbon fixation in *Nitrospira*, as well as comammox *Nitrospira*, occurs via the reverse tricarboxylic acid (rTCA) cycle, suggesting a microaerophilic lifestyle (Daims *et al.*, 2015; Lücker *et al.*, 2010; Palomo *et al.*, 2016, 2018). As explained by Lücker *et al.* (2010), the rTCA cycle is usually found in anaerobic or microaerophilic organisms, due to the oxygen sensitivity of 2-oxoglutarate:ferredoxin oxidoreductase and pyruvate:ferredoxin oxidoreductase. Experimentally this microaerophilic lifestyle is supported by the enrichment of *Ca.* N. nitrosa and *Ca.* N. nitrificans under hypoxic conditions (van Kessel *et al.*, 2015).

Beyond the three species of comammox bacteria that have been cultivated, other comammox bacteria have been described using metagenomics. Shortly after the initial discovery of comammox bacteria, a metagenomic study revealed the presence of comammox bacteria in a drinking water treatment plant, an environment of relatively low ammonia (Pinto *et al.*, 2015). This metagenome assembled genome (MAG) contained genes for ammonia oxidation (*amo* and *hao*) and nitrite oxidation (*nxrA*), though it was missing *nxrB* genes. Highly complete comammox MAGs have also been recovered from soil (three MAGs; Orellana *et al.*, 2017), tap water filters (four MAGs; Wang *et al.*, 2017), rapid sand filters from drinking water treatment plants (four MAGs; Palomo *et al.*, 2018), a ground water well (two MAGs; Daims *et al.*, 2015), a membrane bioreactor of a WWTP (one MAG; Daims *et al.*, 2015), and a lab-scale sequencing batch reactor (one MAG; Camejo *et al.*, 2017). All of these MAGs were highly complete (>75%) with low contamination (<5%). Most of these

comammox bacteria were affiliated with comammox clade A, but three from the rapid sand filters and the two from the ground water well were affiliated with comammox clade B.

1.1.6 Ecology of comammox bacteria

Comammox bacteria can co-exist with nitrite-oxidizing *Nitrospira*, as well as other ammonia oxidizers. In addition, clade A and clade B comammox bacteria have been found in the same environmental samples, such as drinking water treatment plants and rice paddy soils (Pjevac *et al.*, 2017). Co-occurrence of both comammox clades indicates that the two clades have undergone niche specialization to help keep them competitive in their environments. The pure culture of *Ca.* N. inopinata has a high ammonia affinity (reported $K_{m(app)}$ of 49 to 83 nM NH_3), and high growth yield, especially compared to AOB, suggesting comammox bacteria live in oligotrophic environments (Kits *et al.*, 2017). Only the marine AOA *N. maritimus* has a higher reported ammonia affinity than *Ca.* N. inopinata (Kits *et al.*, 2017). Traditionally, AOA were thought to have a higher ammonia affinity than AOB, but now it is known that there is a gradient of ammonia affinities among ammonia oxidizers (Figure 1.4), with some AOA actually having a lower affinity (higher K_m) than some oligotrophic AOB (Hu and He, 2017; Kits *et al.*, 2017). Therefore, with only one pure culture of comammox bacteria with which to study ammonia affinity, it is premature to say that this characteristic of high ammonia affinity can be applied to all comammox species.

The detection of quorum sensing genes in several comammox species via genomic analyses suggests biofilm-associated growth (Kits *et al.*, 2017; Mellbye *et al.*, 2017), consistent with the fact that comammox bacteria are often detected in biofilm samples. These comammox bacteria could have alternative metabolisms for growth, besides using ammonia. The comammox enrichment culture studied by van Kessel *et al.* (2015) converted urea to ammonia, suggesting that comammox bacteria could use urea as a source of ammonia. Additionally, ureases and urea transporters have been found in comammox genomes (van Kessel *et al.*, 2015; Palomo *et al.*, 2016; Camejo *et al.*, 2017; Palomo *et al.*, 2018). The ability to use urea would offer comammox bacteria an advantage over other nitrifiers when

ammonia levels are low (Lawson and Lücker, 2018). Nitrite-oxidizing *Nitrospira* can use hydrogen as an energy source for growth (Koch *et al.*, 2014), but the hydrogenase genes that NOB possess are missing in comammox *Nitrospira* (Camejo *et al.*, 2017). Clade A comammox bacteria do possess a hydrogenase (Palomo *et al.*, 2018), which could allow them to oxidize hydrogen and reduce sulfur (Camejo *et al.*, 2017). Formate can also be used by NOB (Daims *et al.*, 2016), but it appears only clade B comammox bacteria possess a formate dehydrogenase gene (Camejo *et al.*, 2017; Palomo *et al.*, 2018). Comammox bacteria are currently considered to be strict autotrophs, but they possess genes for the degradation of various carbon sources, such as polyhydroxybutyrate (Palomo *et al.*, 2018). This suggests they could be mixotrophic, which has been demonstrated in nitrite-oxidizing *Nitrospira* as well (Daims *et al.*, 2001).

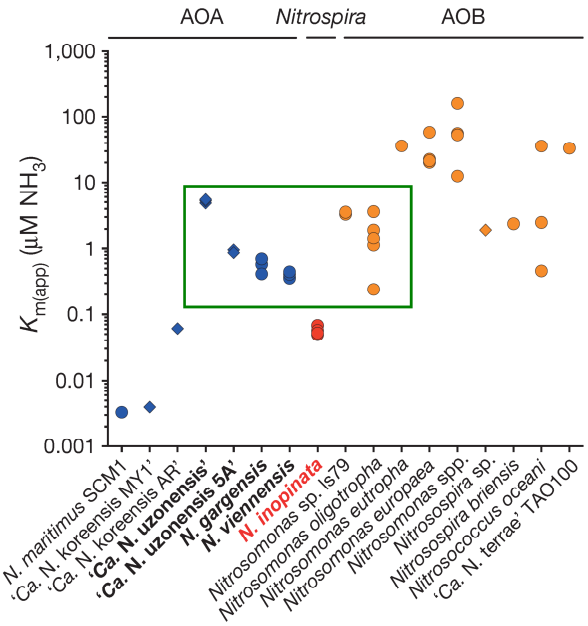

Figure 1.4 Ammonia affinities of AOA, *Nitrospira*, and AOB, adapted from Kits *et al.* (2017). The overlapping K_m values for AOA and AOB are indicated by the green rectangle. Values from enrichment cultures are shown with diamonds, and values from pure cultures are shown with circles.

1.1.7 Comammox bacteria in wastewater treatment plants

Less is known about distributions of comammox bacteria in WWTPs than of AOA. The predicted niche of low ammonia and surface attached growth for comammox bacteria (Costa *et al.*, 2006) is similar to that of AOA (Erguder *et al.*, 2009; Hatzenpichler, 2012; Sauder *et al.*, 2012; Stahl and de la Torre, 2012), and the ammonia affinity for one cultivated comammox bacterium, *Ca.* N. inopinata, is lower than all reported affinities of AOA, except *N. maritimus* (Kits *et al.*, 2017). This suggests that comammox bacteria could directly compete with AOA in lower ammonia environments, although the affinity of *Ca*. N. inopinata may not be representative of comammox bacteria from WWTPs.

Before comammox bacteria had been discovered, *Nitrospira* of lineages I and II were detected in several WWTPs (e.g. Daims *et al.*, 2001; Maixner *et al.*, 2006; Gruber-Dorninger *et al.*, 2015; Ushiki *et al.*, 2013; Fujitani *et al.*, 2014; Spieck *et al.*, 2006). Comammox bacteria were first discovered in WWTPs through screens of metagenomes in public databases (van Kessel *et al.*, 2015; Daims *et al.*, 2015), and multiple operational taxonomic units (OTUs) of clade A comammox bacteria were found in the same WWTP (Pjevac *et al.*, 2017). These clade A comammox bacteria were less abundant than AOB in the WWTP samples but may still have a relevant role in nitrification because 14 to 34% of all sequenced *amoA* genes were affiliated with comammox bacteria. In both activated sludge and the biofilm of another WWTP, *amoA* genes similar to those of *Ca.* N. inopinata were found at low relative abundance (Chao *et al.*, 2016). Another study also reported finding comammox bacteria in activated sludge, but the study was purely based on 16S rRNA gene phylogeny (Gonzalez-Martinez *et al.*, 2016). A one-year study of an activated sludge WWTP detected comammox *amoA* genes at lower abundances than those of AOB and AOA (Fan *et al.*, 2017). Comammox bacteria, along with AOB, were implicated as important nitrifiers in the aerobic granulation process of a sequencing batch reactor (Fan *et al.*, 2018). However, it is important to note that these latter two studies used quantitative PCR primers to specifically target *Ca*. N. inopinata *amoA*, and not all comammox-associated *amoA* genes, therefore these surveys may not have quantified all comammox bacteria in these systems. In addition to

WWTPs with activated sludge systems, comammox bacteria may play an important role in nitrification associated with the biofilm of a lab-scale trickling bioreactor (Scarascia *et al.*, 2017). The hierarchical oligonucleotide primer extension (HOPE) detection method used in this study targeted comammox *Nitrospira*, in addition to nitrite-oxidizing *Nitrospira*, thus it could not differentiate between the two groups.

Nitrospira were dominant nitrifiers in the microaerobic stage of a lab scale biological nutrient removal reactor (Camejo *et al.*, 2017). With few AOA or AOB present, most ammonia oxidation was likely due to the detected *Nitrospira*. The comammox bacteria enriched from this reactor were classified as *Ca*. N. nitrosa. Comammox bacteria have also been found ubiquitously in a study of full scale biological nutrient removal WWTPs (Annavajhala *et al.*, 2018), demonstrating that comammox bacteria could have a role in WWTPs, although further cultivation work must be done to determine how much they contribute to nitrification in these systems.

1.2 Research overview

Given the importance of ammonia oxidizers to wastewater treatment, it is important to understand the distributions and activity of these microorganisms. Wastewater treatment plants typically have high levels of ammonia in their influent waters, and this ammonia must be removed before the water is discharged into the environment. Some WWTPs, such as the Guelph WWTP, located in Guelph, Ontario, Canada, employ a tertiary treatment system in order to achieve high quality effluent that is low in ammonia. Water that enters the tertiary treatment system is lower in ammonia than the water entering the secondary treatment system aeration basin. Water from the secondary clarifiers is pooled and then split among the four trains of rotating biological contactors (RBCs). Each train consists of eight RBC stages. Each RBC has panels for biofilm growth connected to a rotating shaft, for a total surface area of 13 750 m^2 per RBC. The rotation results in the biofilm alternatively being exposed to water beneath the RBC and to air. The activity of nitrifiers present in the RBC biofilm results

in an ammonia gradient, in which ammonia concentrations are higher in RBC 1 and lowest in RBC 8 (Sauder *et al.*, 2012).

The AOA of the RBCs have been a previous research focus in this environment. An earlier study found that the abundances of AOA increase as ammonia concentrations decrease across the RBC flowpath, demonstrating a low ammonia niche for the AOA (Sauder *et al.*, 2012). The AOA community in the RBCs is composed of one species, *Ca.* N. exaquare, which has been cultivated in an enrichment culture (Sauder *et al.*, 2017). Pyruvate stimulates *Ca.* N. exaquare, as do additional organic carbon sources such as the dicarboxylic acids malate and succinate. The mechanism of stimulation is unknown. The genome of *Ca.* N. exaquare encodes for two dicarboxylate transporters, which have been found in additional AOA (Walker *et al.*, 2010; Sauder *et al.*, 2017). This suggests that *Ca.* N. exaquare could use the dicarboxylic acids as carbon sources. Genes for ROS detoxification, including superoxide dismutase, peroxidase, and catalase are also encoded in the *Ca.* N. exaquare genome. Peroxidase has not been found in other sequenced AOA (Sauder *et al.*, 2017). A full catalase gene has only been found in *Nitrososphaera evergladensis* (Zhalnina *et al.*, 2014) and *Nitrosocosmicus oleophilus* (Jung *et al.*, 2016), and a truncated catalase has been found in *Nitrososphaera gargensis* (Spang *et al.*, 2012). Other AOA species do not encode a gene for catalase. This suggests that *Ca.* N. exaquare may be able to manage ROS species directly, and that both pyruvate and dicarboxylic acids could be used as carbon sources. If this is the case, *Ca.* N. exaquare would be the only known example of a mixotrophic AOA. Further studies on the carbon metabolism of this AOA species would help elucidate its role in the RBCs and help determine the breadth of its metabolic capability, or an alternative metabolism.

The RBCs of the Guelph WWTP, with their low ammonia concentrations and surface for biofilm growth, present an ideal environment for comammox bacterial growth. To date, no studies have looked for comammox bacteria in tertiary wastewater treatment systems. This thesis aimed to study the ammonia oxidizing community of the RBCs, with a focus on the abundance and diversity of comammox bacteria. This was achieved using metagenomic

sequencing and quantitative PCR. Additionally, the enrichment culture of *Ca.* N. exaquare was further studied, to determine if this species could utilize specific carbon sources. Overall, this research focused on the microbial ecology of ammonia oxidation in the RBCs.

Chapter 2 Organic carbon utilization by an ammonia oxidizing archaeon

2.1 Introduction

Nitrification is the two-step process involving the oxidation of ammonia to nitrite, and then nitrate. The first step of this process, ammonia oxidation, is considered the rate limiting step. For over a century, ammonia-oxidizing bacteria (AOB) were considered solely responsible for aerobic ammonia oxidation. The discovery of archaea capable of this process (ammonia-oxidizing archaea, AOA) overturned this understanding (Könneke *et al.*, 2005) and, even more recently, bacteria capable of performing both steps of nitrification (complete ammonia oxidation, comammox) have been discovered (Daims *et al.*, 2015; van Kessel *et al.*, 2015). Even though all of these ammonia oxidizers are considered chemolithoautotrophs, using inorganic carbon as a carbon source, the growth of some AOB is stimulated by organic compounds, such as pyruvate, formate, and fructose (Clark and Schmidt, 1966; Krümmel and Harms, 1982; Hommes *et al.*, 2003). Several AOA have also been reported to be stimulated by organic carbon sources, as evidenced by increased growth rate and nitrite production (Tourna *et al.*, 2011; Qin *et al.*, 2014). Furthermore, another study found that AOA did not incorporate labelled inorganic carbon suggesting that AOA may be mixotrophic (Mussmann *et al.*, 2011). A recent study by Kim *et al.* (2016) showed that growth stimulation in AOA due to alpha-keto acids, such as pyruvate, is due to detoxification of reactive oxygen species (ROS), rather than mixotrophy. Via a decarboxylation reaction, alpha-keto acids react non-enzymatically with hydrogen peroxide, converting it to water. Additions of both catalase and alpha-keto acids protected tested AOA from oxidative stress (Kim *et al.*, 2016). No hydrogen peroxide was detected when catalase or pyruvate was added, demonstrating that pyruvate acts as a ROS detoxification agent, and not as an organic carbon source for mixotrophy. Although evidence for mixotrophic growth of AOB (Clark and Schmidt, 1966; Krümmel and Harms, 1982; Hommes *et al.*, 2003) and NOB (Bock *et al.*, 1990; Bock, 1976; Watson *et al.*, 1986) is relatively strong, no clear evidence exists for mixotrophic metabolism by AOA.

Nitrification is an important process in wastewater treatment to prevent high levels of ammonia in treated effluent, which cause toxicity to aquatic organisms and eutrophication. Despite the importance of ammonia oxidizers in wastewater treatment plants (WWTPs), only two species of AOA have been enriched from a WWTP (Sauder *et al.*, 2017; Li *et al.*, 2016). The archaeon *Candidatus* Nitrosocosmicus exaquare was enriched from the rotating biological contactors of the municipal WWTP in Guelph, Ontario. Like several other AOA, ammonia oxidation by *Ca.* N. exaquare is stimulated by organic carbon sources such as pyruvate and succinate (Sauder *et al.*, 2017). It is currently unknown whether ammonia oxidization stimulation by pyruvate is due to ROS detoxification, whether the heterotrophic bacteria growing in the enrichment culture use pyruvate to stimulate *Ca.* N. exaquare indirectly, or whether *Ca*. N. exaquare transports and assimilates pyruvate directly. Dicarboxylic acids do not provide ROS protection, and so stimulation via dicarboxylic acids (i.e. succinate) could be either indirect or direct. The genome of *Ca.* N. exaquare encodes for two dicarboxylate transporters, which have been found in additional AOA (Walker *et al.*, 2010; Sauder *et al.*, 2017), which would allow for *Ca*. N. exaquare to acquire tricarboxylic acid (TCA) cycle as well as 3-hydroxypropionate/ 4-hydroxybutyrate (3HP/4HB) intermediates directly from the environment. Succinate is a key precursor for biosynthesis of carbon compounds in other archaea that use the 3HP/4HB cycle (Estelmann *et al.*, 2011). Succinate could also enter the oxidative TCA cycle, which would offer the benefit of regenerating reducing power, in the form of NADH, as an alternative to reverse electron transport (Spang *et al.*, 2012; Walker *et al.*, 2010; Nunoura *et al.*, 2014). *Ca.* N. exaquare also encodes genes for ROS detoxification, including superoxide dismutase, peroxidase, and catalase. Peroxidase has not been found in other sequenced AOA (Sauder *et al.*, 2017). A full catalase gene has only been found in *Nitrososphaera evergladensis* (Zhalnina *et al.*, 2014) and *Nitrosocosmicus oleophilus* (Jung *et al.*, 2016), and a truncated catalase has been found in *Nitrososphaera gargensis* (Spang *et al.*, 2012). Other AOA species do not encode a gene for catalase. This suggests that *Ca.* N. exaquare may be able to manage ROS species directly, and that both pyruvate and dicarboxylic acids could be used as carbon sources. If this is the

case, *Ca.* N. exaquare and related I.1b *Thaumarchaeota* (Mussmann *et al.*, 2011) would be the only verified examples of mixotrophic or heterotrophic growth by AOA.

This study aimed to identify the relationship of *Ca.* N. exaquare to organic carbon to determine if this archaeon is capable of mixotrophic growth. To test this hypothesis, ammonia oxidation of *Ca.* N. exaquare without any organic carbon sources was compared to ammonia oxidation with pyruvate (alpha-keto acid), catalase, as well as succinate (dicarboxylic acid). Similar stimulation with exogenous catalase as with pyruvate would indicate that the supplied pyruvate is simply acting as a ROS scavenger and not as a carbon source. Because the genome of *Ca.* N. exaquare suggests that it can produce its own catalase and peroxidase, I predicted that exogenous catalase would not stimulate its activity, and that pyruvate would stimulate activity, which could indicate that *Ca.* N. exaquare is not stimulated via ROS scavenging but rather through mixotrophic use of pyruvate.

2.2 Methods

2.2.1 Ca. N. exaquare incubations

The enrichment culture of *Ca.* N. exaquare was grown in a minimal medium (*Nitrososphaera gargensis* medium, Ngm) (Sauder *et al.*, 2017) at 30°C in the dark and with no shaking. Actively growing cultures were centrifuged at 7000 x g for 15 minutes. Cells were washed three times with fresh medium, with repeated centrifugation steps between each wash, and then suspended in fresh medium. Subcultures (1%) were made in 100 mL Schott bottles in 50 mL of Ngm containing 0.5 mM ammonium chloride, and either with or without the addition of organic carbon or catalase (Table 2.1). Organic carbon sources used were sodium pyruvate (0.5 mM) and succinate (0.5 mM). Supplied catalase was either derived from *Aspergillus niger* (50 U/ml; C3515, Sigma-Aldrich, Oakville, ON, Canada) or bovine liver (10 U/ml; C1345, Sigma-Aldrich, Oakville, ON, Canada). The *A. niger* catalase was suspended in ammonium sulfate, and so bovine liver catalase was chosen for the second experiment to eliminate the excess ammonium added to culture upon catalase supplementation. Negative controls involved inactivation of catalase. The *A. niger* catalase

required a higher inactivation temperature than the bovine liver catalase. Inactivation was achieved by heating at 100°C for 3 hours (*A. niger* catalase) or by heating at 65°C for 40 minutes (bovine liver catalase) and the inactivated catalase was added to the cultures at the same volume as the active catalase. Experiments were performed using biological triplicates. At each sampling point, 1 mL of culture was removed and frozen at -20°C until analyzed.

Table 2.1 Treatment conditions for *Ca.* N. exaquare incubations. All additions were added to Ngm containing 0.5 mM ammonium chloride.

Experiment	Treatment	Additions to medium
1	Control	NA
	Catalase	50 U/ml *Aspergillus niger* catalase
	Pyruvate	0.5 mM sodium pyruvate
	Succinate	0.5 mM succinate
	Pyruvate & catalase	0.5 mM sodium pyruvate & 50 U/ml *Aspergillus niger* catalase
	Succinate & catalase	0.5 mM succinate & 50 U/ml *Aspergillus niger* catalase
	Inactivated catalase	50 U/ml heat inactivated *Aspergillus niger* catalase
2	Control	NA
	Catalase	10 U/ml bovine liver catalase
	Pyruvate	0.5 mM sodium pyruvate
	Succinate	0.5 mM succinate
	Inactivated catalase	10 U/ml heat inactivated bovine liver catalase

NA, nothing added

2.2.2 Water chemistry

Growth was monitored by measuring nitrite production according to a previously published protocol (Miranda *et al.*, 2001). Standards of sodium nitrite were prepared in two-fold dilution series, then 100 µl of diluted (1:10 in NH_4-free medium salts) sample or standard was added to clear flat-bottom 96-well plates. Subsequently, 100 µL of Greiss

reagent was added to each well. Plates were incubated for 10 minutes at room temperature and then absorbance values at 550 nm were read on a FilterMax F5 Multi-mode microplate reader (Molecular Devices, San Jose, CA, USA). Ammonium concentrations were measured colorimetrically using Nessler's reagent as described previously (Meseguer-Lloret *et al.*, 2002). Standards were prepared in two-fold dilution series, then 80 µl of sample (or 1:5 diluted sample if *Aspergillus niger* catalase was added) or standard was added to a clear flat-bottom 96 well plate. Then 80 µL of both sodium potassium tartrate (17.7 mM) and Nessler's reagent were added to the wells. Plates were incubated for up to 30 minutes at room temperature and then absorbance values at 450 nm were read on a FilterMax F5 Multi-mode microplate reader (Molecular Devices). All technical replicates were performed in duplicate. Concentrations were determined by comparison to a standard curve using SoftMax Pro 6.4 software (Molecular Devices).

2.2.3 Hydrogen peroxide measurement

Hydrogen peroxide was measured at the time of sampling using the Fluorometric Hydrogen Peroxide Assay kit (MAK165, Sigma-Aldrich, Oakville, ON, Canada) according to the manufacturer's instructions. All technical replicates were performed in duplicate in 96 well opaque flat-bottomed plates. Plates were incubated at room temperature for 20 minutes and then fluorescence at 535 nm excitation and 595 nm emission were read on a FilterMax F5 Multi-mode microplate reader (Molecular Devices, San Jose, CA, USA). Concentrations were determined by comparison to a standard curve using SoftMax Pro 6.4 software (Molecular Devices).

2.2.4 Testing of catalase and pyruvate hydrogen peroxide detoxification activity

Hydrogen peroxide (either 0.5 µM or 1 µM) was added to Ngm medium in 100 mL Schott bottles and hydrogen peroxide levels were measured (as described above) before scavengers (catalase and pyruvate) were added. Then 0.5 mM of sodium pyruvate or 10 U/mL of bovine liver catalase were added to the bottles. Hydrogen peroxide levels were measured directly after adding scavengers and after a 1 hour incubation at room temperature

in the dark. All treatments were done in duplicate, except control bottles which had hydrogen peroxide added, which were done without replication.

2.2.5 Catalase activity monitoring

Catalase activity (for the second experiment, with bovine liver catalase) was detected qualitatively by adding 50 µL of swirled enrichment culture or medium to 50 µL of 3% hydrogen peroxide on an empty Petri plate. Production of bubbles was viewed as a positive reaction for catalase activity.

2.2.6 Catalase testing of enrichment culture heterotrophs

The *Ca.* N. exaquare enrichment culture was diluted in medium salts, then spread plated on either nutrient agar or R2A agar and incubated for one week at 30°C in the dark. Unique isolated colonies were streaked onto fresh plates and incubated for four days at 30°C. Catalase activity of isolated colonies was tested by mixing a bit of colony with 3% hydrogen peroxide on a glass slide. Production of vigorous bubbles within 15 seconds was considered a positive result for catalase production.

2.2.7 Measurement of succinate and pyruvate

Succinate and pyruvate utilization (in the experiment with *A. niger* catalase) was monitored by measuring the amount of these compounds left in the culture supernatant by nuclear magnetic resonance (NMR). Culture aliquots from days 0, 4, 12, 28, and 32 were assayed. The pH of each aliquot was first adjusted to between 6 and 8, if applicable, by adding 200 mM phosphate buffered saline, then 70 µL of internal standard was added to 630 µL of aliquot. The internal standard was 5 mM DSS (4,4-dimethyl-4-silapentane-1-sulfonic acid) dissolved in 99.9% deuterium oxide, with 0.2% w/v sodium azide added to inhibit bacteria (Chenomx Inc., Edmonton, AB, Canada). Sample solutions were measured in 5 mm glass NMR tubes (NE-UL5-7, New Era Enterprises Inc., Vineland, NJ, USA) and scanned on a Bruker Avance 600 MHz spectrometer with triple resonance probe (TXI 600). The first increment of a 1D-NOESY pulse sequence with a 1 second pre-saturation pulse, 100

millisecond mixing time, and a 4 second acquisition was used for the scans. Spectra were analyzed using Chenomx NMR Suite 8.3 software (Chenomx Inc., Edmonton, AB, Canada). Baseline and phase corrections were first performed automatically by the software, then manually adjusted if necessary. All NMR readings were performed in the Department of Chemical Engineering at the University of Waterloo.

2.3 Results

2.3.1 Growth experiment with Aspergillus niger catalase

Nitrite production and ammonium depletion in control incubations was compared to treatments with organic carbon and/or catalase. For culture incubations in the presence of *Aspergillus niger* catalase, nitrite was detected in all incubation conditions by day 16 (Figure 2.1). By the end of the experiment (day 44) the control cultures (no added organic carbon or catalase) had almost reached stationary phase, because the nitrite produced was almost equal to the amount of ammonium put into the media. This corresponded to the measurement of ammonium left in the cultures (Figure 2.2). Conditions could be equally compared at day 32, which is the day that ammonium was depleted in the succinate treatments, due to the presence of excess ammonium in treatments containing catalase, but the experiment was continued until the control incubations depleted ammonium, in order to compare length of time to deplete ammonium across treatments. Succinate treatment stimulated *Ca.* N. exaquare ammonia oxidation, and furthermore, succinate was the most stimulatory organic carbon source added as evidenced by these cultures reaching stationary phase the fastest. Despite the apparent stimulation, nitrite detected at day 32 in the succinate treatments was not significantly different from the nitrite detected in the control incubations (t-test, p=0.11). Ammonium was used up over ten days earlier in the succinate treatment compared to the control. Pyruvate appeared to be stimulatory to the culture, though again nitrite detected was not significantly different to the control at day 32 (p=0.26). Incubations with pyruvate had used up all ammonia by day 40. Ammonium concentrations were higher in catalase-added incubations than those without (Figure 2.2) because the catalase stock was suspended in

ammonium sulfate. When catalase was added, additional ammonium (in the form of ammonium sulfate) was added and was oxidized to nitrite by *Ca.* N. exaquare. Ammonium concentrations in inactivated catalase treatments were lower than in active catalase treatments due to liquid loss during inactivation, and subsequent topping up with medium salts. Comparing at day 32, nitrite production with catalase as a supplement followed that of the control (Figure 2.1). In treatments with pyruvate, in addition to catalase, nitrite production was equivalent to cultures supplemented with pyruvate alone. Furthermore, when succinate was added, in addition to catalase, nitrite production was similar to succinate alone. These observations indicate that catalase did not stimulate ammonia oxidation. Whereas addition of catalase alone did not significantly stimulate *Ca.* N. exaquare by day 32, relative to the control (p=0.66), or even day 36, nitrite concentrations were significantly higher in the incubations with catalase by the end of the experiment (p=0.03) and increased more rapidly than the control. Compared to catalase alone, catalase incubations supplemented with either succinate or pyruvate provided additional stimulation. Incubations with both succinate and catalase oxidized ammonia more rapidly than cultures with only active catalase, and pyruvate plus catalase was the next most stimulatory treatment.

Although pyruvate and succinate were detected in the culture supernatant at day zero, the amount of pyruvate was less than the amount added to the culture (Table 2.2). There was a lag between inoculation and sampling for day zero, and because of this, the quick reduction in pyruvate concentration may have been due to the activity of heterotrophs in the enrichment culture, or due to pyruvate reacting with hydrogen peroxide in the culture, though hydrogen peroxide was not measured in this experiment. No pyruvate or succinate were detected by day four, or at any time point after that, indicating that these compounds were depleted rapidly within the first few hours or days of incubation.

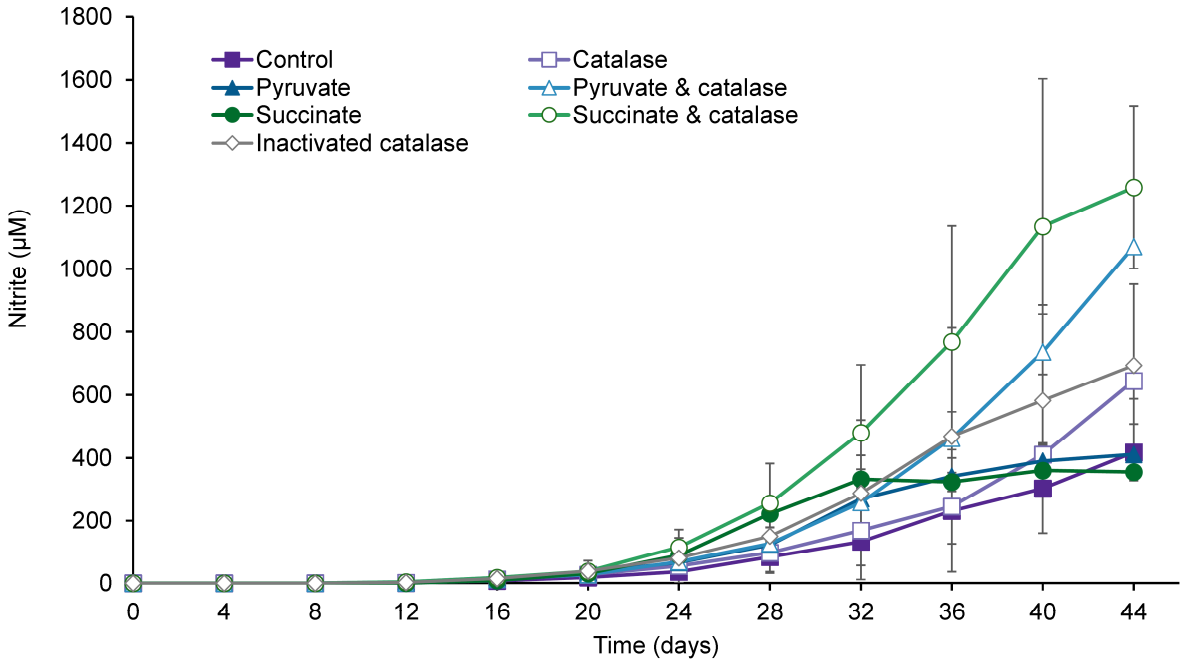

Figure 2.1 Nitrite production of *Ca.* N. exaquare enrichment culture supplemented with organic carbon and/or *A. niger* catalase. Cultures were grown in medium containing 0.5 mM of NH_4Cl at 30°C, and catalase supplementation resulted in additional ammonium added to the medium, due to ammonium sulfate suspension of catalase stock. Error bars represent standard deviation of biological triplicates.

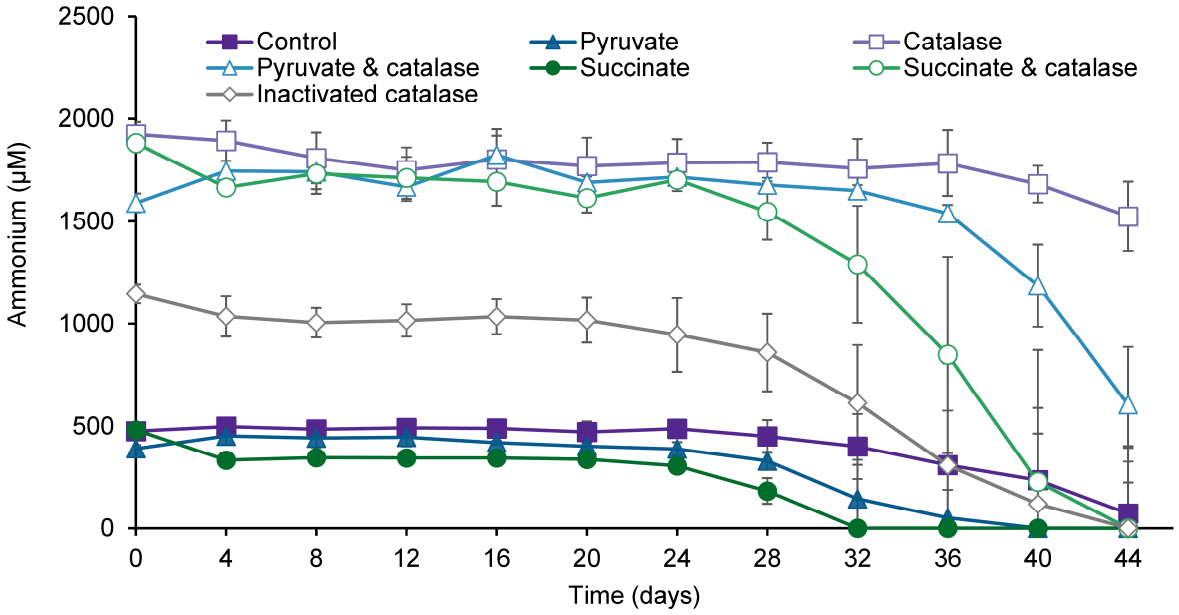

Figure 2.2 Ammonia oxidation of *Ca*. N. exaquare enrichment culture supplemented with organic carbon and/or *A. niger* catalase. Cultures were grown in medium containing 0.5 mM of NH_4Cl at 30°C, and catalase supplementation resulted in additional ammonium added to the medium, due to ammonium sulfate suspension of catalase stock. Error bars represent standard deviation of biological triplicates

Table 2.2 Measurement of pyruvate and succinate in *Ca.* N. exaquare enrichment cultures by NMR analysis.

Culture treatment	Expected day 0 concentration	Day 0	Day 4	Day 12	Day 28	Day 32
Pyruvate (mM)	0.50	0.03	ND	ND	ND	ND
Succinate (mM)	0.50	0.41	ND	ND	ND	ND

ND, not detected (detection limits were 0.02 mM (pyruvate) and 0.01 mM (succinate)

2.3.2 Growth experiments with bovine liver catalase

Nitrite production and ammonium depletion in control incubations was compared to treatments with organic carbon or catalase. The bovine liver catalase used did not introduce excess ammonium into the treatments, eliminating the confounding variable in the above experiment, therefore, only nitrite was measured as a proxy for growth (Figure 2.3), and ammonium concentrations were not measured during this experiment. There was a relatively long lag phase for all treatment incubations, with nitrite only detected in all incubations by day 24. Succinate addition provided some stimulation compared to the control, but this was not significant at day 32 (p=0.46) or day 36 (p=0.91). Nitrite production stopped in the succinate treatment by day 36, and nitrite production did not plateau until day 39 for the control culture. Pyruvate alone did not provide stimulation compared to the control (p=0.35 at day 36). Catalase decreased nitrite production. This was also true of the inactivated catalase treatment. The culture was still able to convert all ammonia to nitrite with the addition of catalase; however, this conversion in the presence of catalase took longer than without the catalase. At day 36, the nitrite detected in the catalase treatments was significantly different than the amount of nitrite detected in the control incubations (p<0.05).

Initial hydrogen peroxide concentrations in the cultures varied depending on treatment (Figure 2.4). The lowest levels of hydrogen peroxide at day zero were in the incubations that had catalase or pyruvate added, indicating hydrogen peroxide removal by these treatments. Overall hydrogen peroxide concentrations in the cultures were low throughout the experiment (i.e., less than 0.35 μM) and the concentrations in all cultures were below 0.2 μM by day eight. This indicated that the enrichment cultures themselves maintained low hydrogen peroxide concentrations, without any additional supplement required. From day eight onwards, hydrogen peroxide concentrations did not vary between treatments, with the exception of the pyruvate treatment.

Catalase activity spot tests revealed that there was very weak activity by days 12 and 16, and no catalase activity was detected by day 24. In the medium control containing

catalase, the catalase was still active on day 32, which was the last day catalase activity was tested. This suggests that the enrichment culture itself leads to the inactivation of catalase.

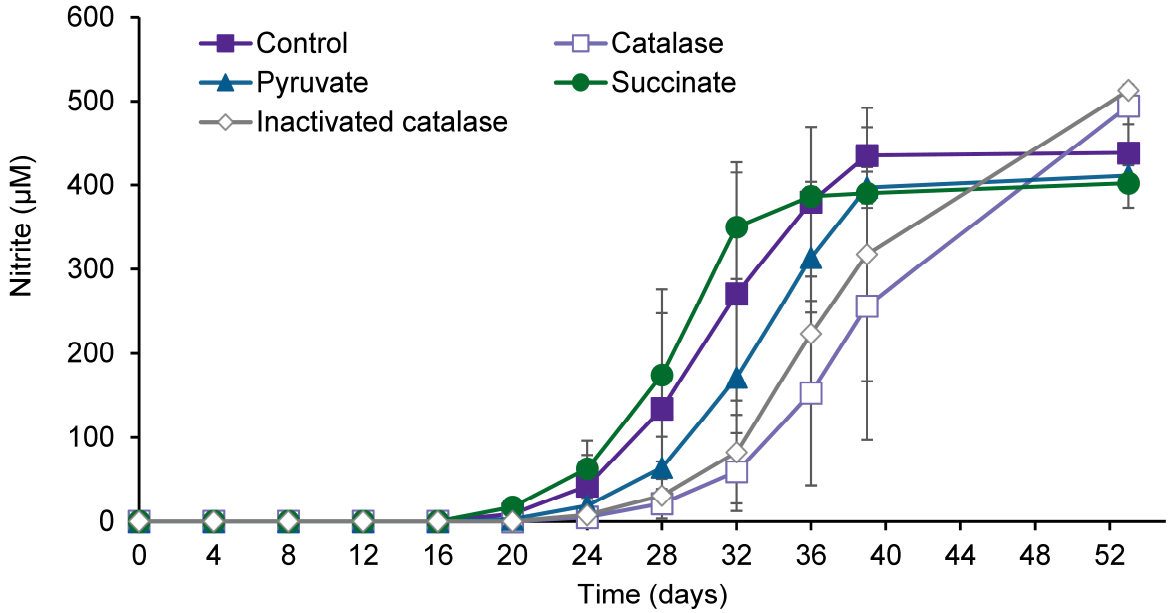

Figure 2.3 Nitrite production of *Ca*. N. exaquare enrichment culture supplemented with organic carbon or bovine liver catalase. Cultures were grown with 0.5 mM of NH_4Cl at 30°C. Error bars represent standard deviation of biological triplicates.

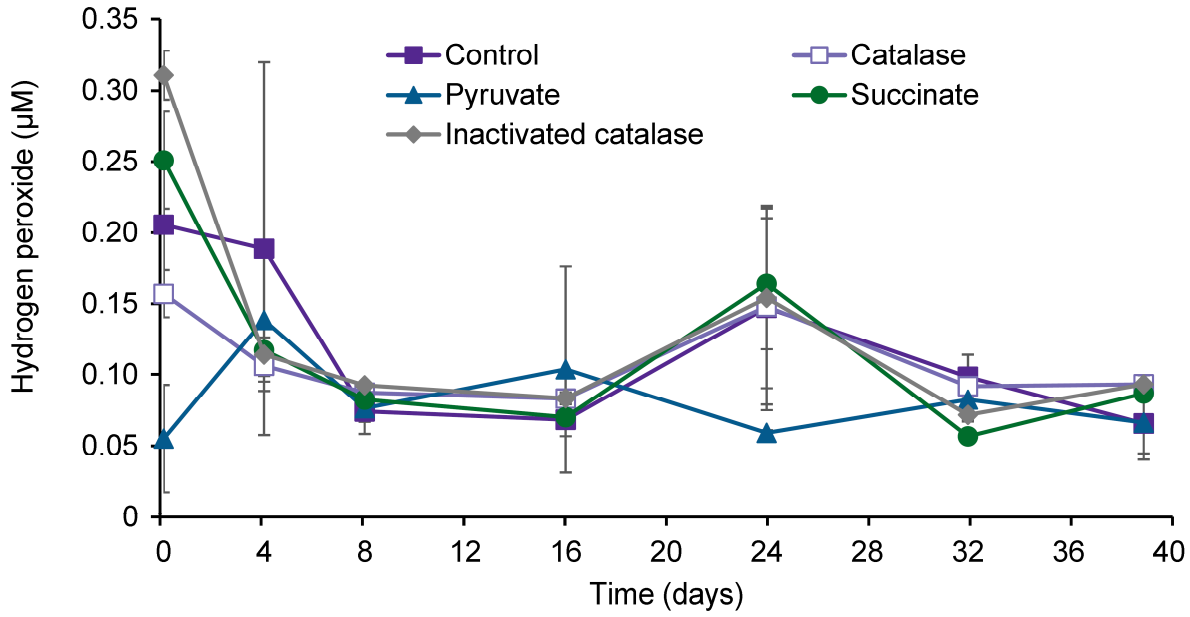

Figure 2.4 Hydrogen peroxide in *Ca*. N. exaquare enrichment culture supplemented with organic carbon or bovine liver catalase. Error bars represent the standard deviation of biological triplicates.

2.3.3 Catalase-producing heterotrophs

Eight unique colony types from the *Ca.* N. exaquare enrichment culture were grown on nutrient agar, and seven unique colony types were grown on R2A agar. Of these colonies, three from the nutrient agar and three from R2A agar tested catalase positive (Table 2.3). Isolates were characterized by colony morphology but not further identified. Type 6 and 7 colony types from nutrient agar looked very similar, and type 3 and 4 from R2A agar looked very similar to each other as well.

Table 2.3 Colony morphology and catalase activity of heterotrophic bacteria isolated from the *Ca.* N. exaquare enrichment culture.

Media	Colony type	Colony morphology	Catalase activity
Nutrient agar	T1	circular, medium, pale yellow, flat, entire margin	+
	T2	circular, small, dark yellow, convex, entire margin	(+)
	T3	circular, small, beige-white, raised, entire margin	(+)
	T4	circular, small, beige, convex, entire margin	-
	T5	circular, small, beige, convex, entire margin	-
	T6	filamentous, large, yellow-beige, undulate, filamentous margin	+
	T7	filamentous, large, yellow-beige, undulate, filamentous margin	+
	T8	circular, small, white-beige, convex, entire margin	-
R2A agar	T1	circular, medium, white, convex, entire margin	-
	T2	circular, medium, white, convex, entire margin	-
	T3	circular, medium, yellow, flat, entire margin	+
	T4	circular, medium, yellow, flat, entire margin	+
	T5	circular, small, pink, raised, entire margin	+
	T6	mixed colony types: filamentous, medium, pink-white; circular, medium, beige	(+); (+)
	T7	filamentous, small, white, filamentous margin	(+)

+, catalase activity

(+), possible weak catalase activity

-, no catalase activity

2.3.4 Testing of catalase and pyruvate hydrogen peroxide detoxification activity

Incubations of Ngm with hydrogen peroxide revealed that hydrogen peroxide was stable over a one hour incubation, and that both catalase and pyruvate reacted with the hydrogen peroxide, making it undetectable (Figure 2.5). Catalase reacted with all the available hydrogen peroxide faster than pyruvate.

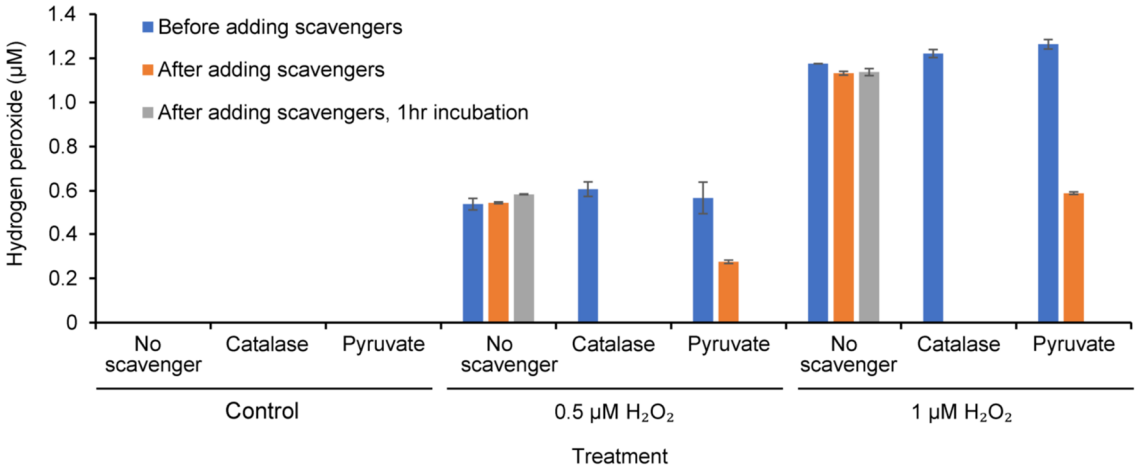

Figure 2.5 Hydrogen peroxide depletion by bovine liver catalase and pyruvate. Hydrogen peroxide (either 0.5 μM or 1 μM) was added to Ngm media and hydrogen peroxide levels were measured before scavengers (catalase and pyruvate) were added. Hydrogen peroxide levels were measured directly after adding scavengers and after a 1 hr incubation. Error bars indicate standard deviation of duplicate treatments. Control bottles (no hydrogen peroxide added) had no treatment duplicates.

2.4 Discussion

To determine how the previously reported organic carbon additions stimulate growth of *Ca.* N. exaquare (Sauder *et al.*, 2017), two different experiments were performed with pyruvate, succinate, and catalase additions to the cultures. Catalase was not stimulatory, and succinate and pyruvate could be stimulatory to *Ca.* N. exaquare ammonia oxidation, though the differences in nitrite production were not significant. This indicates the potential for *Ca.* N. exaquare to use organic carbon sources to increase activity; however, the mechanism of this stimulation is unclear. Mixotrophy through the assimilation of organic carbon is one possible mechanism. Alternatively, the stimulation could be indirect, through the stimulation of the heterotrophs in the culture, which in turn provide a different stimulus to the ammonia-oxidizing archaea.

Nitrite production with catalase addition was not the same as with pyruvate addition in either of the two experiments of the current study. In fact, nitrite production with catalase lagged behind that with pyruvate addition, particularly in the second experiment with bovine liver catalase. This indicated that, in contrast to the five AOA cultures tested by Kim *et al.* (2016) and the two AOA strains tested by Qin *et al.* (2017), catalase did not provide any nitrite-associated growth stimulation to *Ca.* N. exaquare. By day 40, *A. niger* catalase appeared to stimulate nitrite production, but this may be due to the excess ammonium in the media from the ammonium sulfate catalase suspension (Figure 2.2). The excess ammonium may be the cause of stimulation in all treatments with the *A. niger* catalase, because the heat inactivated catalase treatment also provided stimulation over the control. Additional exogenous catalase was unimportant for reducing hydrogen peroxide concentrations over the course of the experiment. Even after bovine liver catalase activity could no longer be detected, hydrogen peroxide levels did not increase over the rest of the experiment (Figure 2.4). Concentrations of hydrogen peroxide did not fluctuate greatly or build up to high levels over the course of the experiment, indicating that hydrogen peroxide was scavenged in the enrichment culture. In contrast, a closely related species of AOA, *Nitrososphaera viennensis*, produces hydrogen peroxide during ammonia oxidation (Kim *et al.*, 2016). Hydrogen peroxide accumulation in the *Ca.* N. exaquare enrichment culture may have been limited by production of catalase by *Ca.* N. exaquare, or by the catalase of other bacteria in the enrichment culture. Catalase activity of *Ca.* N. exaquare could not be tested specifically but catalase activity of the heterotrophic bacteria was tested. Catalase positive colony types (Table 2.3) may have been the species responsible for the low hydrogen peroxide levels in the culture supernatant. Co-inoculation of an AOA culture with catalase producing bacteria was shown to stimulate growth in the same manner as pyruvate, and to provide protection from ROS by maintaining low levels of extracellular hydrogen peroxide (Kim *et al.*, 2016). The *Ca.* N. exaquare enrichment culture is similar to this co-inoculation experiment because it also contains several catalase-producing species.

Pyruvate was one of the organic carbon compounds that was previously shown to stimulate *Ca.* N. exaquare (Sauder *et al.*, 2017). In the first experiment of the current study, pyruvate provided some stimulation, though not significant, but in the second experiment it did not. This inconsistency makes it difficult to draw conclusions on whether *Ca.* N. exaquare can use pyruvate as a carbon source. This inconsistency may be due to the number of cells that were used in the incubations. Sauder *et al.* (2017) used a 0.1% inoculum in their setup, and the current study used a 1% inoculum. The smaller number of AOA and heterotrophic bacterial cells in the 0.1% inoculum may be the cause of the greater nitrite production shown with pyruvate in that experiment. The two experiments in the current study both used a 1% inoculum of AOA that were at a similar stage of growth before subculturing, but exact cell numbers and the ratio of AOA to heterotrophic bacteria may have differed, leading to inconsistent results.

This current study indicates that succinate was not significantly stimulatory. Compared to the control cultures, succinate supplementation always resulted in an increased rate of nitrite production. However, compared to the study by Sauder *et al.* (2017), the degree of stimulation that succinate provides is much lower in the current study, and not statistically significant. Even between the two experimental setups in the current study, the level of stimulation varied, which could be explained by the culture inoculum differences described above.

Further experiments are needed to determine whether *Ca.* N. exaquare is capable of mixotrophic growth, such as experiments using labelled organic carbon sources to detect assimilation of these compounds. However, before this further work can be performed, *Ca.* N. exaquare must be isolated as a pure culture. Pyruvate and succinate were used up within a few days in the enrichment cultures, presumably by the heterotrophs (Table 2.2) and stimulation by pyruvate and succinate addition was not observed in the first few days of the experiments. Heterotrophs must be removed in order to properly assess the effect of pyruvate and catalase on *Ca.* N. exaquare. Furthermore, published findings of pyruvate stimulation of AOA were done using pure AOA cultures. Obtaining a pure culture of *Ca.* N. exaquare and

demonstrating increased ammonia oxidation in the presence of exogenous pyruvate and succinate, independent of whether catalase is added, would be an important first step toward demonstrating that the stimulation arises from assimilation of these organic compounds.

In summary, stimulation of *Ca.* N. exaquare by pyruvate and succinate was inconsistent; these results do not address the potential for organic carbon stimulation by *Ca.* N. exaquare. Catalase was not stimulatory to the culture, suggesting that this enrichment culture of *Ca.* N. exaquare already possesses the ability to enzymatically deplete hydrogen peroxide. Purification of *Ca.* N. exaquare and further incubation experiments such as the ones described in this thesis are required to demonstrate organic carbon assimilation and determine whether this WWTP archaeon is uniquely capable of mixotrophic growth.

Chapter 3: Metagenomic analysis of RBC biofilm

3.1 Introduction

Municipal wastewater contains ammonia that is removed by wastewater treatment plants (WWTPs) in order to prevent eutrophication, oxygen depletion, and toxicity to aquatic animals in the receiving waters. The nitrification process oxidizes ammonia to nitrate via nitrite in two enzymatic steps that were historically thought to be mediated by distinct groups of microorganisms. Aerobic ammonia oxidation was thought to be conducted by only ammonia-oxidizing bacteria (AOB) and ammonia-oxidizing archaea (AOA), and nitrite oxidation was carried out by nitrite-oxidizing bacteria (NOB). The existence of microorganisms capable of catalyzing both steps of nitrification in the process of complete ammonia oxidation (comammox) was suggested over a decade ago, with a prediction that such bacteria would be slow growing and inhabit biofilms exposed to relatively low ammonia concentrations (Costa *et al.*, 2006). Recently these predictions were confirmed by the discovery of species of *Nitrospira* that are capable of catalyzing comammox (Daims *et al.*, 2015; van Kessel *et al.*, 2015). To date, all comammox bacteria belong to lineage II of the genus *Nitrospira*. Two clades of comammox bacteria have been described, based on ammonia monooxygenase (*amoA*) gene phylogeny, with existing cultivated species of comammox bacteria belonging to clade A (van Kessel *et al.*, 2015; Daims *et al.*, 2015).

Little is known about the abundance and diversity of comammox bacteria in WWTPs. First detected in WWTP metagenomes (Daims *et al.*, 2015; van Kessel *et al.*, 2015), all comammox bacteria detected in WWTPs belong to comammox clade A (Pjevac *et al.*, 2017; Daims *et al.*, 2015). These bacteria were found at lower abundances than AOA and AOB (Pjevac *et al.*, 2017; Chao *et al.*, 2016; Fan *et al.*, 2017). Comammox bacteria have also been found in engineered environments with low ammonia concentrations, such as drinking water treatment plants (Pjevac *et al.*, 2017; Pinto *et al.*, 2015; Palomo *et al.*, 2016; Wang *et al.*, 2017). Although the detection of *amoA* genes of *Nitrospira* spp. has thus far been used as evidence for contributions to comammox activity, the detection of genes for both ammonia

and nitrite oxidation in the same genome offer increased evidence for complete ammonia oxidation. Previous studies examining comammox bacterial distributions in WWTPs have focused on activated sludge secondary treatment systems (Gonzalez-Martinez *et al.*, 2016; Fan *et al.*, 2017; Chao *et al.*, 2016). To date, no studies have investigated comammox bacteria in tertiary biological wastewater treatment systems.

Rotating biological contactors (RBCs) are used in the tertiary treatment system of the Guelph wastewater treatment plant (Ontario, Canada). Representing a total of 440,000 m^2 of surface area for nitrifying biofilm, the RBCs are organized into "trains", each composed of eight individual RBC "stages" (Figure 3.1). Water from secondary clarifiers is pooled and then distributed among the four trains, flowing from RBC 1 to RBC 8. The rotation of central RBC shafts results in alternating exposure of RBC biofilm to wastewater and air, and ammonia decreases sequentially along the flowpath due to nitrification (Sauder et al., 2012). Because of the relatively low ammonia concentrations entering the RBCs, compared to aeration basins, and their fixed-film design, these RBCs present a valuable opportunity to study distributions and relative abundances of nitrifiers. Both AOA and AOB abundances in these RBCs have previously been studied, demonstrating that AOA abundances increase along the RBC flowpath (Sauder *et al.*, 2012). In addition, the sole AOA species present in the RBCs, *Candidatus* Nitrosocosmicus exaquare, has been cultivated (Sauder *et al.*, 2017). This AOA enrichment culture incorporates labelled inorganic carbon during ammonia oxidation, indicating that it is chemolithoautotrophic. However, no incorporation of inorganic carbon by AOA was observed in the RBC biofilm incubations. Ammonia oxidation in these biofilm incubations was partially inhibited by a differential inhibitor targeting AOA, indicating that the AOA may contribute to ammonia oxidation in the RBCs. However, results for differential inhibitors targeting AOB were inconsistent. Additionally, *Nitrospira* were also labelled during the RBC biofilm incubations. This labelling, along with the inconsistencies in activity assessments with the differential inhibitors, could be attributed to comammox bacteria, as suggested by Sauder *et al.* (2017). Comammox bacteria need to be considered in any future studies of the RBC biofilm. Currently, the relative abundances of

AOA, AOB, and comammox bacteria in the RBCs are unknown. This information is the first step towards understanding these groups' contribution to ammonia oxidation and other functions in the biofilm.

Due to the predicted adaptation to low ammonia concentrations and biofilm growth of comammox bacteria (Costa *et al.*, 2006; Daims *et al.*, 2015), I hypothesized that, like for AOA (Sauder *et al.*, 2012), the relative abundance of comammox bacteria would increase as ammonia concentrations decreased along the RBC flowpath. To test this hypothesis, and to test whether comammox bacteria are present in the RBCs, a combination of qPCR and metagenomic sequencing of selected RBC samples was used to assess the relative abundance and diversity of comammox bacteria, in relation to AOA and traditional AOB, in this tertiary treatment system environment. The stability of RBC biofilm communities was also tested by including samples from three different time points in 2010 and one time point in 2016. Furthermore, through assembly and binning of metagenome sequences, bins containing genes for both ammonia oxidation and nitrite oxidation were investigated to show that some of the *Nitrospira* species present in the RBCs were genetically capable of complete ammonia oxidation.

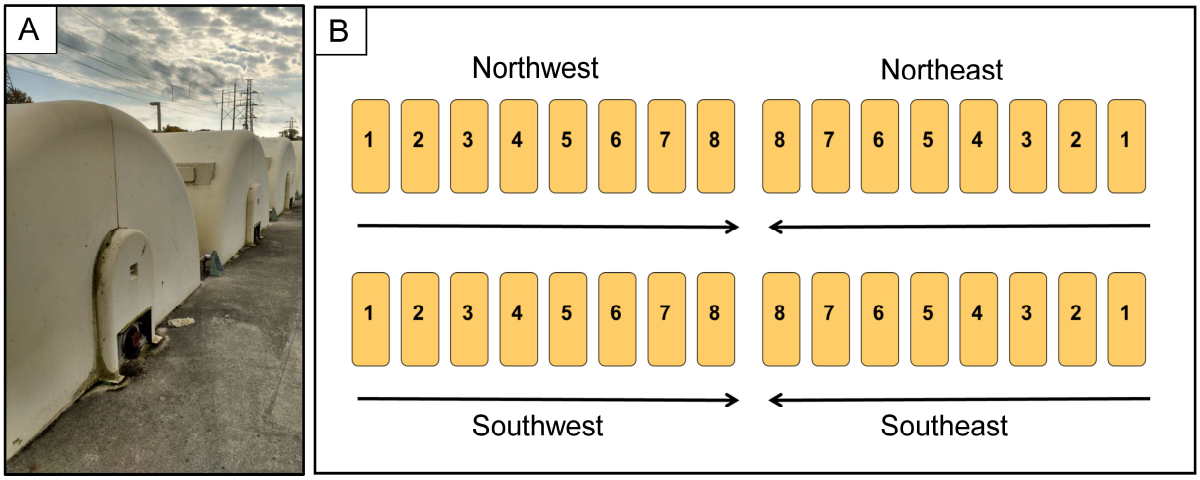

Figure 3.1 Rotating biological contactors (RBCs) of the Guelph wastewater treatment plant (WWTP). (A) External view of the RBCs and (B) schematic of the RBC trains. Arrows indicate the direction of water flow.

3.2 Methods

3.2.1 Sampling

Using ethanol cleaned spatulas, biofilm samples were removed from RBC biofilm surfaces. Samples were stored on dry ice until delivered to the lab and were kept at -70°C until analyzed. Biofilm was sampled in February, June, and September in 2010 and in October 2016. In June and September 2010 all eight stages of both the northeast (NE) and southeast (SE) trains were sampled, and in February 2010 only the eight stages of the NE train were sampled (Sauder *et al.*, 2012), but only the NE RBC 1 and RBC 8 samples were used in this current study (Table 3.1). All RBCs from all four trains were sampled in 2016, except for RBC 1 of the SE train and RBC 2 of the southwest (SW) train, which were not operational. Water samples were also collected from RBC 1 and RBC 8 and kept on ice until delivered to the lab. The pH of all water samples was measured using a Delta 30 pH meter

(Mettler Toledo, Mississauga, Ontario, Canada), and then samples were stored at -20°C until further analyzed.

Table 3.1 RBC samples used in this study.

Abbreviation	RBC stage	RBC train	Month	Year	Study	Analysis
FNE1	RBC 1	NE train	February	2010	Sauder et al., 2012	qPCR, metagenomics
FNE8	RBC 8	NE train	February	2010	Sauder et al., 2012	qPCR, metagenomics
JNE1	RBC 1	NE train	June	2010	Sauder et al., 2012	qPCR, metagenomics
JNE8	RBC 8	NE train	June	2010	Sauder et al., 2012	qPCR, metagenomics
SNE1	RBC 1	NE train	September	2010	Sauder et al., 2012	qPCR, metagenomics
SNE8	RBC 8	NE train	September	2010	Sauder et al., 2012	qPCR, metagenomics
NE1	RBC 1	NE train	October	2016	This study	qPCR, metagenomics
NE2	RBC 2	NE train	October	2016	This study	qPCR
NE3	RBC 3	NE train	October	2016	This study	qPCR
NE4	RBC 4	NE train	October	2016	This study	qPCR
NE5	RBC 5	NE train	October	2016	This study	qPCR
NE6	RBC 6	NE train	October	2016	This study	qPCR
NE7	RBC 7	NE train	October	2016	This study	qPCR
NE8	RBC 8	NE train	October	2016	This study	qPCR, metagenomics
NW1	RBC 1	NW train	October	2016	This study	qPCR, metagenomics
NW2	RBC 2	NW train	October	2016	This study	qPCR
NW3	RBC 3	NW train	October	2016	This study	qPCR
NW4	RBC 4	NW train	October	2016	This study	qPCR
NW5	RBC 5	NW train	October	2016	This study	qPCR
NW6	RBC 6	NW train	October	2016	This study	qPCR
NW7	RBC 7	NW train	October	2016	This study	qPCR
NW8	RBC 8	NW train	October	2016	This study	qPCR, metagenomics
SE2	RBC 2	SE train	October	2016	This study	qPCR, metagenomics
SE3	RBC 3	SE train	October	2016	This study	qPCR
SE4	RBC 4	SE train	October	2016	This study	qPCR
SE5	RBC 5	SE train	October	2016	This study	qPCR
SE6	RBC 6	SE train	October	2016	This study	qPCR
SE7	RBC 7	SE train	October	2016	This study	qPCR
SE8	RBC 8	SE train	October	2016	This study	qPCR, metagenomics
SW1	RBC 1	SW train	October	2016	This study	qPCR, metagenomics
SW3	RBC 3	SW train	October	2016	This study	qPCR
SW4	RBC 4	SW train	October	2016	This study	qPCR
SW5	RBC 5	SW train	October	2016	This study	qPCR
SW6	RBC 6	SW train	October	2016	This study	qPCR
SW7	RBC 7	SW train	October	2016	This study	qPCR
SW8	RBC 8	SW train	October	2016	This study	qPCR, metagenomics

3.2.2 Water chemistry

Total ammonium ($NH_3 + NH_4^+$) was measured fluorometrically using orthophthaldialdehyde (OPA) reagent (Holmes *et al.*, 1999) according to the method by Poulin and Pelletier (2007), with the following modifications. Volumes of 100 µL of sample and 200 µL of OPA working reagent were added to a 96-well opaque flat-bottomed plate. Plates were incubated for four hours in the dark before being measured. Nitrite and nitrate concentrations were measured colorimetrically using Greiss reagent as described by Miranda *et al.* (2001). All samples were measured as technical duplicates at 360 nm excitation, 465 nm emission (ammonium), and 550 nm (nitrite/nitrate) using a FilterMax F5 Multi-Mode Microplate reader (Molecular Devices, San Jose, CA, USA). Measurements reflect total ammonium ($NH_3 + NH_4^+$) as nitrogen, and nitrite and nitrate as nitrogen. Monthly and yearly ammonia concentrations (measured as total ammonia as nitrogen) of secondary effluent (RBC influent) and the southeast RBC train were compiled for the years 2010 to 2017. Data were obtained from WWTP operators. Plant influent and effluent data were retrieved from the Guelph WWTP annual reports for 2010 to 2016, and the data are available at https://guelph.ca/living/environment/water/wastewater/.

3.2.3 DNA extractions

Extracted DNA from RBC 1 and 8 biofilm samples of the northeast train from 2010 was used for quantitative PCR (qPCR) and metagenomic sequencing (6 samples) (Table 3.1). The 2010 biofilm samples used were the same samples collected and analyzed via qPCR by Sauder and colleagues (2012), but DNA extractions were performed again, at the same time as the 2016 samples. The DNA extracts from all four trains in 2016 were used for qPCR, but only DNA from RBCs 1 and 8 were used for metagenomic sequencing (8 samples; SE2 replaced SE1). All extractions were done with the PowerSoil DNA Isolation Kit (Mo Bio, Carlsbad, CA, USA) according to the manufacturer's instructions, except that beadbeating was conducted with a FastPrep-24 (MP Biomedicals, Santa Ana, CA, USA) at 5.5 m/s for 45 s. Genomic DNA was visualized on a 1% agarose gel and quantified using a NanoDrop 2000

(Thermo Scientific, Waltham, MA, USA) and Qubit dsDNA high sensitivity assay kit (Thermo Scientific).

3.2.4 Quantitative PCR

Archaeal and bacterial 16S rRNA genes were quantified using the primers 771F/957R (Ochsenreiter *et al.*, 2003) and 341F/518R (Muyzer *et al.*, 1993), respectively. Quantification of AOB *amoA* genes was carried out using the primers amoA1F/amoA2R (Rotthauwe *et al.*, 1997). Comammox clade A and clade B were amplified using equimolar primer mixes of comaA-244f (a-f) and comaA-659r (a-f), and comaB-244f (a-f) and comaB-659r (a-f), respectively (Pjevac *et al.*, 2017). Primers for each of comammox clades A and B were used first in end-point PCR, but clade B primers produced no amplicons. Subsequent qPCR was only performed with clade A primers. All qPCR amplifications were carried out as technical duplicates on a CFX96 thermal cycler (Bio-Rad, Hercules, CA, USA). Each 10 µL PCR contained 1X iQ SYBR Green Supermix (Bio-Rad; containing 50 U/ml iTaq DNA polymerase, 0.4 mM dNTPs, 6 mM $MgCl_2$, 100 mM KCl, 40 mM Tris-HCl, 20 nM fluorescein, stabilizers, and SYBR Green I dye), primers (see below for concentrations), 0.5 µg bovine serum albumin, and 2-20 ng of DNA as template. Primers were used at a final concentration of 0.2 µM, except for the comaA primers, which were used at 0.5 µM. Conditions for qPCR of bacterial 16S rRNA, AOA 16S rRNA, and AOB *amoA* genes were 95°C for 3 minutes, followed by 35 cycles of 95°C for 30 s, 55°C for 30 s, and 72°C for 30 s, with a fluorescence reading at each step. Melt curve analysis was performed from 65-95°C, in increments of 0.5°C. The qPCR conditions for comammox bacterial *amoA* genes were the same except that the annealing temperature was 52°C and the extension time at 72°C was 1 minute. Standard curves were generated using 10-fold dilutions of standards that were made using the same primer pairs used for qPCR. For comammox bacterial *amoA* genes, template DNA was extracted from the RBC biofilm. For AOB *amoA* genes and AOA 16S rRNA genes, template DNA was extracted from cultures of *Nitrosomonas europaea* and *Candidatus* Nitrosocosmicus exaquare, respectively. Extracted DNA from *Escherichia coli* was used to

prepare standards for bacterial 16S rRNA genes. Gene copies were calculated based on the amount of DNA present in the original extractions but were not normalized further to account for copy number.

3.2.5 Metagenomic sequencing

DNA shearing, library preparation, and sequencing was performed at The Centre for Applied Genomics (TCAG) in Toronto, Ontario. Approximately 1 µg of DNA per sample was sent to TCAG. Extracted DNA was quantified by Qubit dsDNA High Sensitivity assay (Thermo Scientific, Waltham, MA, USA). Subsequently, 500 ng of input DNA was sheared to 550 bp using a Covaris LE220 (Covaris, Woburn, MA, USA). Library preparation was done with the TruSeq PCR-free Library Prep Kit (Illumina Inc. San Diego, CA, USA). Paired-end sequencing (2x250 bases) was performed on a HiSeq 2500 (Illumina) using the HiSeq Rapid SBS Kit v2 (500 Cycle) (Illumina), resulting in a total of ~250 million paired-end reads.

3.2.6 Sequence quality control

Quality trimming and removal of adaptor sequences was performed using AdapterRemoval version 2.2.2 (Schubert *et al.*, 2016) and the quality of the reads was checked with FastQC version 0.11.5 (Andrews, 2010). Reports were combined using MultiQC version 1.0 (Ewels *et al.*, 2016).

3.2.7 Analysis of unassembled reads

Using forward trimmed reads, open reading frames (ORFs) were predicted on the unmerged and unassembled forward reads using FragGeneScan-Plus (Kim *et al.*, 2015). Profile hidden Markov models (HMMs) for a taxonomic marker (*rpoB*) and functional genes (*amoA*, *nxrB*) were used to quantify the relative abundances and taxonomic affiliations of nitrifiers from the unassembled reads using MetAnnotate (Petrenko *et al.*, 2015). The database used for taxonomic classification was RefSeq release 80. Functional gene HMMs (*amoA*_AOA, *amoA*_AOB, and *nxrB*) and the taxonomic marker gene HMM (*rpoB*) were

downloaded from FunGene (Fish *et al.*, 2013). Within each sample, length-normalized HMM hits for each functional gene were divided by the total number of length-normalized HMM hits for *rpoB*. This was done in order to facilitate cross-HMM and cross-sample comparisons. Therefore, the proportional numbers for each functional gene can be thought of as their total community contribution relative to *rpoB*. Barplots were generated using R version 3.4 using a custom script (available at https://github.com/jmtsuji/metannotate-analysis).

3.2.8 Assembly and binning of metagenomic reads

Metagenomic reads were processed through the entire ATLAS pipeline (release 1.0.22), which includes quality control, assembly, annotation, binning, and read mapping steps (White et al., 2017). Quality control was performed using BBduk2 from the BBMap tools (Bushnell, 2017). Several assembly and binning strategies were performed (Table 3.2, Table 3.3). First, samples were assembled individually using metaSPAdes (Nurk et al., 2017) as an assembler (k-mers 21, 33, 55), Prokka (Seemann, 2014) for annotation, and MaxBin2 (Wu et al., 2016) for binning (Table 3.3). Several co-assembly combinations (Table 3.2) were tested using Megahit (Li *et al.*, 2015) as an assembler (k-min=21, k-max=121, k-step=20), Prokka (Seemann, 2014) for annotation, and MetaBAT (Kang *et al.*, 2015) for binning (Table 3.3). Only contigs >1 kb were used for binning. The extension script for the ATLAS co-assemblies can be found at https://github.com/jmtsuji/atlas-extensions/releases/tag/1.0.22-coassembly-r3. Bin completeness and contamination were assessed using CheckM (Parks *et al.*, 2015). *Nitrospira* genome bins from assembly attempts were compared and dereplicated to find identical genomes using dRep (Olm *et al.*, 2017). Average nucleotide identity (ANI) analysis was performed on the representative ("winning") AOA genome selected by dRep, as well as the high quality (>75% completion, <25% contamination) *amoA*-containing *Nitrospira* bins, using ANIm on the JSpecies webserver (Richter *et al.*, 2016).

Table 3.2 Co-assembly combinations used in ATLAS for metagenome assembly and binning.

Co-assembly name	Co-assemblies	Samples used in co-assembly
2016 all	NE	NE1, NE8
	NW	NW1, NW8
	SE	SE1, SE8
	SW	SW1, SW8
Upper 2016	Upper 2016	NE1, NW1, SE2, SW1
NE8-NW8	NE8-NW8	NE8, NW8
NE 2010	NE1 2010	FNE1, JNE1, SNE1
	NE8 2010	FNE8, JNE8, SNE8

Table 3.3 Metagenomic sequencing assembly and binning data for RBC samples.

	Sample	Sequenced reads (million)	Reads after quality filtering (million)	Number of contigs	Total size of contigs (Mb)	Average G + C content (%)	N50	Total number of bins
Individual assembly	1FNE	19.6	19.6	57480	220.2	60.4	6651	41
	8FNE	16.2	16.1	44033	189.1	60.6	4137	36
	1JNE	20.3	20.3	70247	295.3	53.6	6934	39
	8JNE	21.6	21.5	62986	265.4	52.0	5907	37
	1SNE	19.3	19.3	56438	227.9	61.5	4988	40
	8SNE	21.6	21.6	80168	286.4	62.9	8402	54
	NE1	17.0	17.0	52916	223.6	63.1	5567	40
	NE8	11.4	11.4	37321	120.3	63.4	5633	23
	NW1	20.3	20.3	73276	289.6	63.1	8093	49
	NW8	10.5	10.5	31808	107.7	63.3	3877	20
	SE2	20.7	20.7	66997	261.3	62.2	7762	45
	SE8	16.2	16.1	46074	190.5	63.5	4733	34
	SW1	19.6	19.6	71123	263.0	62.0	8197	43
	SW8	18.4	18.4	59735	242.1	62.6	5862	46
Co-assembly	2016 all NE	28.4	28.3	123049	397.7	63.7	18271	108
	2016 all NW	30.8	30.8	147057	450.7	63.7	23012	126
	2016 all SE	36.9	36.8	166156	502.6	63.4	28212	136
	2016 all SW	38.1	38.0	199019	592.9	62.5	32814	156
	Upper 2016	77.6	77.5	374818	1193.0	62.4	59179	273
	NE8-NW8	21.9	21.8	101851	310.0	63.8	17130	64
	NE1 2010	59.3	59.1	295362	945.0	60.1	47513	234
	NE8 2010	59.4	59.2	317986	1013.1	60.5	52045	229

3.2.9 Phylogenetic analysis

Nitrospira amoA gene ORFs from assembled contigs were compiled and clustered into groups based on nucleotide sequence at a 99% identity threshold using cd-hit (Li and Godzik, 2006). All *amoA* gene ORFs that were classified as the genus *Nitrospira* were included. The corresponding amino acid sequences of these genes were aligned, along with comammox AmoA sequences from cultivated species and environmental surveys downloaded from NCBI, using Muscle (Edgar, 2004) within MEGA7 (Kumar *et al.*, 2016). Phylogenetic analysis was inferred using maximum likelihood analysis based on the Le Gascuel evolutionary model (Le and Gascuel, 2008), using MEGA7.

3.2.10 Abundance of comammox bacteria bins

Representative bins for each *amoA* RBC cluster (determined during the phylogenetic analysis) were selected for each group. For RBC groups that had a corresponding high quality bin, the winning bin as selected by dRep was used. Group G was the exception, because the winning bin did not contain *amoA*, and so the bin containing the *amoA* gene was selected, which was also of a higher completeness than the winning bin for that cluster. When only one bin contained the RBC group, that bin was selected, even though the bin quality was not high (Groups I, J, K, L). Bins containing RBC groups E and D were clustered into the same dRep cluster, and so the selected bin (group E) represented both of these closely related sequence groups. Read mapping (using quality trimmed reads) to representative bins was performed using BBMap (Bushnell, 2017) version 38.22 (with the flags perfectmode=t and ambiguous=best). Reads from all samples were iteratively mapped to each bin, and average coverage was calculated. Depth of coverage per nucleotide was determined using the depth tool within Samtools (Li *et al.*, 2009) version 1.9 (with the -aa flag), and then these values were averaged to get the average bin coverage per sample. Hierarchical clustering of bins for the heatmap was performed using R version 3.4.4, using the Pearson correlation coefficient as a distance measure.

3.3 Results

3.3.1 Water chemistry

Ammonium concentrations were higher in RBC 1 than RBC 8 for all treatment trains (Figure 3.2, Table 3.4). The highest ammonium concentration was in NE1 RBC (16.3 μM) and the lowest concentration was in NW8 RBC (0.2 μM). In all RBC 1s, the ammonium concentration was at least 9 μM, whereas the ammonium concentration was below 4 μM in all RBC 8s. Nitrite concentrations were higher than ammonium concentrations, whereas nitrate concentrations were the highest of all measured nitrogen forms (Table 3.4). Data from the WWTP operators showed that the ammonia concentrations of the RBC influent were lowest in 2012 (0.23 mg/L, equivalent to 16.4 μM NH_3-N) and 2016 (0.31 mg/L, equivalent to 22.1 μM NH_3-N) (Figure 3.3). Data for 2010 only included two months of data, so the 2010 data cannot be fairly compared to the 2016 data. However, 2011 data was complete and can be compared. The ammonia concentration in 2016 (0.31 mg/L NH_3-N) was lower than in 2011 (1.14 mg/L NH_3-N) but this was not a significant difference at a significance level of 0.05 (t-test, p=0.07). The plant influent and effluent ammonia concentrations were stable over the years 2010 to 2016 (Figure 3.4).

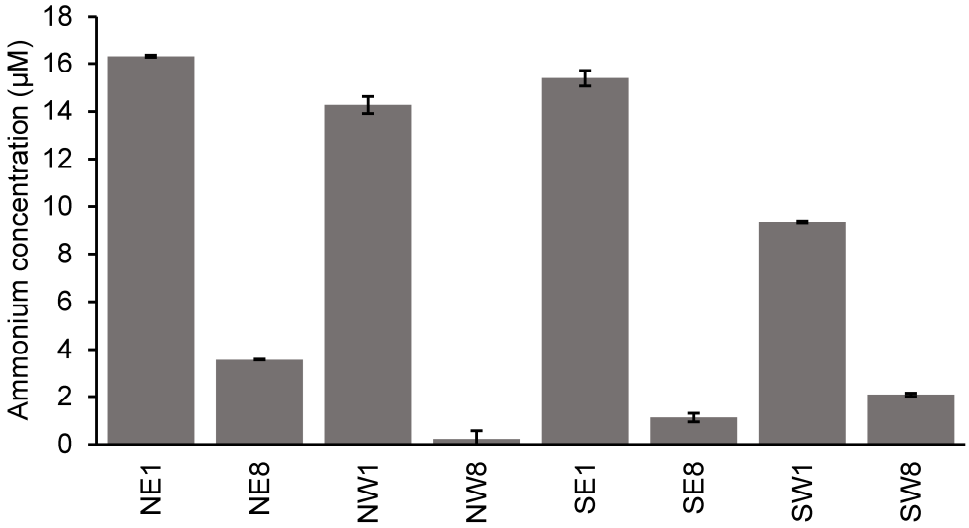

Figure 3.2 Ammonium concentrations in RBC water sampled at the same time as biofilm collection in October 2016. Error bars indicate standard deviation of technical duplicates. NE, Northeast train; NW, Northwest train; SE, Southeast train; SW, Southwest train.

Table 3.4 Water chemistry for October 2016 RBC samples.

Sample	Ammonium (µM)	Nitrite (µM)	Nitrate (µM)
NE1	16.3	66.1	1777.8
NE8	3.6	3.3	1471.3
NW1	14.3	31.5	681.8
NW8	0.2	0.9	358.5
SE1	15.4	27.7	566.5
SE8	1.1	6.2	632.6
SW1	9.3	18.4	478.0
SW8	2.1	9.8	970.1

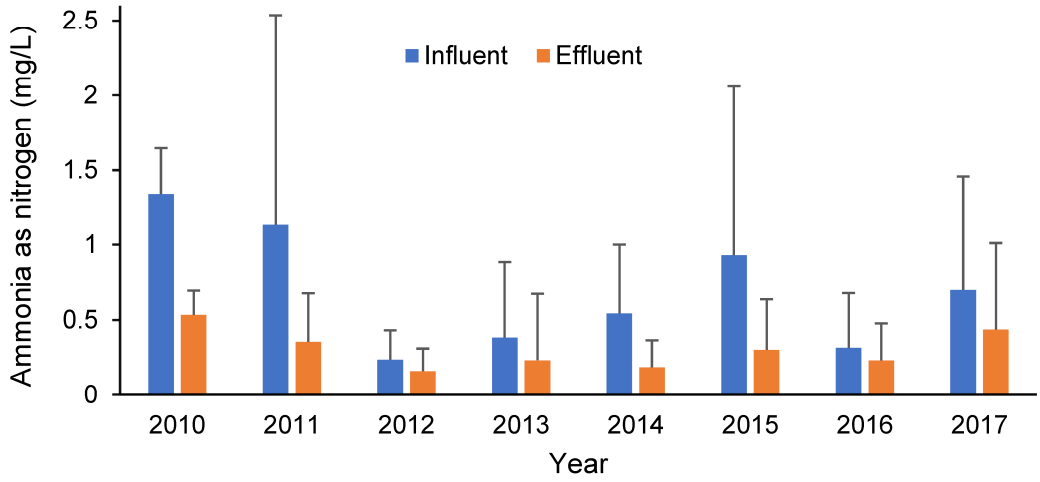

Figure 3.3 Average ammonia concentrations for RBC influent and effluent. Values were obtained from WWTP operators. The RBC influent values were measured as the secondary effluent, and the RBC effluent values were from the southeast train. Averages for each month were calculated, and then averaged for the year. Error bars indicate standard deviation of yearly averages.

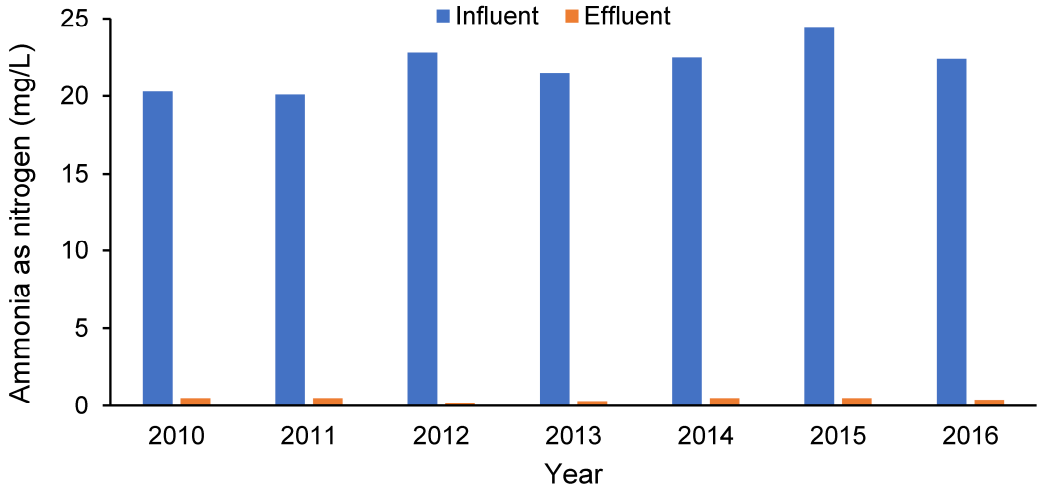

Figure 3.4 Yearly average ammonia concentrations for Guelph WWTP influent and effluent. Values were obtained from the Guelph WWTP annual reports available online.

3.3.2 Quantitative PCR

Thaumarchaeotal 16S rRNA genes, AOB *amoA,* and comammox *amoA* genes were detected in all samples (Figure 3.5, Figure 3.6, Table 3.5). The overall bacterial 16S rRNA gene abundance was higher in RBC 1 than 8 in all sample pairs in both years, except for the June samples from 2010 (Figure 3.5, Figure 3.6). Comammox *amoA* genes were more abundant in RBC 1 samples than RBC 8 samples for each RBC 1 and 8 pairing for 2010 and 2016 samples and were usually within the same order of magnitude. The proportion of comammox bacteria to the total community was consistently higher in RBC 1 than RBC 8 across all sample pairs (Table 3.5). Thaumarchaeotal 16S rRNA genes were most abundant in RBC 8 and less abundant in RBC 1 for 2010 samples. In addition, the proportion of AOA to the total community was consistently higher in RBC 8 compared to RBC 1 in the same month in 2010. But in 2016 AOA *amoA* gene abundance was higher in RBC 1 than 8 in all four trains. When comparing the proportion of AOA to the total community, the proportion of AOA was also higher in RBC 1 than RBC 8 of the same train in 2016. AOB *amoA* gene abundances were higher in RBC 1 than RBC 8 in both years, but in 2016 their abundances were one to two orders of magnitude lower.

In most samples, comammox *amoA* genes dominated those corresponding to other ammonia oxidizers (Figure 3.5, Table 3.5). In 2010, comammox genes outnumbered AOA and AOB genes in all samples, except for the September RBC 8 sample, in which AOA genes outnumbered the genes of the other ammonia oxidizers. The AOB genes outnumbered AOA genes in RBC 1 at all timepoints for 2010 samples, whereas AOA genes either outnumbered AOB genes in RBC 8, or their abundances were roughly equal. In 2016, comammox *amoA* genes outnumbered the corresponding genes of other ammonia oxidizers, except in NE8 and NW8, in which the AOA *amoA* genes outnumbered those of comammox bacteria. The AOA genes greatly outnumbered AOB genes in RBC 1 and 8 in all trains in the 2016 samples. Analysis of all 2016 RBC stages showed a general trend of decreasing gene abundance across each RBC flowpath for all genes quantified (Figure 3.6).

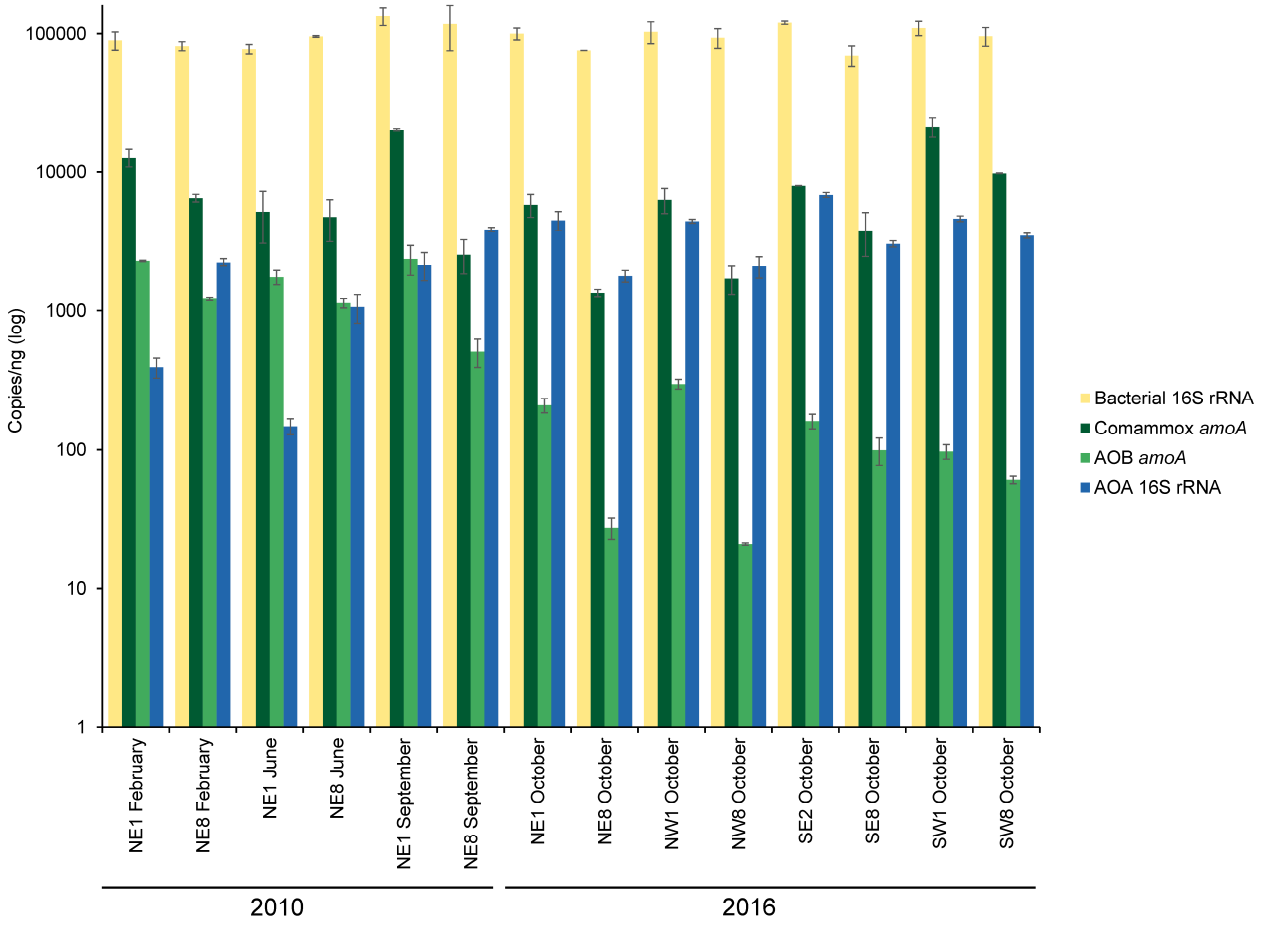

Figure 3.5 Bacterial 16S rRNA, comammox, and AOB *amoA*, and archaeal 16S rRNA gene abundances for samples paired with metagenome sequencing. Error bars indicate standard deviation of qPCR technical duplicates. NE, northeast train; NW, northwest train; SE, southeast train; SW, southwest train.

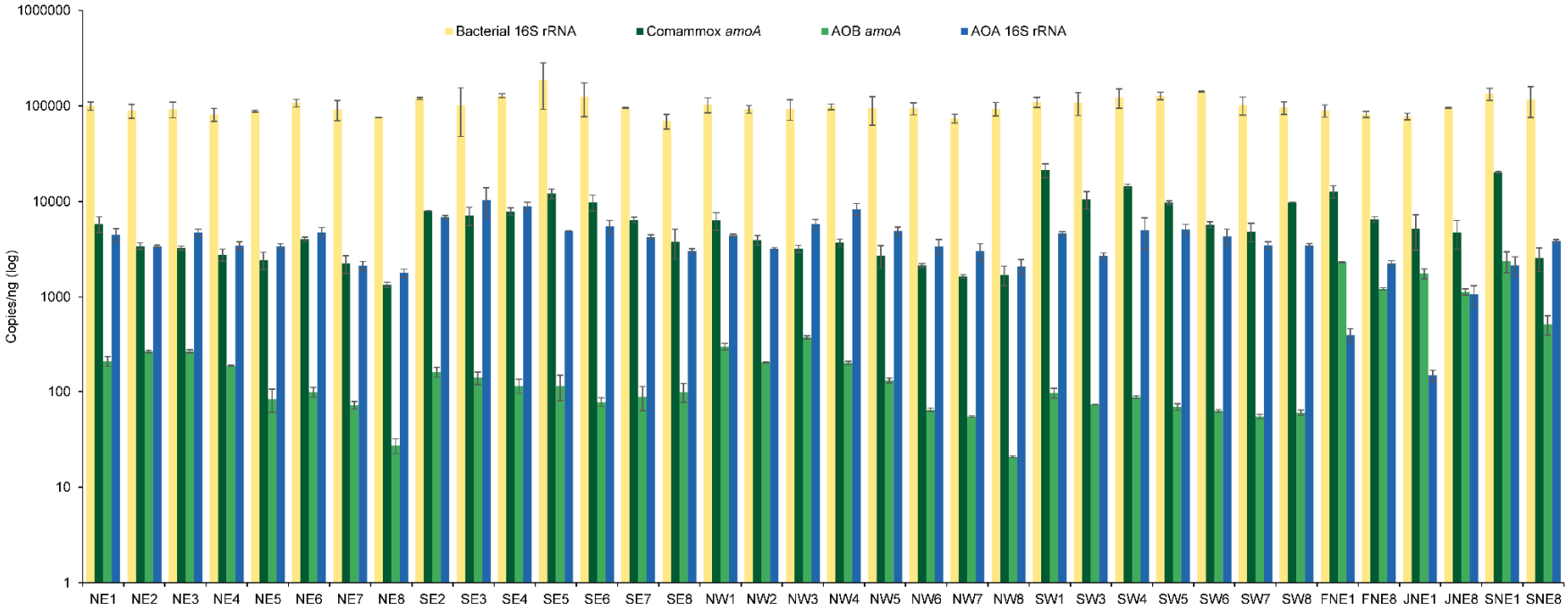

Figure 3.6 Bacterial 16S rRNA, comammox and AOB *amoA*, and archaeal 16S rRNA gene abundances for all RBC samples. Error bars indicate standard deviation of qPCR technical duplicates. NE, northeast train; NW, northwest train; SE, southeast train; SW, southwest train.

Table 3.5 Quantitative PCR results for RBC biofilm samples.

	Bacterial 16S rRNA		Comammox *amoA*		AOA 16S rRNA		AOB *amoA*		Total AOP						
Biofilm sample	Copies/ng genomic DNA	SD	Copies/ng genomic DNA	SD	Copies/ng genomic DNA	SD	Copies/ng genomic DNA	SD	Copies/ng genomic DNA	AOA of total AOP (%)	Comammox of total AOP (%)	AOB of total AOP (%)	AOA of TC (%)	Comammox of TC (%)	AOB of TC (%)
FNE1	89448.4	13333.9	12754.2	1892.1	391.6	64.5	2314.9	25.0	15460.7	2.5	82.5	15.0	0.4	14.3	2.6
FNE8	81515.3	6043.9	6517.2	413.7	2256.6	144.1	1216.4	34.9	9990.1	22.6	65.2	12.2	2.7	8.0	1.5
JNE1	77612.8	5965.3	5180.4	2101.9	147.7	19.2	1754.6	205.8	7082.7	2.1	73.1	24.8	0.2	6.7	2.3
JNE8	95455.4	1332.3	4752.1	1588.3	1063.2	248.6	1131.3	86.2	6946.6	15.3	68.4	16.3	1.1	5.0	1.2
SNE1	133594.7	19158.7	20149.7	513.2	2150.2	497.6	2387.2	582.8	24687.2	8.7	81.6	9.7	1.6	15.1	1.8
SNE8	117388.9	41913.8	2554.0	705.8	3863.2	139.0	507.8	117.7	6925.0	55.8	36.9	7.3	3.2	2.2	0.4
NE1	99901.3	9882.5	5823.8	1093.8	4499.5	709.7	208.6	24.5	10532.0	42.7	55.3	2.0	4.3	5.8	0.2
NE8	75882.7	0.00*	1348.2	80.2	1783.0	173.6	27.2	4.7	3158.4	56.5	42.7	0.9	2.3	1.8	0.0
NW1	103216.4	18344.9	6333.7	1301.6	4437.3	143.9	296.9	24.0	11067.9	40.1	57.2	2.7	4.1	6.1	0.3
NW8	93546.2	15073.5	1709.5	394.0	2098.6	376.1	20.8	0.4	3828.9	54.8	44.6	0.5	2.2	1.8	0.0
SE2	119854.2	3149.3	7977.7	21.2	6868.2	279.7	160.7	19.2	15006.7	45.8	53.2	1.1	5.4	6.7	0.1
SE8	69611.6	12123.0	3804.4	1315.2	3050.5	155.0	99.4	22.2	6954.4	43.9	54.7	1.4	4.2	5.5	0.1
SW1	109594.3	12892.9	21263.5	3460.4	4628.6	214.6	97.0	11.6	25989.2	17.8	81.8	0.4	4.1	19.4	0.1
SW8	95913.4	14632.1	9779.0	61.0	3482.9	141.4	60.3	3.7	13322.3	26.1	73.4	0.5	3.5	10.2	0.1

* no technical duplicate available

SD, standard deviation of technical duplicates

AOP, ammonia-oxidizing prokaryotes (AOA plus AOB plus comammox)

TC, total community (bacterial plus thaumarchaeotal 16S rRNA genes)

3.3.3 HMM searches on unassembled reads

Based on analysis of unassembled metagenomic sequence data with an HMM for the RNA polymerase subunit B gene (*rpoB*), the combined abundance of all detected taxa at ≥1% relative abundance comprised less than 50% of the total sequenced community (Figure 3.7). Based on metagenomic analysis, *Nitrospira* sequences dominated all samples and were relatively stable in abundance between the two sampling years. The *Nitrospira rpoB* gene relative abundances, like those of the overall community, were higher in RBC 1 than 8 of the corresponding train. *Nitrosomonas*-affiliated *rpoB* gene sequences were only detected at ≥1% in the 2010 samples. Overall, the community composition appeared to be stable between seasonal timepoints in 2010, and these profiles were different than those detected in 2016. The main difference was the absence of *Nitrosomonas rpoB* genes at ≥1% abundance in 2016, making *Nitrospira* the only potential ammonia oxidizer present at ≥1% abundance in those samples. Due to the decreased specificity of taxonomic assignment at the species level (Petrenko *et al.*, 2015), taxonomic classification occurred at the genus level and, as such, taxonomic markers such as *rpoB* cannot indicate whether these *Nitrospira* spp. were strict nitrite oxidizers or were *amoA*-containing comammox bacteria.

The HMM search for the *amoA* gene of AOA detected this gene at low relative abundance in the metagenomic dataset (<2% relative to *rpoB*). For 2010 samples, *amoA* gene sequences that affiliated with *Thaumarchaeota* were more abundant in RBC 8 than RBC 1, whereas in 2016 they were more abundant in RBC 1 than RBC 8 samples (except in the NE 2016 samples) (Figure 3.8A). The raw HMM hits for AOA *amoA* genes were low (with only 64 hits to this HMM for all samples combined). Despite this, the pattern of *amoA* sequence abundance (normalized to *rpoB*) significantly correlated with the corresponding relative abundances determined via qPCR for the proportion of AOA 16S rRNA genes within the total community (Spearman's rank correlation, $p<0.01$).

The *amoA* HMM for AOB detected sequences of both comammox bacteria and AOB. The *amoA* that taxonomically assigned to *Nitrospira* are considered indicative of comammox bacteria. Overall, the relative abundances of these comammox-specific genes were higher in

RBC 1 than RBC 8 of the corresponding sample pairs in both years and dominated *amoA* genes in most sequenced metagenomes. In 2010, *Nitrosomonas* spp. (AOB) *amoA* sequences and *Nitrospira* spp. (comammox bacteria) *amoA* sequences were at roughly equal abundances, whereas *Nitrospira* was the dominant ammonia oxidizer detected in 2016 metagenomes (Figure 3.8B). The *rpoB* and bacterial *amoA* gene relative abundances for *Nitrospira* were consistent, suggesting that a majority of the *Nitrospira* present in the RBCs were likely affiliated with comammox bacteria. Across all samples, *amoA* gene sequences of comammox bacteria represented between ~5-30% of the total microbial community (as measured as relative to *rpoB* HMM hits). However, these proportions assumed that each comammox bacterium encoded one copy of the *amoA* gene. These relative abundance patterns for AOB ($p<0.001$) and comammox bacteria ($p<0.001$) *amoA* genes were significantly correlated to their corresponding relative abundances determined via qPCR for the proportion of their *amoA* genes within the total community.

The HMM search for *nxrB* showed that sequences affiliated with this gene were highly prevalent in the sequenced RBC biofilm community, with combined hits at over 50% abundance relative to *rpoB* (Figure 3.8C). Further evidence for *Nitrospira* dominance in the RBCs was the high relative abundance of *Nitrospira nxrB* genes. As with *rpoB*, *nxrB* genes of *Nitrospira* were the most abundant of any genus relative to *rpoB*. The relative abundances of *Nitrospira nxrB* genes were higher in RBC 1 than RBC 8 across all samples. The relative abundances of *nxrB* were higher than *rpoB* gene numbers because most *Nitrospira* spp. have multiple copies of *nxrB* (up to six copies) (Pester *et al.*, 2014), whereas *rpoB* is a single copy gene (Dahllof *et al.*, 2000).

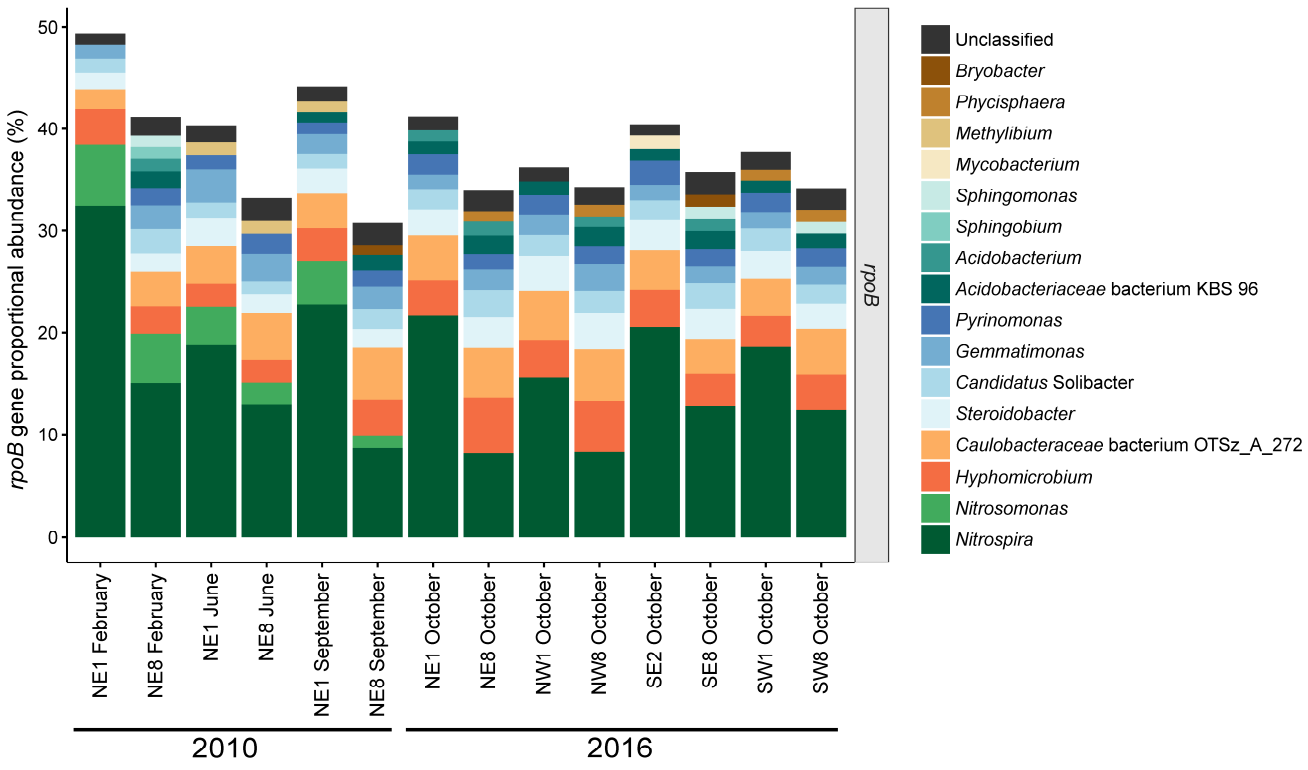

Figure 3.7 Taxonomic profiling of RBC microbial community by the hidden Markov model (HMM) for *rpoB* (RNA polymerase beta subunit). Stacked bars represent the relative abundance of unassembled *rpoB* metagenomic reads classified at the genus level. Genera shown are at greater than or equal to 1% relative abundance. Green shaded bars represent nitrifiers. NE, northeast train; NW, northwest train; SE, southeast train; SW, southwest train.

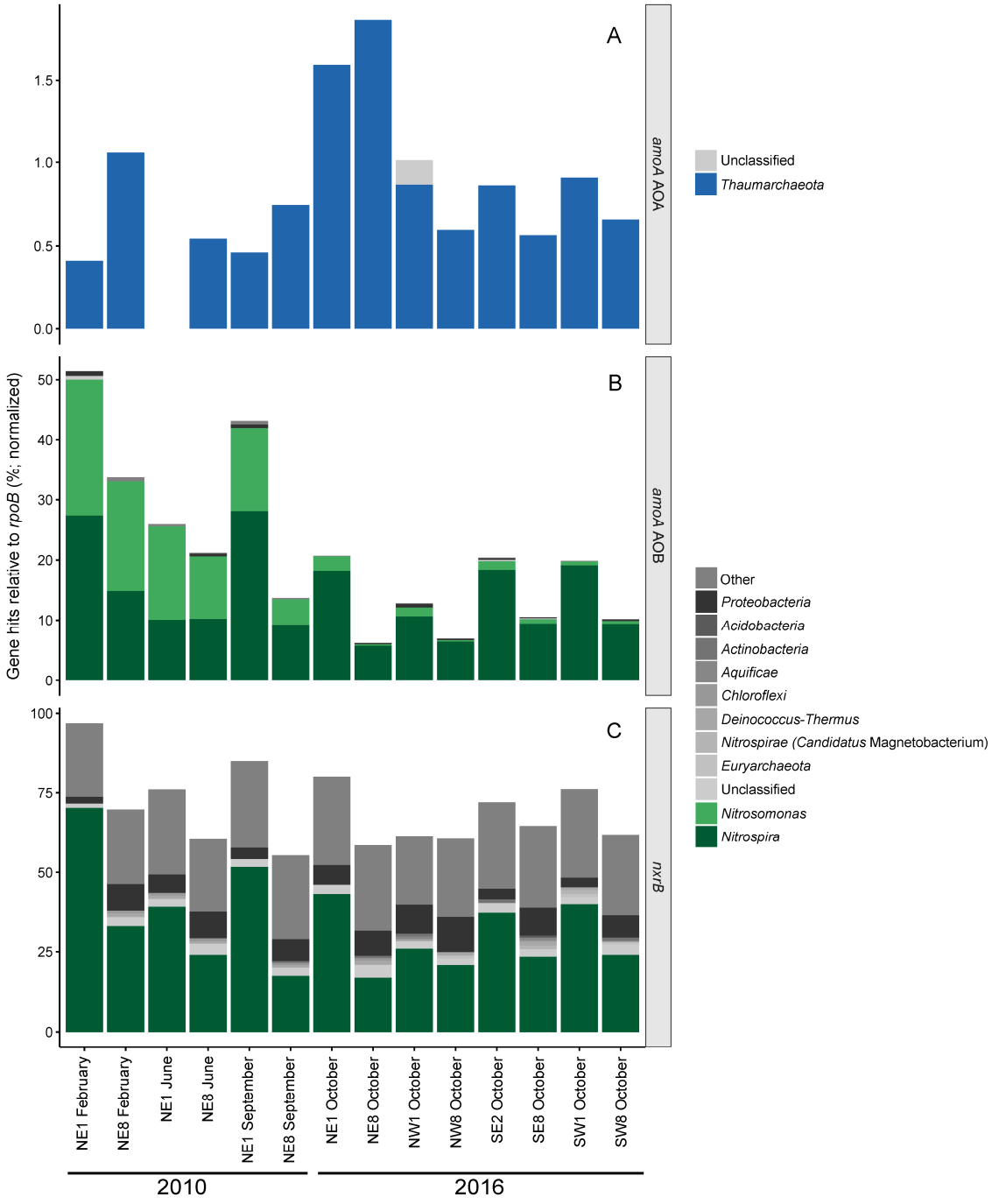

Figure 3.8 Functional gene profiling of nitrifiers in RBC microbial communities by hidden Markov models (HMMs). Stacked bars represent the relative abundance of functional genes from unassembled metagenomic reads, classified to the genus level (B, C) or phylum level

(A). Within each sample, length-normalized HMM hits for each functional gene were divided by the total number of length-normalized HMM hits for *rpoB*. Green and blue bars represent nitrifiers. Other taxa were classified to the genus level, but collapsed to the phylum level for clarity, and are shown in grey. (A) *amoA* gene of ammonia-oxidizing archaea. No HMM hits were found for sample NE1 June 2010. (B) *amoA* gene of ammonia-oxidizing bacteria and comammox bacteria. (C) *nxrB* gene of *Nitrospira*. Taxa shown are at greater than or equal to 1% relative abundance at the genus level relative to the HMM used. Taxa at less than 1% relative abundance are represented by the uppermost grey bar. *amoA*, ammonia monooxygenase subunit A gene; *nxrB*, nitrite oxidoreductase, NE, northeast train; NW, northwest train; SE, southeast train; SW, southwest train.

3.3.4 Metagenome bins

Several metagenomic bins classified as *Nitrospira* were obtained from multiple assembly attempts (Table 3.6). Assembly of the individual samples was performed first. Despite finding *Nitrospira amoA* genes in every sample using MetAnnotate, and despite annotating *Nitrospira amoA* genes on assembled contigs from every sample, *Nitrospira* bins containing *amoA* were not obtained from every sample. From individual assembly, 13 metagenomic bins were assigned to the family *Nitrospiraceae* and contained an *amoA* gene. Of these, four were high quality bins (i.e., ≥75% completeness, <25% contamination). Two of the high quality bins also contained both *nxrB* and *hao* genes. With communities being stable in composition, but changing in relative abundances across the RBCs, especially in the samples taken during the same year, co-assembly was attempted with different combinations of samples to recover high quality *Nitrospira* bins. It was expected that a co-assembly-based approach would yield better results than individual assembly because it would allow for the use of a differential abundance binning algorithm (MetaBAT; Kang *et al.*, 2015), which has been shown to produce high quality genome bins when the abundance of the species of interest varies across many samples. Out of the four different co-assembly attempts, only five *Nitrospira* bins containing *amoA* were recovered, and three were high quality bins. None of these bins contained *nxrB* genes. All bins with highest completeness and lowest

contamination, with genes for both ammonia oxidation and nitrite oxidation, were obtained from the individual assemblies rather than co-assemblies (Table 3.6).

Co-assembly and differential abundance binning yielded a *Thaumarchaeota* bin (Table A 1). Although individual assembly also yielded high quality *Thaumarchaeota* bins, a high quality bin (as described above) was not obtained for every sample. In contrast, a higher quality bin was obtained with every co-assembly combination tried. When all of these *Thaumarchaeota* genome bins were dereplicated using dRep, all were >99% similar to each other (Table A 1), indicating that there was one *Thaumarchaeota* species present in the RBCs, as shown previously (Sauder *et al.*, 2012, 2017). However, this *Thaumarchaeota* bin was not classified as the species enriched from the RBC biofilm, *Candidatus* Nitrosocosmicus exaquare. This is likely because the genome of *Ca.* N. exaquare is not in the RefSeq database, and CheckM uses NCBI taxonomy. Average nucleotide identity (ANI) analysis was done between the dereplicated AOA bin (CA-NE8-2010.39, Appendix A) and the *Ca.* N. exaquare genome (accession number CP017922.1) to confirm that the AOA detected were indeed *Ca.* N. exaquare. The AOA bin was 96.8% similar to the *Ca.* N. exaquare genome, indicating that via metagenomics, the same sole AOA species was detected as previously reported.

Bins assigned to the family *Nitrospiraceae* that did not contain *amoA* genes were also obtained from the assembly attempts. To determine which *Nitrospira* bins were the same across all assemblies and samples, dereplication was performed on all bins classified as *Nitrospira* using dRep (53 bins). Based on clustering and dereplication, 16 distinct populations of *Nitrospira* spp. (with an average nucleotide identity of greater than 99%) were present across all RBC samples (Figure 3.9). A winning genome bin was selected based on the corresponding dRep scores. This clustering also helped determine if *Nitrospira* bins without *amoA* were truly strict nitrite-oxidizing *Nitrospira*, or if the bins were incomplete. Seven of these *Nitrospira* bins (representing five different clusters) contained *amoA* genes. The dendrogram shows a distinct clade of *Nitrospira* bins that do not contain any *amoA* genes (clusters 1 through 5). Most of these bins were missing genes, with most missing the

nxrB gene characteristic of all known *Nitrospira*. The clade of clusters 8 through 14 are likely all comammox *Nitrospira,* because bins within this clade had an *amoA* gene. Not all of the *Nitrospira* bins in these clusters had *amoA*, but most likely the bins were incomplete. Clusters 6 and 7 could represent comammox bacteria because one bin in cluster 6, which was >90% complete with <5% contamination, contains an *amoA* gene. Altogether, the binning and dereplication process indicated that the *Nitrospira* community in the RBCs was composed of both comammox *Nitrospira* and strict nitrite-oxidizing *Nitrospira*. Most of these are likely comammox *Nitrospira,* as demonstrated above by the HMM searches on the unassembled reads.

There is further metagenomic evidence that these *amoA*-encoding *Nitrospira* are capable of complete ammonia oxidation. Comammox *Nitrospira* encode genes for ammonia oxidation (*amo, hao*) as well as nitrite oxidation (*nxr*) (van Kessel *et al.*, 2015; Daims *et al.*, 2015). Of the seven high quality (pre-dereplication) *Nitrospira* bins containing *amoA*, three of them also included a *nxrB* gene, indicating that these *Nitrospira* species are truly comammox bacteria, because they encode genes for both ammonia oxidation and nitrite oxidation. Two bins from the individual assembly attempt, NE8.001 and SNE8.002, contained *amoAB, hao*, and *nxrB* genes. These bins were nearly complete (92.2%) with low contamination (2.7%), and substantially complete (76.8%) with medium contamination (5.8%), respectively (Table 3.6). These bins also represent different comammox populations, as they were grouped into different clusters by dRep. The *nxrB* gene was misannotated by Prokka as *ddhB,* and so MetAnnotate was used to search for the *nxrB* HMM on the assembled contigs. The *nxrA* gene was not searched for. In bin NE8.001, the *amoAB* and *hao* genes were on the same contig. This provided evidence that these genes for ammonia oxidation are found in the same organism in the same genomic area, and their co-occurrence is not simply due to a binning error. In some comammox *Nitrospira* genomes, these genes are found in the same genomic region (van Kessel *et al.*, 2015). A *cycA* gene (cytochrome c554) was also found on the same contig as *amoAB* and *hao*, consistent with published comammox genomes showing that the *cycAB* genes are found next to *hao*. In bin SNE8.002,

the *amoAB* and *hao* genes were not on the same contig, but the level of contamination calculated by CheckM (only 5.8%) indicates that these different contigs are likely not binned together incorrectly. The contig containing *hao* in this bin also contains the *ccmH* and *ccmF* genes (for cytochrome c biogenesis), which are only found near *hao* in comammox *Nitrospira*, not in AOB (van Kessel *et al.*, 2015; Daims *et al.*, 2015). The *nxrB* genes were not located on the same contig as the genes for ammonia oxidation in either of these bins. This is not surprising, given that the genes for ammonia oxidation and nitrite oxidation are not located in the same genomic area (van Kessel *et al.*, 2015; Daims *et al.*, 2015).

The seven high-quality *Nitrospira* bins containing *amoA* were compared to each other, to cultivated comammox species, and to nitrite-oxidizing *Nitrospira* using ANI analysis (Table 3.7). The similarity of the bins to each other matched the dRep cut-off thresholds for clustering, indicating the robustness of the dereplication process. All of these comammox bins were less than 95% similar to any of the cultivated comammox bacterial genomes, as well as the NOB genomes, indicating that these bins represent species separate from these cultivated ones.

Table 3.6 Summary of dereplicated high quality *Nitrospira* bins (≥75% completion, <25% contamination). Bins included were winning genomes for their cluster, as determined by dRep.

	SW1.007	CA-NE8-2010.42	Upper-2016.254	JNE1.001	CA-NE1-2010.95	CA-NE8-2010.148	Upper-2016.235	NW1.001	SNE8.002	SE8.002	SW.74	NE8.001	CA-NE8-2010.156	CA-NE8-2010.193	CA-NE8-2010.35	SW1.001
Completeness (%)	94.0	92.2	86.8	78.0	87.3	79.7	75.6	89.9	76.8	91.4	78.1	92.2	96.8	87.0	95.9	87.8
Contamination (%)	1.9	0.9	1.1	4.6	1.6	1.3	4.4	2.8	5.8	21.6	2.3	2.7	2.7	5.8	3.8	4.0
dRep cluster	1_1	2_1	3_1	4_0	5_0	6_1	7_0	8_1	8_2	8_3	9_1	10_1	11_1	12_1	13_1	14_1
Genome size (Mbp)	4.1	4.0	3.0	2.9	3.7	2.4	4.7	3.0	2.5	5.2	2.6	4.0	4.4	4.1	3.9	3.4
Bin N50	24075	125286	8041	8005	9186	5233	17866	13033	8324	23758	5942	26973	48920	18888	117006	12389
GC content (%)	49.8	59.5	58.8	58.9	58.6	55.3	59.2	55.1	54.5	57.9	54.4	54.9	54.4	55.1	54.9	55.2
amoA	-	-	-	-	-	-	-	+	+	-	-	+	-	+	-	-
amoB	-	-	-	-	-	-	-	+	+	-	-	+	+	+	+	+
amoC	-	-	-	-	-	-	-	-	-	-	-	-	-	-	-	-
amt	-	-	-	-	-	-	-	+	-	-	+	+	+	+	+	+
hao	-	-	-	-	-	-	-	+	+	+	+	+	+	+	+	+
nxrB	-	-	-	-	+	-	-	-	+	+	-	+	-	-	+	-
ure	-	-	+	-	-	+/-	+	+	+	+/-	+	+	+	+	+	+
ccm	-	-	-	-	-	+	-	+	+	+	+	+	+	+	+	+
cyc	-	-	-	-	-	-	-	+	-	-	-	+	+	+	+	+
rpoB	+	+	+	+	-	+	-	-	+	+	+	+	+	-	+	+
hyb	+/-	-	+/-	-	-	-	+/-	+/-	+/-	-	-	+/-	+/-	+/-	-	-
hyd	-	-	-	-	-	-	-	-	-	-	-	-	-	-	-	-
hyp	+/-	-	+/-	-	-	+/-	+/-	+/-	+/-	+/-	-	+/-	+/-	+/-	-	-
fdh	-	-	+	-	-	-	-	-	-	+	-	-	-	-	-	-
cynS	+	+	+	+	+	-	+	-	-	+	-	-	-	-	+	-

+/- indicates only some of the subunits are present

amo, ammonia monooxygenase; *amt*, ammonia transporter; *hao,* hydroxylamine oxidoreductase; *nxrB*, nitrite oxidoreductase; *ure*, urease; *ccm*, cytochrome c biogenesis; *cyc*, cytochrome c; *rpoB, RNA polymerase; hyb* and *hyd*, group 3 [Ni-Fe] sulfur-reducing hydrogenase; *hyp*, hydrogenase accessory protein; *fdh*, formate dehydrogenase; *cyn*, cyanate hydratase

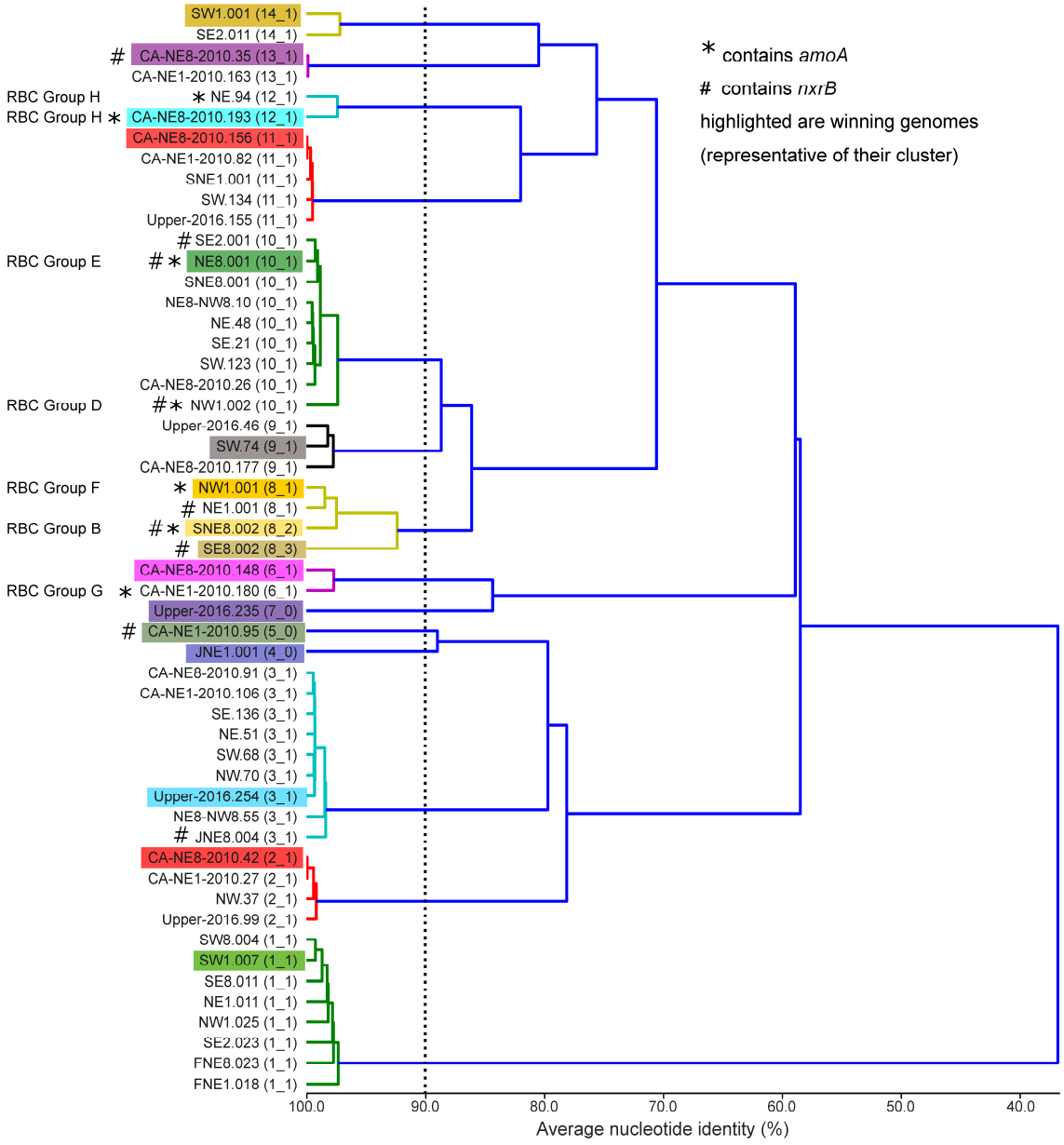

Figure 3.9 Metagenome bin clustering dendrogram for *Nitrospira* bins. Bins classified as *Nitrospira* were dereplicated using dRep. Bins included in dereplication were at least 75% complete and had less than 25% contamination. Primary clusters were built at 90% similarity, and secondary clusters refined these primary clusters at 99% similarity. Dendrogram was generated as dRep output. RBC Groups corresponding to AmoA phylogeny are also indicated for each bin containing an *amoA* gene.

Table 3.7 ANI analysis of high quality *amoA*-containing *Nitrospira* bins.

	SNE8.002	CA-NE1-2010.180	CA-NE8-2010.193	NE.94	NE8.001	NW1.001	NW1.002	*Ca.* Nitrospira nitrificans	*Ca.* Nitrospira nitrosa	*Ca.* Nitrospira inopinata	*Nitrospira defluvii*	*Nitrospira moscoviensis*
SNE8.002	*	83.7 [18.9]	83.9 [5.1]	84.1 [4.1]	89.2 [72.0]	99.0 [75.0]	88.7 [56.3]	84.1 [11.4]	83.8 [4.3]	85.0 [1.6]	84.3 [0.5]	83.1 [0.8]
CA-NE1-2010.180	83.7 [12.1]	*	84.5 [4.3]	85.6 [2.6]	83.4 [18.9]	83.7 [14.5]	83.9 [14.0]	83.2 [5.6]	83.5 [4.4]	85.1 [0.8]	83.0 [0.2]	83.1 [0.7]
CA-NE8-2010.193	83.9 [3.3]	84.5 [4.1]	*	99.4 [54.5]	83.9 [4.6]	83.7 [4.1]	84.0 [3.9]	83.7 [7.2]	86.9 [56.2]	84.5 [0.8]	85.2 [0.4]	82.7 [0.8]
NE.94	84.1 [3.7]	85.6 [3.6]	99.4 [79.9]	*	84.2 [4.7]	84.5 [5.7]	84.0 [4.3]	83.1 [7.0]	87.3 [58.3]	83.6 [0.4]	88.4 [1.9]	82.0 [0.9]
NE8.001	89.2 [45.2]	83.4 [18.7]	83.9 [4.7]	84.2 [3.3]	*	87.8 [47.9]	99.3 [68.2]	84.2 [13.6]	83.3 [4.5]	84.0 [1.0]	85.5 [0.7]	82.9 [1.2]
NW1.001	99.0 [63.7]	83.7 [19.5]	83.7 [5.5]	84.5 [5.4]	87.8 [65.1]	*	87.1 [47.0]	84.0 [11.5]	83.3 [4.5]	83.2 [1.1]	90.0 [1.3]	83.2 [1.1]
NW1.002	88.7 [34.4]	83.9 [13.3]	84.0 [4.0]	84.0 [2.9]	99.3 [67.5]	87.1 [33.6]	*	84.0 [10.0]	83.8 [3.2]	84.7 [0.9]	88.9 [6.2]	83.1 [0.9]
Ca. Nitrospira nitrificans	84.1 [6.8]	83.2 [5.6]	83.7 [7.2]	83.1 [4.8]	84.2 [13.3]	84.1 [8.2]	84.1 [10.0]	*	83.7 [8.9]	84.4 [2.2]	85.1 [0.9]	83.4 [2.6]
Ca. Nitrospira nitrosa	83.8 [2.6]	83.5 [3.9]	86.9 [52.3]	87.3 [36.6]	83.3 [4.2]	83.3 [3.1]	83.7 [3.1]	83.7 [8.0]	*	86.7 [1.1]	86.4 [0.6]	84.2 [0.9]
Ca. Nitrospira inopinata	85.0 [1.2]	85.1 [0.9]	84.2 [1.0]	83.1 [0.4]	84.0 [1.3]	83.2 [1.0]	84.7 [1.1]	84.4 [2.8]	86.7 [1.5]	*	86.3 [0.5]	83.0 [3.2]
Nitrospira defluvii	84.3 [0.3]	83.0 [0.2]	85.2 [0.4]	88.4 [1.2]	85.5 [0.7]	90.0 [0.9]	88.9 [4.6]	85.3 [0.7]	86.4 [0.6]	86.3 [0.4]	*	83.1 [2.0]
Nitrospira moscoviensis	83.1 [0.5]	83.1 [0.8]	82.7 [0.9]	82.0 [0.6]	82.9 [1.3]	83.2 [0.9]	83.2 [0.8]	83.3 [2.2]	84.2 [1.2]	83.0 [2.4]	83.1 [2.2]	*

Value in brackets indicates the percentage aligned

Identities >95% are highlighted in red

3.3.5 Phylogenetic analysis

From all assembly attempts, there were a total of 71 *amoA* gene sequences belonging to *Nitrospira* obtained from the assembled contigs. Of these, 19 were placed into bins (Table 3.8). One bin, SW8.001, had two *amoA* genes, whereas the rest had only one copy. High quality bins were analyzed by dRep and there were seven *amoA*-containing bins in total, as described above. The RBC groups with AmoA sequences belonging to one of these high-quality bins are indicated by an asterisk on the phylogenetic tree (Figure 3.10).

Although all sequenced *amoA* genes of *Nitrospira* spp. belonged to comammox clade A (Figure 3.10), our bin data suggest multiple distinct populations of *amoA*-containing comammox *Nitrospira* in the RBCs. There were up to 13 distinct groups of comammox *Nitrospira* according to *amoA* DNA sequence identity (Table 3.8, Figure 3.10), although it is possible that closely related sequences represent the same population. For example, the *amoA* sequences belonging to RBC groups E and D were assigned to separate bins, but after dereplication these bins were assigned to the same cluster (10_1). Therefore, based on *amoA* amino acid sequence identity and the average nucleotide identity of the bins they belong to, RBC groups E and D likely represent the same microorganism. In contrast, RBC groups F and B have differing *amoA* DNA and amino acid sequences but are closely related in terms of AmoA phylogeny. Both groups have higher quality bins that were dereplicated into closely related genome clusters (8_1 and 8_2 respectively). This indicates congruency between AmoA phylogeny and bin average nucleotide identity and suggests that comammox species in groups F and B are closely related but unique populations of comammox bacteria.

A majority of detected *amoA* gene sequences (RBC groups B, C, D, E, F, I, L, and M) clustered with uncultivated comammox species from a metagenomic survey of water treatment systems (Wang *et al.*, 2017) and a rice paddy soil from China (Genbank accession AKD44274). The other RBC groups clustered more closely with cultivated species of

comammox bacteria or uncultivated comammox species detected from other environments, including drinking water systems and another WWTP.

Table 3.8 All RBC *Nitrospira amoA* sequence groups, based on 99% similarity DNA clustering.

RBC group	*amoA* sequences	Placed in a bin*
A	1	0
B	12	3
C	4	0
D	5	4
E	14	4
F	1	1
G	4	1
H	13	2
I	3	1
J	6	1
K	4	1
L	3	1
M	1	0
Total	71	19

* placed in a *Nitrospira* bin, regardless of bin quality

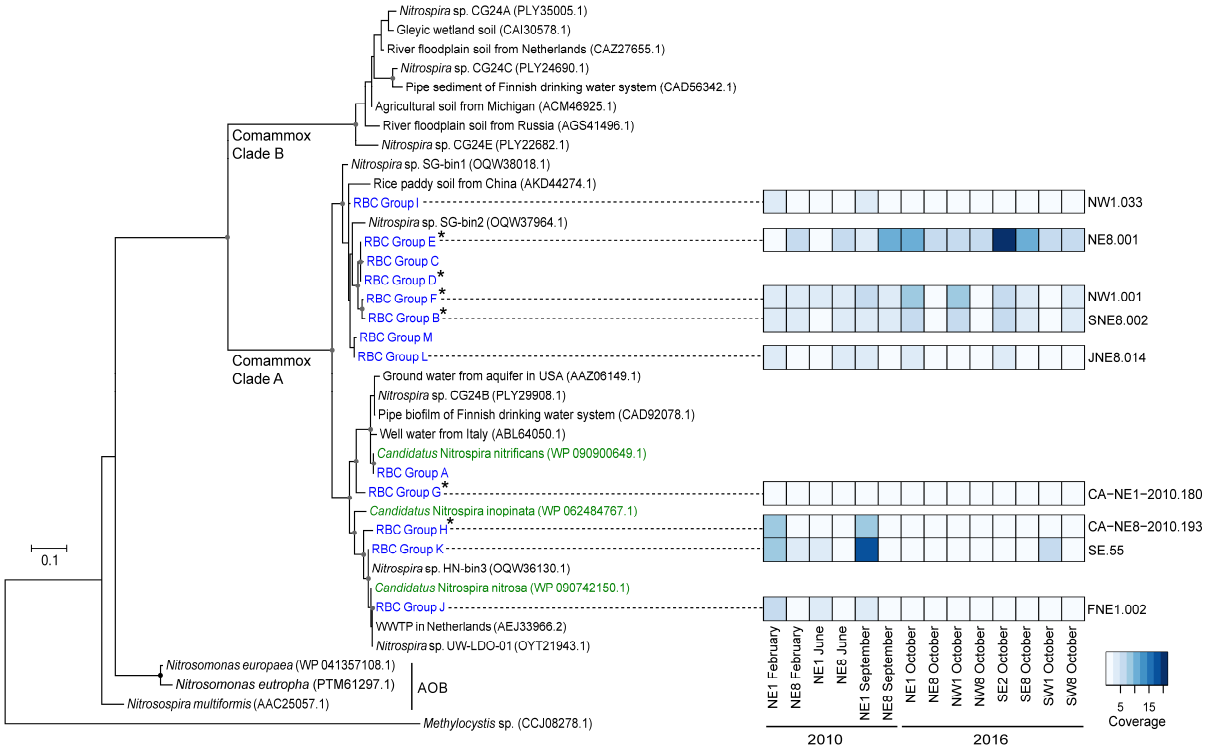

Figure 3.10 Phylogeny of *Nitrospira* AmoA sequences, and average coverage of *amoA*-containing *Nitrospira* bins across samples. The *Nitrospira amoA* genes were from assembled contigs of all assembly combinations, and translated amino acid sequences were used to build an alignment using Muscle (Edgar, 2004). Phylogenetic analysis of *Nitrospira* AmoA was inferred using maximum likelihood analysis based on the Le Gascuel evolutionary model (Le and Gascuel, 2008). Bootstrap values are based on 500 replicates, and those over 60% are shown and indicated with a grey dot, those at 100% are shown with a black dot. The tree is drawn to scale, with branch lengths measured in the number of amino acid substitutions per site. The tree was made using MEGA7 (Kumar *et al.*, 2016). The AmoA sequences from RBCs were grouped according to 99% identity at the DNA level and are shown in blue. Cultivated comammox species are shown in green. Comammox AmoA sequences from environmental surveys are shown in black. *Methylocystis* sp. PmoA was used as an outgroup. The * indicate bins that are ≥75% complete and have <25% contamination which contain the indicated RBC *amoA* group. Reads from each sample were mapped to each individual bin, and average coverage of the bins within each sample is depicted in the heatmap.

3.3.6 Comammox bacteria bin abundances

The abundances of representative comammox bacteria bins were analyzed by read mapping unassembled reads to the individual *Nitrospira* bins. Average coverage for each bin was calculated and used as a measure of abundance for each bin across the samples. Bins NW1.001 and SNE1.002, which contained *amoA* genes corresponding the RBC Groups F and B, respectively, showed similar abundance trends across the RBC samples (Figure 3.11). Bin NE8.001, which contained the *amoA* gene corresponding the RBC Group E, also showed similar abundance patterns to these bins. All three of these bins represent closely related RBC groups, according to AmoA phylogeny (Figure 3.10). Across all samples, these bins also appeared to be the most abundant (as measured by average bin coverage), and NE8.001 represented the most abundant population of comammox in 2016. Several phylogenetically distinct populations displayed similar abundance trends, as NW1.033 clustered with FNE1.002, CA-NE8-2010.193, and SE.55. The latter three were closely related to each other and to cultivated comammox bacteria species, but NW1.033 was not. Likewise, bins JNE8.014 and CA-NE1-210.180 also had similar abundance patterns, and these are also not closely related populations. Bin CA-NE1-210.180 was detected at very low abundance across all samples. Multiple comammox populations were found in the same RBC. This high strain heterogeneity of comammox bacteria contrasts the AOA diversity (only one species) in the RBCs. Compared to AOA, comammox bacteria of the RBCs were much more diverse.

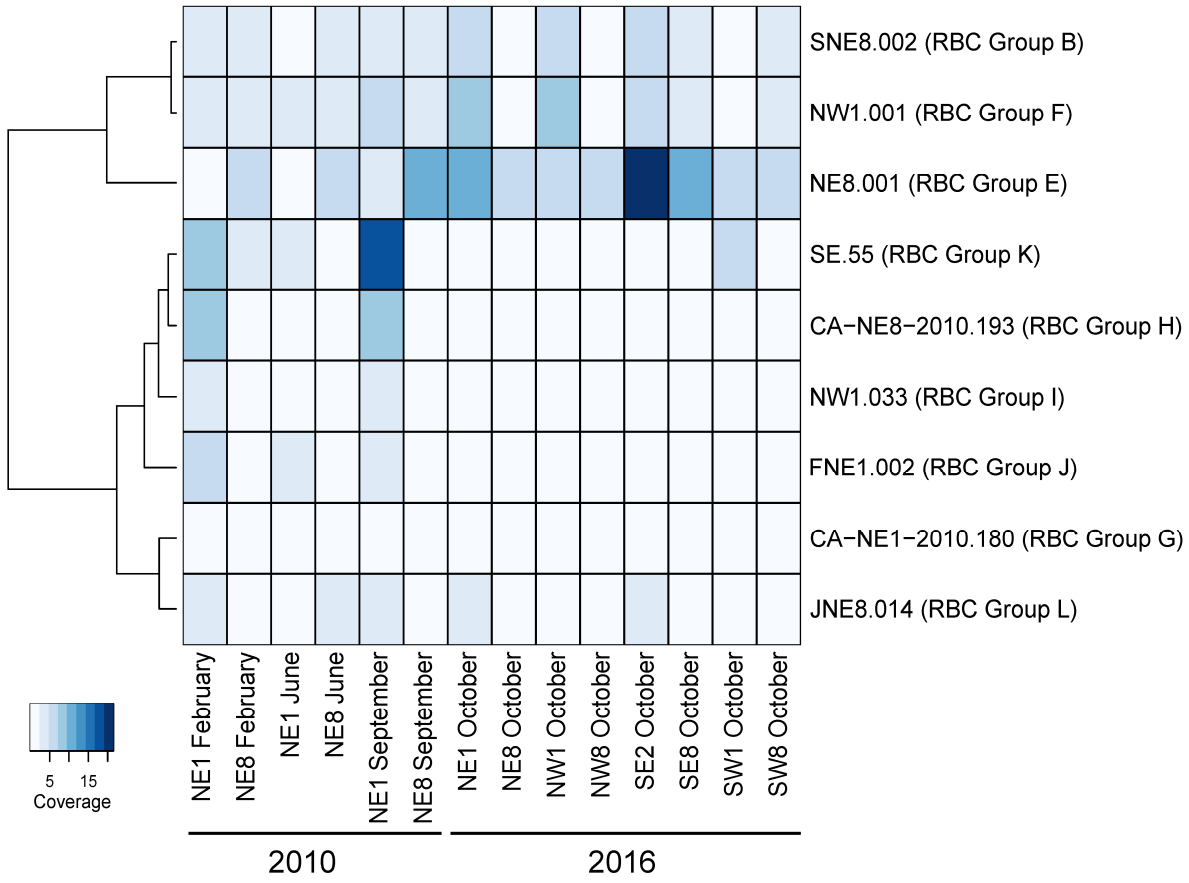

Figure 3.11 Hierarchical clustering of bin coverage across RBC samples. Reads from each sample were mapped to each individual representative *amoA*-containing *Nitrospira* bin and average coverage of the bin within each sample was calculated. Hierarchical clustering was calculated using the Pearson correlation coefficient distance measure.

3.4 Discussion

Taken together, metagenomic and qPCR data indicated that *amoA*-containing *Nitrospira* (comammox bacteria) were the dominant ammonia oxidizers in the RBC biofilm (Figure 3.5, Figure 3.8). This study is the first time comammox have been reported as dominant ammonia oxidizers in a WWTP. Due to their recent discovery (Daims *et al.*, 2015;

van Kessel *et al.*, 2015), comammox bacteria were never previously investigated within the Guelph WWTP. The qPCR data indicated that the comammox bacteria *amoA* genes made up over 50% of all ammonia-oxidizing prokaryote genes in most samples, although multiple gene copies were not accounted for in the calculations (Table 3.5). In terms of the proportion of the total community, comammox bacteria genes ranged from around 2% to almost 20%. Based on metagenomic data, comammox bacteria genes comprised ~5-30% of the total microbial community. The difference between the two methods can be attributed to the different genome copy numbers of genes used to assess the total microbial community, as well as limitations of the methods themselves, such as primer biases and HMM specificity. Nonetheless, these data offer strong evidence supporting comammox bacteria as the dominant ammonia oxidizers in the RBCs. This is in contrast to other studies on full-scale activated sludge WWTPs that found comammox at a lower abundance than AOA and AOB (Pjevac *et al.*, 2017; Chao *et al.*, 2016; Fan *et al.*, 2017). At the Guelph WWTP, the RBCs are located downstream of the aeration basin (activated sludge) secondary treatment system. The RBCs provide a larger solid surface for biofilm attachment, and the water contains lower concentrations of ammonia, compared to the aeration basins. Given the predicted low ammonia niche for comammox bacteria (Costa *et al.*, 2006; Daims *et al.*, 2015), and their biofilm growth, it is likely that the RBCs provide a better environment for the comammox bacteria, compared to aeration basins. The ammonia concentrations measured in the Guelph RBCs are around two orders of magnitude lower than at the top of the aeration basins. In the study by Fan *et al.* (2017), the ammonia concentrations ranged from 12 to 51 mg/L NH_4^+-N across the sampling period, which is comparable to the ammonia concentrations in the Guelph aeration basins. This may explain why comammox bacteria have not been found in high abundance in studies of full scale WWTPs, because those studies looked at systems with higher ammonia levels. A future study on the abundance of all three types of ammonia-oxidizing prokaryotes in the aeration basins of the Guelph WWTP could help determine if the RBCs provide an optimal environment for growth, compared to the aeration basins. Finding evidence for comammox bacteria in the RBCs, especially at high abundances, is

important because it suggests a correspondingly important role for nitrification by comammox bacteria in the RBCs.

High abundances of comammox bacteria were reported for other engineered environments with low ammonia levels, such as drinking water systems. Shortly after the discovery of comammox bacteria, these bacteria were found in a drinking water treatment plant via metagenomics (Pinto *et al.*, 2015). Moreover, comammox bacteria were widely distributed in drinking water distribution systems (Wang *et al.*, 2017), and they were more abundant than other ammonia oxidizers in a groundwater well studied by Pjevac *et al.* (2017). In drinking water treatment plants, comammox bacteria were found to be the most abundant nitrifier in groundwater fed rapid sand filters (Fowler *et al.*, 2018). In those filters, clade B comammox bacteria were the dominant type of comammox, in contrast to the comammox bacteria detected in the Guelph RBCs. Another engineered environment comparable to the RBCs is an aquaculture system. Recirculating aquaculture system biofilters use similar strategies to WWTPs. A study on the filters in these systems found that comammox were more abundant than AOA and AOB (Bartleme *et al.*, 2017). Along with these other studies, the dominance of comammox bacteria in the RBCs suggests that these engineered environments with low ammonia concentrations are environments where comammox bacteria thrive.

Given the phylogenetic diversity of *Nitrospira amoA* genes, and the diversity of the comammox *Nitrospira* bins, it is clear that multiple unique populations of comammox bacteria can be found in the RBC biofilm (Figure 3.9, Figure 3.10). These comammox bacteria all belong to comammox clade A, which is consistent with other studies reporting comammox in WWTPs (Pjevac *et al.*, 2017; Chao *et al.*, 2016). Multiple populations of comammox within the same WWTP have been reported previously (Pjevac *et al.*, 2017), but the potential diversity of comammox in the RBCs (Figure 3.10) is much higher than what was found in other WWTPs. Several populations of comammox were present in the same RBC, suggesting that in the environment of the RBCs, these comammox bacteria have adapted to co-exist, likely occupying separate niches. Over time, niche partitioning occurs as

species evolve, as seen in *Escherichia coli* after 765 generations (Helling *et al.*, 1987). The comammox bacteria may not directly compete because they are in separate niches within the RBCs, for example, in microenvironments with different oxygen concentrations within the biofilm. Several closely related comammox bins had correlating abundance patterns (e.g. NW1.001 and SNE8.002; Figure 3.11). It could be that these bins represent the same species, and therefore reads mapped equally as well to each bin. Or these could be closely related strains of comammox bacteria that have similar abundance patterns.

Two phylogenetically distinct clades of comammox bacteria were apparent in the RBCs (Figure 3.10). One of these clades (Groups A, G, H, K, and J) is related to the cultivated species of comammox bacteria. The other clade (Groups I, E, C, D, F, B, M, and L) has no cultured representative, indicating high novelty. The AmoA sequences that are closely related to these sequences are found in metagenomes of a drinking water system (Wang *et al.*, 2017) and a PCR clone from a rice paddy (Genbank accession AKD44274). This clade would be an ideal target for cultivation of comammox bacteria from the RBCs because it is unique from all the species of comammox bacteria cultivated so far. Comparisons of the high quality comammox bins to cultivated comammox genomes shows low similarity (Table 3.7), which is further evidence that at least some of the comammox bacteria in the RBC represent novel species. This high strain heterogeneity is likely why the co-assembly did not yield many *Nitrospira* bins with *amoA* (Table 3.6). Although *amoA* genes belonging to *Nitrospira* were co-assembled and annotated, most were not placed into bins. Indeed, the presence of multiple different strains of the same species has been noted to negatively affect the quality of assembly and binning, often causing a more fragmented assembly, particularly in regions of high strain level variation (Sczyrba *et al.*, 2017; Olm *et al.*, 2017).

It should be noted that the presence of comammox bacteria is based on *amoA* genes classified as belonging to *Nitrospira*. Based on current knowledge of comammox bacteria, all cultivated species of *Nitrospira* that encode *amoA* genes are capable of complete ammonia oxidation (van Kessel *et al.*, 2015; Daims *et al.*, 2015). Further evidence of complete

ammonia oxidation metabolism in the *Nitrospira* of the RBCs is demonstrated by finding genes for both ammonia oxidation and nitrite oxidation in the same genome (Table 3.6). The *amoA* phylogeny (Figure 3.10) matched the bin clustering and dereplication analysis (Figure 3.9), with closely related *amoA* sequences belonging to closely related bins (e.g. RBC groups F and B belong in clusters 8_1 and 8_2, respectively). The congruency between these two methods is strong evidence supporting strain heterogeneity for comammox bacteria in the RBCs.

Although comammox bacteria were numerically dominant, it is unclear whether they also contributed the most to nitrification in the RBCs. Cultivation experiments with differential inhibitors will help determine the contributions of each ammonia oxidizer present. However, currently no inhibitor specific to comammox bacteria has been reported. Enrichment and isolation of the comammox strains will also be important to confirm that these organisms are capable of complete ammonia oxidation and to assess possible alternate metabolisms.

All clade A comammox bacteria described so far possess genes for urease (van Kessel *et al.*, 2015; Daims *et al.*, 2015; Palomo *et al.*, 2018; Lawson and Lücker, 2018). Furthermore, comammox bacteria enrichment cultures have been shown to use urea (Daims *et al.*, 2015; van Kessel *et al.*, 2015). An almost complete *ure* operon was annotated on a contig in several *amoA*-containing *Nitrospira* bins (Table 3.6). This suggests that these comammox bacteria of the RBCs are capable of hydrolyzing urea to ammonia, using this as an ammonia source for nitrification. Only strict NOB *Nitrospira* and clade B comammox bacteria possess the *fdh* genes for formate dehydrogenase, whereas clade A comammox bacteria do not (Palomo *et al.*, 2018). Consistent with these findings, the *Nitrospira amoA*-containing bins in the current study also did not contain any *fdh* genes, indicating they likely cannot use formate as an alternative electron donor. The comammox bins did not contain any of the genes for the group 3b [Ni-Fe] sulfur reducing hydrogenase (*hydBGDA* and *hybD*) described previously (Camejo *et al.*, 2017; Palomo *et al.*, 2018), but they did contain several *hyp* genes and a *hybG* gene, which are accessory genes involved in the maturation and

processing of hydrogenase enzymes. This suggests that these comammox species likely either lost the genes for hydrogenases, or that these genes were missing from the assembly and/or annotation.

These comammox bacteria, although numerically dominant, were not the sole nitrifiers present in the RBC biofilm. Both HMM search data and qPCR data indicated that AOA, AOB, and comammox bacteria were present. Additionally, dereplication of the *Nitrospira* bins indicated that some of these bins were strict NOB, and some were comammox bacteria. These comammox bacteria were diverse, and the AOB population, consisting of *Nitrosomonas* spp., was less diverse (Table A 1). Only one species of AOA, the previously described *Candidatus* Nitrosocosmicus exaquare (Sauder *et al.*, 2017), was present (Table A 1). Even in the relatively low ammonia environment of the RBCs, all three types of ammonia oxidizers appear to co-exist in the RBC biofilm. Although some studies have found all three ammonia oxidizers in wastewater treatment systems (Fan *et al.*, 2018, 2017; Camejo *et al.*, 2017), and others have found only AOB and comammox bacteria in WWTPs (Annavajhala *et al.*, 2018; Gonzalez-Martinez *et al.*, 2016; Chao *et al.*, 2016), little is known about the co-occurrence of ammonia oxidizers in tertiary wastewater treatment systems. This study of the Guelph WWTP RBCs is the first to look at presence and abundance of all three ammonia-oxidizing prokaryotes in a tertiary treatment system of a municipal WWTP.

The consistency in the overall microbial community, as well as the ammonia oxidizing community, between the 2010 timepoints indicated that the communities were stable (Figure 3.7, Figure 3.8). Distinct abundance patterns of taxa were observed in RBC 1 compared to RBC 8 across all 2010 timepoints. Though these patterns shifted in 2016 (e.g. AOA abundance patterns), trends were seen consistently across all trains for the respective RBC (e.g., higher relative abundance of comammox *Nitrospira* in RBC 1 than 8). These patterns imply a relationship between the environmental conditions of the RBCs and the microbial ammonia-oxidizing community.

Comammox bacteria were predicted to have higher abundances in RBC 8 than RBC 1 due to the predicted low ammonia niche of comammox bacteria (Costa *et al.*, 2006). For both years tested in this study, the relative abundances of *Nitrospira amoA* genes were higher in RBC 1 than RBC 8 of the same train. This was demonstrated in both the qPCR (Figure 3.5, Table 3.5) and metagenomic sequencing data (Figure 3.8B). The ammonia levels in the first RBCs were already relatively low (<18 μM for the 2016 samples, Figure 3.2), and it may be that the ammonia concentrations at the end of the train (<4 μM) were below the optimum for these comammox species. The ammonia affinity of only one comammox species (*Ca.* Nitrospira inopinata) has been determined so far, and it has one of the highest reported affinities of all ammonia oxidizers (reported $K_{m(app)}$ of 0.65 to 1.1 μM total ammonium) (Kits *et al.*, 2017). The affinity of the RBC comammox bacteria is unknown, but given their higher abundance in RBC 1 than RBC 8, they may prefer higher ammonia concentrations than *Ca.* N. inopinata, and have a lower affinity for ammonia (higher K_m). Other factors that likely also lead to the differences in relative abundances of comammox bacteria across RBCs could include oxygen requirements, growth rates, growth yields, and biofilm formation capabilities (Lawson and Lücker, 2018). Cultivation of the comammox species from biofilms, as well as microcosm experiments, will help determine factors that influence comammox abundance and activity in these RBCs.

Given previous research showing that the abundance of AOA increases towards RBC 8 (Sauder *et al.*, 2012), I predicted that abundances of AOA would be higher in RBC 8 than RBC 1 in the current study. Indeed, the observed pattern of AOA *amoA* abundances for 2010 samples analyzed in this study were consistent with previous data, and this trend was consistent using both an archaeal *amoA* HMM search on the metagenomic reads and qPCR detection of the 16S rRNA gene of Thaumarchaeota. In contrast to 2010 samples, in 2016 AOA were at a lower relative abundance in RBC 8 compared to RBC 1 (Figure 3.5), which was confirmed by the metagenomic data (Figure 3.8A). This indicates that a change in the RBC environment occurred, leading to the shift in AOA abundance. Cleaning of all RBC trains occurred in 2014 and samples taken in December 2015, after RBC cleaning and

biofilm regeneration had taken place, indicated that there was a higher relative abundance of AOA 16S rRNA genes in RBC 1 than RBC 8 (Sauder *et al.*, 2017). Combined with lower overall ammonia concentrations in the tertiary treatment system in recent years (e.g., 0.31 mg/L NH_3-N in 2016, 1.14 mg/L NH_3-N in 2011, which are equivalent to 22.13 µM and 81.39 µM NH_3-N, respectively; Figure 3.3), both a microbial community disturbance and lower incoming ammonia concentrations would have influenced the established biofilm community sampled in 2016. The abundances of AOB also shifted between 2010 and 2016. Despite differences between qPCR (Figure 3.5) and metagenomic data (Figure 3.8B) for AOB *amoA* abundance relative to *Nitrospira*, both methods indicated a decrease in AOB *amoA* relative abundance in the 2016 samples, compared to 2010. It is likely that AOB, like the AOA, were also affected by the decrease in ammonia concentrations entering the RBCs and/or the RBC cleaning. The decreased ammonia levels entering the RBCs in 2016 would mean that ammonia oxidizers with a higher ammonia affinity would dominate, outcompeting those with a lower ammonia affinity like AOB. The abundances of comammox *Nitrospira* did not drastically shift like those of the AOA and AOB, indicating that they were not affected the same way by the environmental changes that occurred between 2010 and 2016. This suggests that the factors that drive AOA, AOB, and comammox abundance and diversity are different, indicating that these groups of ammonia oxidizers occupy distinct niches within the RBC biofilm environment.

This was the first study to report comammox bacteria as the dominant ammonia oxidizer in a WWTP and is also the first to look for comammox bacteria in a tertiary wastewater system. These comammox bacteria exhibited a high level of strain heterogeneity, with some populations displaying similar abundance trends across samples. Even though these highly abundant *Nitrospira* were considered comammox based on the presence of the *amoA* gene, there is further genetic evidence that these presumed comammox *Nitrospira* were indeed capable of complete ammonia oxidation. They encoded genes for both ammonia and nitrite oxidation, as well as other genes typical of comammox *Nitrospira*. Cultivation of

these *Nitrospira* will be needed to demonstrate that they do carry out complete ammonia oxidation.

The comammox bacteria co-existed with the AOA species *Ca.* N. exaquare, and AOB species in the RBC biofilm. These nitrifiers displayed distinct abundance differences between RBCs within the same train, and these different ammonia oxidizers were affected differently by environmental changes that occurred between 2010 and 2016. The comammox *Nitrospira amoA* genes were consistently more abundant in RBC 1 compared to RBC 8, and their abundances were relatively stable between the sampling years. These RBCs are an ideal system to study the ecology of comammox bacteria and other nitrifiers. Low levels of ammonia in the effluent of the WWTP are essential because the receiving water for the Guelph WWTP is a relatively small river (i.e., Speed River). Understanding the microorganisms that are present and what they are potentially doing is an important step towards understanding the microbial contributions to nitrification in these RBCs and may eventually help guide operational practices for improved effluent quality.

Chapter 4 Conclusions and future directions

4.1 Summary

An important goal of microbial ecology is to characterize microbially mediated processes, and a critical prerequisite for this is to characterize microorganisms and their encoded functions within Earth's many environments. This goal is particularly important for WWTPs, where microorganisms involved in nitrification are critical for maintaining the sustainability of receiving water ecosystems. The aim of this research was to contribute to the understanding of ammonia oxidation within the RBCs of the Guelph WWTP. Low ammonia concentrations within these effluents are important because the associated Speed River is a relatively small river. This work represents an important step toward understanding the microbial contributions to nitrification in these systems and may in future help inform WWTP design and management practices for improved effluent quality.

Although most characterized aerobic nitrifiers are chemolithoautotrophic, this work examined potential organic carbon source utilization of *Ca.* N. exaquare (Chapter 2) which is an AOA representative enriched from the Guelph RBCs. Expanding known contributors to ammonia oxidation within these RBCs, a large-scale metagenomic study of RBCs indicated that comammox bacteria are not only present in the RBC biofilm, but they are the dominant ammonia oxidizers detected (Chapter 3). This thesis builds upon a previous body of work studying ammonia oxidation within RBCs of the Guelph WWTP (Sauder *et al.*, 2012, 2017). Together, this work further underlines the value of these RBCs as study sites to investigate the ecology of ammonia oxidation because of the combination of AOB (including comammox bacteria) and AOA in one nitrifying biofilm gradient with well characterized operational parameters.

4.1.1 Organic carbon source utilization of an AOA

Cultivation of a microorganism allows further insight into its metabolism and physiology, which leads to understanding of its potential roles within the RBC community.

The cultivation of *Ca.* N. exaquare by Sauder *et al.* (2017) allowed for testing of hypotheses around its metabolism. For example, because this AOA representative encodes dicarboxylate transporters and is stimulated by dicarboxylic acids, this thesis expanded on the work of Sauder *et al.* (2017), which confirmed the possibility of autotrophic growth, to determine whether *Ca.* N. exaquare is also capable of assimilating organic carbon directly from the environment of the RBCs. As pointed out by Mussmann *et al.* (2011), AOA may not be strict chemolithoautotrophs, which is consistent with a lack of bicarbonate assimilation by AOA within RBC biofilm (Sauder *et al.*, 2017). Studying alternative metabolisms of AOA is important for determining the full scope and scale of contributions of these AOA to nitrification and carbon cycling, further shedding light on the functional role of AOA in the RBCs.

Experiments with the *Ca.* N. exaquare enrichment culture did not yield consistent results for organic carbon source utilization. Both succinate and pyruvate were previously found to be stimulatory to ammonia oxidation of this archaeal species (Sauder *et al.*, 2017); however, the response of *Ca*. N. exaquare to succinate and pyruvate in my experiments was inconsistent (Figure 2.1, Figure 2.3). Catalase was not stimulatory to the culture, indicating that this enrichment culture already had the capacity to remove reactive oxygen species (ROS), consistent with its genome-encoded ability to detoxify ROS. Pyruvate is therefore likely not used as a hydrogen peroxide scavenger by *Ca*. N. exaquare, and it may instead serve as an organic carbon source. Conversely, pyruvate and a representative dicarboxylic acid (succinate) were both depleted rapidly within incubations (Table 2.2), likely by heterotrophic culture contaminants, and were no longer detected once the stimulation of ammonia oxidation was measurable. The data highlight the importance of obtaining a pure culture of *Ca.* N. exaquare to clarify the relationship of *Ca*. N. exaquare to pyruvate or dicarboxylic acid intermediates of the tricarboxylic acid cycle.

4.1.2 Metagenomic analysis of the RBC biofilm

Shotgun metagenomics provided access to the microbial community members present within biofilm of RBCs and the genome-encoded metabolic functions. Assembly and binning of the sequencing data linked functions to taxonomy, demonstrating that *Nitrospira* encoding genes for complete ammonia oxidation were present in the biofilm. Not only were these comammox bacteria present, they were also the dominant ammonia oxidizers detected (Figure 3.8B). The comammox bacteria were also very diverse, with multiple populations present across RBC trains and within individual RBCs (Figure 3.10). Before this study, the only reported ammonia oxidizers in the RBCs were AOA and AOB (Sauder *et al.*, 2012, 2017). This discovery of comammox bacteria in the RBCs changes how we view the ecology of ammonia oxidation at the Guelph WWTP. Despite low ammonia concentrations, all three types of ammonia oxidizers co-existed across all RBC trains sampled (Figure 3.6). Because nitrite-oxidizing *Nitrospira* were also detected, the RBCs serve as an ideal location to study the microbial ecology of aerobic nitrification in a general sense. This metagenomic analysis serves as the first step in understanding how nitrification is catalyzed by RBC biofilm.

Distinct patterns in ammonia oxidizer relative abundances emerged from both the metagenomic and qPCR data. The shift in relative abundance of AOA-associated genes across RBC 1 and 8 reported in 2010 (higher in RBC 8 than 1) was inconsistent with the results from 2016 (higher in RBC 1 than 8), suggesting a change to the conditions of wastewater being treated by the RBCs. These changes coincided with a decrease in the relative abundance of AOB-associated genes in 2016 (Figure 3.5, Figure 3.8). The relative abundances of *Nitrospira amoA* genes in RBC 1 and 8 in 2010 and 2016 were similar, suggesting that the same factors that govern AOA and traditional AOB distributions are distinct from those that govern comammox *Nitrospira*, which may hint at a unique niche for these newly discovered nitrifiers. Whether ammonia concentration is the sole factor responsible for these changes, or not, will remain an open question to be addressed by future research, but this study does indicate that environmental factors affect the AOA, AOB, and comammox bacteria differentially.

4.2 Future directions

4.2.1 Cultivation experiments with Ca. N. exaquare

A pure culture of *Ca.* N. exaquare is required for future study of organic carbon substrate utilization by AOA related to *Nitrosocosmicus*. Even if incorporation of organic carbon is seen in the enrichment culture, for example using DNA stable-isotope probing (DNA-SIP; Neufeld *et al.*, 2007), it may be the result of cross-feeding and not direct assimilation of the carbon source. Further purification of the enrichment culture could be achieved through serial dilutions, as shown by Tourna *et al.* (2011) and Könneke *et al.* (2005), and attempted previously (data not shown). Furthermore, the culture of *Ca.* N. exaquare can grow at 40°C (Sauder *et al.*, 2017) and therefore cultivation at higher temperatures may help inhibit the growth of heterotrophs. The use of antibiotics may also be of use again, because different heterotrophs may have been introduced to the culture over time via laboratory contamination.

Once purified, cultivation experiments using labelled organic carbon can be performed to measure assimilation. Experiments could involve DNA-SIP (Neufeld *et al.*, 2007), total carbon analysis using a C/N analyzer linked to a mass spectrometer (Hommes *et al.*, 2003), through membrane lipid analysis (Kim *et al.*, 2016), or through catalyzed reporter deposition fluorescence *in situ* hybridization (CARD-FISH) associated with microautoradiography (Sauder *et al.*, 2017). Because some of the heterotrophs in the enrichment culture produced catalase, experiments testing catalase and pyruvate stimulation of *Ca.* N. exaquare should also be repeated with the pure culture to test whether these additives are sufficient to produce the same level of ammonia oxidation stimulation reported previously.

Given the high ammonia tolerance (20 mM) reported for *Ca.* N. exaquare (Sauder *et al.*, 2017), and the low ammonia environment in which it lives, determining the ammonia affinity of this AOA would increase understanding of AOA niche specialization. It was recently suggested that the S-layer, which most AOA have, partially explains the high

affinity of AOA for ammonia (Li *et al.*, 2018). The charged S-layer concentrates ammonium in the pseudo-periplasmic space, helping AOA thrive in environments with very low ammonia. However, *Ca.* N. exaquare does not have an S-layer (Sauder *et al.*, 2017), which suggests it may have a lower ammonia affinity, and may explain its high ammonia tolerance. AOA have a range of ammonia affinities (Kits *et al.*, 2017) and it is currently unknown where *Ca.* N. exaquare fits into this spectrum. Furthermore, knowing the ammonia affinity of this species will help determine whether it is a competitive ammonia oxidizer in the RBC environment.

Apart from ammonia concentrations, copper should be considered as a factor affecting growth of *Ca.* N. exaquare. Copper is required for many AOA enzymes, most notably as a cofactor for ammonia monooxygenase (Walker *et al.*, 2010). The availability of copper can limit AOA growth (Amin *et al.*, 2013). Under conditions of ammonia limitation and copper stress, AOA upregulate cobalamin (vitamin B_{12}) biosynthesis. Cobalamin is required as an enzyme cofactor in several AOA enzymes (Doxey *et al.*, 2015). This upregulation in times of stress is due to the reaction of cobalamin with nitric oxide and oxygen to generate nitrocobalamin, which is not biologically active (Qin *et al.*, 2018). To make up for this, cobalamin synthesis is upregulated (Qin *et al.*, 2018; Heal *et al.*, 2018). Cobalamin biosynthesis draws on TCA and 3HP/4HB cycle intermediates (Dailey *et al.*, 2017). Organic carbon could replenish these intermediates. This would demonstrate an interplay between copper availability and organic carbon, and therefore, copper concentrations (in addition to ammonia concentrations) must be carefully considered in future work. Additionally, copper concentrations in the water entering the RBCs could have an effect on *Ca.* N. exaquare distributions and activity *in situ*.

4.2.2 Further RBC biofilm analysis and cultivation

Because metagenomic analysis provides access to functional information for a microbial community of interest, such analyses can help generate hypotheses and support subsequent cultivation results. The metagenomic data generated from this study represents

hundreds of high quality metagenome-assembled genomes (MAGs) that have yet to be explored. My research focused on nitrifiers, but there are many other MAGs that should be explored in more detail, such as denitrifiers, methanotrophs, and representatives associated with the candidate phylum radiation (data not shown). Metagenomes can also be used to find novel taxa, or to assign new functions to taxa. Given that AOA were first suggested based on metagenomic sequence data from the Sargasso Sea (Venter *et al.*, 2004), and more recently even nitrite-oxidizing archaea have been proposed based on metagenomic data (Kitzinger *et al.*, 2018) the data generated from my research will serve as a valuable foundation for future microbial ecology discovery.

There were several high quality (≥75% completeness, <25% contamination) *Nitrospira* bins containing *amoA* that did not contain *nxrB* genes (Table 3.6, Figure 3.9). In order for these *Nitrospira* to be considered comammox bacteria, they must encode genes for both ammonia oxidation and nitrite oxidation. Further bin refining with tools such as Anvi'o (Eren *et al.*, 2015) could help complete bins and reduce contamination, or potentially reveal that *Nitrospira* bacteria exist that are solely involved in ammonia oxidation as AOB.

The comammox bacteria of the RBCs were diverse, with unique populations distributed differentially among the RBCs (Figure 3.10). High strain-level heterogeneity of comammox bacteria is in stark contrast to the sole species of thaumarchaeotal AOA detected in the RBCs. This suggests niche-specialization occurred within the comammox bacteria, with individual strains adapted to unique micro-environments within the RBC biofilm. With many of these detected comammox strains being highly distinct to those from reported cultures, these populations of *Nitrospira* are ideal targets for future cultivation efforts. Strategies for enriching the growth of comammox bacteria could include using a chemostat to establish conditions with low ammonia concentrations and dilution rates. These parameters would favour the growth of comammox bacteria with a high substrate affinity and low growth rate (Costa *et al.*, 2006). Indeed, low ammonia concentrations were essential for enriching *Ca.* N. inopinata (Kits *et al.*, 2017). The use of dilution series and antibiotics could

also help with purifying comammox bacteria (Daims *et al.*, 2015; Kits *et al.*, 2017). The dilution series is an especially useful strategy when comammox bacteria dominate, like in the RBCs, and genome-informed antibiotic use would help inhibit the growth of contaminating bacteria. Once additional pure comammox cultures are obtained, biochemical experiments can be performed to determine their substrate affinities, growth kinetics, and potential use of alternative metabolic pathways, such as hydrogen oxidation and urea degradation. This will help determine the optimal conditions for comammox bacterial growth, and how they compete and interact with other nitrifiers.

Although it is likely that comammox bacteria contribute to ammonia oxidation in the RBCs, future research will be required to identify the ammonia oxidation potential of AOA and various AOB. The use of differential inhibitors originally led to estimations of AOA and AOB contributions to ammonia oxidation, but the discovery of comammox bacteria in the RBCs complicates these results, as suggested might be the case by the study authors (Sauder *et al.* 2017). Differential inhibitors can be used to determine the relative contributions of AOA and AOB to ammonia oxidation in environmental samples by selectively inhibiting one ammonia oxidizer type and determining the proportion of ammonia oxidation inhibited. The ammonia-oxidizing activity of AOB can be inhibited by compounds such as allylthiourea (ATU) (Martens-Habbena *et al.*, 2015; Shen *et al.*, 2013) and octyne (Taylor *et al.*, 2013). Scavengers of nitric oxide have been used to inhibit AOA activity (Sauder *et al.*, 2016), such as 2-phenyl-4,4,5,5-tetramethylimidazoline-1-oxyl 3-oxide (PTIO) (Martens-Habbena *et al.*, 2015; Shen *et al.*, 2013). Although ATU inhibits tested comammox bacteria (van Kessel *et al.*, 2015), this is not surprising because the ammonia oxidation enzymes in AOB and comammox are homologous. Because ATU inhibits both AOB and comammox bacteria, the contributions of AOB and comammox bacteria cannot be separated if they are both present in the same environment. In addition, the inhibition profile of comammox bacteria in the presence of PTIO is unknown, so previous activity data will need to be examined once these data become available. Identifying an inhibitor that will selectively inhibit only comammox bacteria ammonia oxidation will be a very important step towards determining comammox

bacteria activity under environmentally relevant conditions and will be needed to determine the contributions to nitrification of all the ammonia oxidizers in the RBC biofilm. Some research suggests that chlorate, a potent inhibitor of nitrite oxidation, may be an effective ammonia oxidation inhibitor of only comammox bacteria (Tatari *et al.*, 2017) and future research should assess its effectiveness for use as a general inhibitor of ammonia-oxidizing *Nitrospira*.

Given that AOA, AOB, comammox bacteria, and nitrite-oxidizing *Nitrospira* all co-exist in the RBC biofilm, this environment is an ideal place to study the interactions among all three types of ammonia oxidizers. The ammonia oxidizers and *Nitrospira* are in close proximity to each other in the biofilm (Sauder *et al.*, 2017). These aggregates are typical of nitrifiers, and are viewed as mutualistic, where the ammonia oxidizers provide nitrite for the NOB and the NOB provide nitrite detoxification for the ammonia oxidizers (Daims *et al.*, 2016). How the comammox bacteria fit into this is currently unknown. Observing where the different nitrifiers are spatially to each other would provide context for the possible interactions between them. This could be achieved using gene fluorescence *in situ* hybridization (GeneFISH), which connects cell identity to the presence of genes of interest (Moraru *et al.*, 2010). This method could be used to generate an image showing the spatial distributions of all nitrifier types present in the biofilm and form the basis of future research on nitrifier interactions in the RBCs.

Overall, RBCs associated with the Guelph WWTP house a diverse community of characterized and novel microorganisms, and an especially diverse complement of nitrifiers. Although there is still much to be discovered about the microbial processes carried out in the RBC biofilm, this research is an important step towards understanding these processes within the context of nitrification, setting the stage for future metagenomics- and cultivation-based research to further clarify the microbial ecology of ammonia-oxidizing archaea, ammonia-oxidizing bacteria, and complete ammonia-oxidizing bacteria in a municipal wastewater treatment plant.

Bibliography

Amin SA, Moffett JW, Martens-Habbena W, Jacquot JE, Han Y, Devol A, *et al.* (2013). Copper requirements of the ammonia-oxidizing archaeon *Nitrosopumilus maritimus* SCM1 and implications for nitrification in the marine environment. *Limnol Oceanogr* **58**: 2037–2045.

Andrews S. (2010). FastQC: a quality control tool for high throughput sequence data. http://www.bioinformatics.babraham.ac.uk/projects/fastqc.

Annavajhala MK, Kapoor V, Santo-Domingo J, Chandran K. (2018). Comammox functionality identified in diverse engineered biological wastewater treatment systems. *Environ Sci Technol Lett* **5**: 110–116.

Arp DJ, Stein LY. (2003). Metabolism of inorganic N compounds by ammonia-oxidizing bacteria. *Crit Rev Biochem Mol Biol* **38**: 471–495.

Bai Y, Sun Q, Wen D, Tang X. (2012). Abundance of ammonia-oxidizing bacteria and archaea in industrial and domestic wastewater treatment systems. *FEMS Microbiol Ecol* **80**: 323–330.

Bartleme RP, Mclellan SL, Newton RJ. (2017). Freshwater recirculating aquaculture system operations drive biofilter bacterial community shifts around a stable nitrifying consortium of ammonia-oxidizing archaea and comammox *Nitrospira*. *Front Microbiol* **8**: 101.

Blainey PC, Mosier AC, Potanina A, Francis CA, Quake SR. (2011). Genome of a low-salinity ammonia-oxidizing archaeon determined by single-cell and metagenomic analysis. *PLoS One* **6**: e16626.

Bock E. (1976). Growth of *Nitrobacter* in the presence of organic matter. *Arch Microbiol* **108**: 305–312.

Bock E, Koops H-P, Möller UC, Rudert M. (1990). A new facultatively nitrite oxidizing bacterium, *Nitrobacter vulgaris* sp. nov. *Arch Microbiol* **153**: 105–110.

Bushnell B. (2017). BBMap. https://sourceforge.net/projects/bbmap/.

Camejo PY, Santo Domingo J, McMahon KD, Noguera DR. (2017). Genome-enabled insights into the ecophysiology of the comammox bacterium "*Candidatus* Nitrospira nitrosa". *mSystems* **2**: e00059-17.

Caranto JD, Lancaster KM. (2017). Nitric oxide is an obligate bacterial nitrification intermediate produced by hydroxylamine oxidoreductase. *Proc Natl Acad Sci U S A* **114**: 8217–8222.

Chao Y, Mao Y, Yu K, Zhang T. (2016). Novel nitrifiers and comammox in a full-scale hybrid biofilm and activated sludge reactor revealed by metagenomic approach. *Appl Microbiol Biotechnol* **100**: 8225–8237.

Clark C, Schmidt EL. (1966). Effect of mixed culture on *Nitrosomonas europaea* simulated by uptake and utilization of pyruvate. *J Bacteriol* **91**: 367–373.

Costa E, Pérez J, Kreft J-U. (2006). Why is metabolic labour divided in nitrification? *Trends Microbiol* **14**: 213–219.

Dahllof I, Baillie H, Kjelleberg S. (2000). *rpoB*-based microbial community analysis avoids limitations inherent in 16S rRNA gene intraspecies heterogeneity. *Appl Environ Microbiol* **66**: 3376–3380.

Dailey HA, Dailey TA, Gerdes S, Jahn D, Jahn M, O'Brian MR, *et al.* (2017). Prokaryotic heme biosynthesis: multiple pathways to a common essential product. *Microbiol Mol Biol Rev* **81**: e00048-16.

Daims H, Lebedeva E V., Pjevac P, Han P, Herbold C, Albertsen M, *et al.* (2015). Complete nitrification by *Nitrospira* bacteria. *Nature* **528**: 504–509.

Daims H, Lücker S, Wagner M. (2016). A new perspective on microbes formerly known as nitrite-oxidizing bacteria. *Trends Microbiol* **24**: 699–712.

Daims H, Nielsen JL, Nielsen PH, Schleifer KH, Wagner M. (2001). In situ characterization

of *Nitrospira*-like nitrite-oxidizing bacteria active in wastewater treatment plants. *Appl Environ Microbiol* **67**: 5273–5284.

Ding K, Wen X, Li Y, Shen B, Zhang B. (2015). Ammonia-oxidizing archaea versus bacteria in two soil aquifer treatment systems. *Appl Microbiol Biotechnol* **99**: 1337–1347.

Doxey AC, Kurtz DA, Lynch MD, Sauder LA, Neufeld JD. (2015). Aquatic metagenomes implicate *Thaumarchaeota* in global cobalamin production. *ISME J* **9**: 461–471.

Edgar RC. (2004). MUSCLE: Multiple sequence alignment with high accuracy and high throughput. *Nucleic Acids Res* **32**: 1792–1797.

Eren AM, Esen ÖC, Quince C, Vineis JH, Morrison HG, Sogin ML, *et al.* (2015). Anvi'o: an advanced analysis and visualization platform for 'omics data. *PeerJ* **3**: e1319.

Erguder TH, Boon N, Wittebolle L, Marzorati M, Verstraete W. (2009). Environmental factors shaping the ecological niches of ammonia-oxidizing archaea. *FEMS Microbiol Rev* **33**: 855–869.

Estelmann S, Hügler M, Eisenreich W, Werner K, Berg IA, Ramos-Vera WH, *et al.* (2011). Labeling and enzyme studies of the central carbon metabolism in *Metallosphaera sedula*. *J Bacteriol* **193**: 1191–200.

Ewels P, Magnusson M, Lundin S, Käller M. (2016). MultiQC: summarize analysis results for multiple tools and samples in a single report. *Bioinformatics* **32**: 3047–3048.

Fan X-Y, Gao J-F, Pan K-L, Li D-C, Dai H-H. (2017). Temporal dynamics of bacterial communities and predicted nitrogen metabolism genes in a full-scale wastewater treatment plant. *RSC Adv* **7**: 56317–56327.

Fan X-Y, Gao J-F, Pan K-L, Li D-C, Zhang L-F, Wang S-J. (2018). Shifts in bacterial community composition and abundance of nitrifiers during aerobic granulation in two nitrifying sequencing batch reactors. *Bioresour Technol* **251**: 99–107.

Fish JA, Chai B, Wang Q, Sun Y, Brown CT, Tiedje JM, *et al.* (2013). FunGene: the

functional gene pipeline and repository. *Front Microbiol* **4**: 291.

Fowler SJ, Palomo A, Dechesne A, Mines PD, Smets BF. (2018). Comammox *Nitrospira* are abundant ammonia oxidizers in diverse groundwater-fed rapid sand filter communities. *Environ Microbiol* **20**: 1002–1015.

French E, Kozlowski JA, Mukherjee M, Bullerjahn G, Bollmann A. (2012). Ecophysiological characterization of ammonia-oxidizing archaea and bacteria from freshwater. *Appl Environ Microbiol* **78**: 5773–5780.

Fujitani H, Ushiki N, Tsuneda S, Aoi Y. (2014). Isolation of sublineage I *Nitrospira* by a novel cultivation strategy. *Environ Microbiol* **16**: 3030–3040.

Gao J-F, Luo X, Wu G-X, Li T, Peng Y-Z. (2013). Quantitative analyses of the composition and abundance of ammonia-oxidizing archaea and ammonia-oxidizing bacteria in eight full-scale biological wastewater treatment plants. *Bioresour Technol* **138**: 285–296.

Gao J, Fan X, Wu G, Li T, Pan K. (2016). Changes of abundance and diversity of ammonia-oxidizing archaea (AOA) and bacteria (AOB) in three nitrifying bioreactors with different ammonia concentrations. *Desalin Water Treat* **57**: 21463–21475.

Gao J, Luo X, Wu G, Li T, Peng Y. (2014). Abundance and diversity based on *amoA* genes of ammonia-oxidizing archaea and bacteria in ten wastewater treatment systems. *Appl Microbiol Biotechnol* **98**: 3339–3354.

Gonzalez-Martinez A, Rodriguez-Sanchez A, van Loosdrecht MCM, Gonzalez-Lopez J, Vahala R. (2016). Detection of comammox bacteria in full-scale wastewater treatment bioreactors using tag-454-pyrosequencing. *Environ Sci Pollut Res* **23**: 25501–25511.

Gruber-Dorninger C, Pester M, Kitzinger K, Savio DF, Loy A, Rattei T, *et al.* (2015). Functionally relevant diversity of closely related *Nitrospira* in activated sludge. *ISME J* **9**: 643–655.

Hatzenpichler R. (2012). Diversity, physiology, and niche differentiation of ammonia-oxidizing archaea. *Appl Environ Microbiol* **78**: 7501–7510.

Hatzenpichler R, Lebedeva E V, Spieck E, Stoecker K, Richter A, Daims H, *et al.* (2008). A moderately thermophilic ammonia-oxidizing crenarchaeote from a hot spring. *Proc Natl Acad Sci U S A* **105**: 2134–2139.

Heal KR, Qin W, Amin SA, Devol AH, Moffett JW, Virginia Armbrust E, *et al.* (2018). Accumulation of NO_2 -cobalamin in nutrient-stressed ammonia-oxidizing archaea and in the oxygen deficient zone of the eastern tropical North Pacific. *Environ Microbiol Rep* **10**: 453–457.

Helling RB, Vargas CN, Adams J. (1987). Evolution of *Escherichia coli* during growth in a constant environment. *Genetics* **116**: 349–358.

Holmes AJ, Costello A, Lidstrom ME, Murrell JC. (1995). Evidence that particulate methane monooxygenase and ammonia monooxygenase may be evolutionarily related. *FEMS Microbiol Lett* **132**: 203–208.

Holmes RM, Aminot A, Kérouel R, Hooker BA, Peterson BJ. (1999). A simple and precise method for measuring ammonium in marine and freshwater ecosystems. *Can J Fish Aquat Sci* **56**: 1801–1808.

Hommes NG, Sayavedra-Soto LA, Arp DJ. (2003). Chemolithoorganotrophic growth of *Nitrosomonas europaea* on fructose. *J Bacteriol* **185**: 6809–6814.

Hu H-W, He J-Z. (2017). Comammox---a newly discovered nitrification process in the terrestrial nitrogen cycle. *J Soils Sediments* **17**: 2709–2717.

Huo Y, Bai Y, Qu J. (2017). Unravelling riverine microbial communities under wastewater treatment plant effluent discharge in large urban areas. *Appl Microbiol Biotechnol* **101**: 6755–6764.

Jung MY, Kim JG, Sinninghe Damsté JS, Rijpstra WIC, Madsen EL, Kim SJ, *et al.* (2016). A hydrophobic ammonia-oxidizing archaeon of the *Nitrosocosmicus* clade isolated from coal tar-contaminated sediment. *Environ Microbiol Rep* **8**: 983–992.

Kang DD, Froula J, Egan R, Wang Z. (2015). MetaBAT, an efficient tool for accurately

reconstructing single genomes from complex microbial communities. *PeerJ* **3**: e1165.

van Kessel MAHJ, Speth DR, Albertsen M, Nielsen PH, Op den Camp HJM, Kartal B, *et al.* (2015). Complete nitrification by a single microorganism. *Nature* **528**: 555–559.

Kim D, Hahn AS, Wu SJ, Hanson NW, Konwar KM, Hallam SJ. (2015). FragGeneScan-plus for scalable high-throughput short-read open reading frame prediction. In: *2015 IEEE Conference on Computational Intelligence in Bioinformatics and Computational Biology, CIBCB 2015*. IEEE, pp 1–8.

Kim J-G, Park S-J, Damsté JSS, Schouten S, Rijpstra WIC, Jung M-Y, *et al.* (2016). Hydrogen peroxide detoxification is a key mechanism for growth of ammonia-oxidizing archaea. *Proc Natl Acad Sci U S A* **113**: 7888–7893.

Kits KD, Sedlacek CJ, Lebedeva E V., Han P, Bulaev A, Pjevac P, *et al.* (2017). Kinetic analysis of a complete nitrifier reveals an oligotrophic lifestyle. *Nature* **549**: 269–272.

Kitzinger K, Koch H, Lücker S, Sedlacek CJ, Herbold C, Schwarz J, *et al.* (2018). Characterization of the first '*Candidatus* Nitrotoga' isolate reveals metabolic versatility and separate evolution of widespread nitrite-oxidizing bacteria. *MBio* **9**: e01186-18.

Koch H, Galushko A, Albertsen M, Schintlmeister A, Gruber-Dorninger C, Lücker S, *et al.* (2014). Growth of nitrite-oxidizing bacteria by aerobic hydrogen oxidation. *Science* **345**: 1052–1054.

Könneke M, Bernhard AE, de la Torre JR, Walker CB, Waterbury JB, Stahl DA. (2005). Isolation of an autotrophic ammonia-oxidizing marine archaeon. *Nature* **437**: 543–546.

Könneke M, Schubert DM, Brown PC, Hügler M, Standfest S, Schwander T, *et al.* (2014). Ammonia-oxidizing archaea use the most energy-efficient aerobic pathway for CO_2 fixation. *Proc Natl Acad Sci U S A* **111**: 8239–8244.

Kozlowski JA, Stieglmeier M, Schleper C, Klotz MG, Stein LY. (2016). Pathways and key intermediates required for obligate aerobic ammonia-dependent chemolithotrophy in bacteria and Thaumarchaeota. *ISME J* **10**: 1836–1845.

Krümmel A, Harms H. (1982). Effect of organic matter on growth and cell yield of ammonia-oxidizing bacteria. *Arch Microbiol* **133**: 50–54.

Kumar S, Stecher G, Tamura K. (2016). MEGA7: Molecular Evolutionary Genetics Analysis version 7.0 for bigger datasets. *Mol Biol Evol* **33**: 1870–1874.

Lawson CE, Lücker S. (2018). Complete ammonia oxidation: an important control on nitrification in engineered ecosystems? *Curr Opin Biotechnol* **50**: 158–165.

Le SQ, Gascuel O. (2008). An improved general amino acid replacement matrix. *Mol Biol Evol* **25**: 1307–1320.

Lebedeva E V, Off S, Zumbrägel S, Kruse M, Shagzhina A, Lücker S, *et al.* (2011). Isolation and characterization of a moderately thermophilic nitrite-oxidizing bacterium from a geothermal spring. *FEMS Microbiol Ecol* **75**: 195–204.

Lehtovirta-Morley LE. (2018). Ammonia oxidation: Ecology, physiology, biochemistry and why they must all come together. *FEMS Microbiol Lett* **365**: fny058.

Lehtovirta-Morley LE, Ge C, Ross J, Yao H, Nicol GW, Prosser JI. (2014). Characterisation of terrestrial acidophilic archaeal ammonia oxidisers and their inhibition and stimulation by organic compounds. *FEMS Microbiol Ecol* **89**: 542–552.

Lewis WM, Morris DP. (1986). Toxicity of nitrite to fish: a review. *Trans Am Fish Soc* **115**: 183–195.

Li D, Liu C-M, Luo R, Sadakane K, Lam T-W. (2015). MEGAHIT: an ultra-fast single-node solution for large and complex metagenomics assembly via succinct *de Bruijn* graph. *Bioinformatics* **31**: 1674–1676.

Li H, Handsaker B, Wysoker A, Fennell T, Ruan J, Homer N, *et al.* (2009). The Sequence Alignment/Map format and SAMtools. *Bioinformatics* **25**: 2078–2079.

Li P-N, Herrmann J, Tolar BB, Poitevin F, Ramdasi R, Bargar JR, *et al.* (2018). Nutrient transport suggests an evolutionary basis for charged archaeal surface layer proteins. *ISME J*

e-pub ahead of print: 10.1038/s41396-018-0191-0.

Li W, Godzik A. (2006). Cd-hit: a fast program for clustering and comparing large sets of protein or nucleotide sequences. *Bioinformatics* **22**: 1658–1659.

Li Y, Ding K, Wen X, Zhang B, Shen B, Yang Y. (2016). A novel ammonia-oxidizing archaeon from wastewater treatment plant: Its enrichment, physiological and genomic characteristics. *Sci Rep* **6**: 23747.

Limpiyakorn T, Sonthiphand P, Rongsayamanont C, Polprasert C. (2011). Abundance of *amoA* genes of ammonia-oxidizing archaea and bacteria in activated sludge of full-scale wastewater treatment plants. *Bioresour Technol* **102**: 3694–3701.

Lücker S, Wagner M, Maixner F, Pelletier E, Koch H, Vacherie B, *et al.* (2010). A *Nitrospira* metagenome illuminates the physiology and evolution of globally important nitrite-oxidizing bacteria. *Proc Natl Acad Sci U S A* **107**: 13479–13484.

Maixner F, Noguera DR, Anneser B, Stoecker K, Wegl G, Wagner M, *et al.* (2006). Nitrite concentration influences the population structure of *Nitrospira*-like bacteria. *Environ Microbiol* **8**: 1487–1495.

Martens-Habbena W, Berube PM, Urakawa H, de la Torre JR, Stahl DA. (2009). Ammonia oxidation kinetics determine niche separation of nitrifying Archaea and Bacteria. *Nature* **461**: 976–979.

Martens-Habbena W, Qin W, Horak REA, Urakawa H, Schauer AJ, Moffett JW, *et al.* (2015). The production of nitric oxide by marine ammonia-oxidizing archaea and inhibition of archaeal ammonia oxidation by a nitric oxide scavenger. *Environ Microbiol* **17**: 2261–2274.

Mellbye BL, Spieck E, Bottomley PJ, Sayavedra-Soto LA. (2017). Acyl-homoserine lactone production in nitrifying bacteria of the genera *Nitrosospira*, *Nitrobacter*, and *Nitrospira* identified via a survey of putative quorum-sensing genes. *Appl Environ Microbiol* **83**: e01540-17.

Meseguer-Lloret S, Molins-Legua C, Campins-Falco P. (2002). Ammonium determination in water samples by using OPA-NAC reagent: A comparative study with Nessler and ammonium selective electrode methods. *Int J Environ Anal Chem* **82**: 475–489.

Miranda KM, Espey MG, Wink DA. (2001). A rapid, simple spectrophotometric method for simultaneous detection of nitrate and nitrite. *Nitric Oxide* **5**: 62–71.

Moraru C, Lam P, Fuchs BM, Kuypers MMM, Amann R. (2010). GeneFISH - an in situ technique for linking gene presence and cell identity in environmental microorganisms. *Environ Microbiol* **12**: 3057–3073.

Mussmann M, Brito I, Pitcher A, Sinninghe Damste JS, Hatzenpichler R, Richter A, *et al.* (2011). Thaumarchaeotes abundant in refinery nitrifying sludges express *amoA* but are not obligate autotrophic ammonia oxidizers. *Proc Natl Acad Sci U S A* **108**: 16771–16776.

Muyzer G, de Waal EC, Uitterlinden AG. (1993). Profiling of complex microbial populations by denaturing gradient gel electrophoresis analysis of polymerase chain reaction-amplified genes coding for 16S rRNA. *Appl Environ Microbiol* **59**: 695–700.

Neufeld JD, Vohra J, Dumont MG, Lueders T, Manefield M, Friedrich MW, *et al.* (2007). DNA stable-isotope probing. *Nat Protoc* **2**: 860–866.

Nunoura T, Takaki Y, Kazama H, Kakuta J, Shimamura S, Makita H, *et al.* (2014). Physiological and genomic features of a novel sulfur-oxidizing gammaproteobacterium belonging to a previously uncultivated symbiotic lineage isolated from a hydrothermal vent. *PLoS One* **9**: e104959.

Nurk S, Meleshko D, Korobeynikov A, Pevzner PA. (2017). metaSPAdes: a new versatile metagenomic assembler. *Genome Res* **27**: 824–834.

Ochsenreiter T, Selezi D, Quaiser A, Bonch-Osmolovskaya L, Schleper C. (2003). Diversity and abundance of Crenarchaeota in terrestrial habitats studied by 16S RNA surveys and real time PCR. *Environ Microbiol* **5**: 787–797.

Olm MR, Brown CT, Brooks B, Banfield JF. (2017). dRep: a tool for fast and accurate

genomic comparisons that enables improved genome recovery from metagenomes through de-replication. *ISME J* **11**: 2864–2868.

Orellana LH, Chee-Sanford JC, Sanford RA, Löffler FE, Konstantinidis KT. (2017). Year-round shotgun metagenomes reveal stable microbial communities in agricultural soils and novel ammonia oxidizers responding to fertilization. *Appl Environ Microbiol* **84**: e01646-17.

Palomo A, Fowler SJ, Gülay A, Rasmussen S, Sicheritz-Ponten T, Smets BF. (2016). Metagenomic analysis of rapid gravity sand filter microbial communities suggests novel physiology of *Nitrospira* spp. *ISME J* **10**: 2569–2581.

Palomo A, Pedersen AG, Fowler SJ, Dechesne A, Sicheritz-Pontén T, Smets BF. (2018). Comparative genomics sheds light on niche differentiation and the evolutionary history of comammox *Nitrospira*. *ISME J* **12**: 1779–1793.

Pan K-L, Gao J-F, Li H-Y, Fan X-Y, Li D-C, Jiang H. (2018). Ammonia-oxidizing bacteria dominate ammonia oxidation in a full-scale wastewater treatment plant revealed by DNA-based stable isotope probing. *Bioresour Technol* **256**: 152–159.

Park H-D, Wells GF, Bae H, Criddle CS, Francis CA. (2006). Occurrence of ammonia-oxidizing archaea in wastewater treatment plant bioreactors. *Appl Environ Microbiol* **72**: 5643–5647.

Parks DH, Imelfort M, Skennerton CT, Hugenholtz P, Tyson GW. (2015). CheckM: assessing the quality of microbial genomes recovered from isolates, single cells, and metagenomes. *Genome Res* **25**: 1043–1055.

Pelissari C, Guivernau M, Viñas M, de Souza SS, García J, Sezerino PH, *et al.* (2017). Unraveling the active microbial populations involved in nitrogen utilization in a vertical subsurface flow constructed wetland treating urban wastewater. *Sci Total Environ* **584–585**: 642–650.

Pester M, Maixner F, Berry D, Rattei T, Koch H, Lücker S, *et al.* (2014). *NxrB* encoding the beta subunit of nitrite oxidoreductase as functional and phylogenetic marker for nitrite-

oxidizing *Nitrospira*. *Environ Microbiol* **16**: 3055–3071.

Pester M, Rattei T, Flechl S, Gröngröft A, Richter A, Overmann J, *et al.* (2012). *amoA*-based consensus phylogeny of ammonia-oxidizing archaea and deep sequencing of *amoA* genes from soils of four different geographic regions. *Environ Microbiol* **14**: 525–539.

Petrenko P, Lobb B, Kurtz DA, Neufeld JD, Doxey AC. (2015). MetAnnotate: function-specific taxonomic profiling and comparison of metagenomes. *BMC Biol* **13**: 92.

Pinto AJ, Marcus DN, Ijaz Z, Bautista-de los Santos QM, Dick GJ, Raskin L. (2015). Metagenomic evidence for the presence of comammox *Nitrospira*-like bacteria in a drinking water system. *mSphere* **1**: e00054-15.

Pjevac P, Schauberger C, Poghosyan L, Herbold CW, Kessel MA van, Daebeler A, *et al.* (2017). *AmoA*-targeted polymerase chain reaction primers for the specific detection and quantification of comammox *Nitrospira* in the environment. *Front Microbiol* **8**: 1508.

Poulin P, Pelletier É. (2007). Determination of ammonium using a microplate-based fluorometric technique. *Talanta* **71**: 1500–1506.

Prosser JI, Nicol GW. (2012). Archaeal and bacterial ammonia-oxidisers in soil: The quest for niche specialisation and differentiation. *Trends Microbiol* **20**: 523–531.

Purkhold U, Pommerening-Röser A, Juretschko S, Schmid MC, Koops HP, Wagner M. (2000). Phylogeny of all recognized species of ammonia oxidizers based on comparative 16S rRNA and *amoA* sequence analysis: Implications for molecular diversity surveys. *Appl Environ Microbiol* **66**: 5368–5382.

Qin W, Amin SA, Lundeen RA, Heal KR, Martens-Habbena W, Turkarslan S, *et al.* (2018). Stress response of a marine ammonia-oxidizing archaeon informs physiological status of environmental populations. *ISME J* **12**: 508–519.

Qin W, Amin SA, Martens-Habbena W, Walker CB, Urakawa H, Devol AH, *et al.* (2014). Marine ammonia-oxidizing archaeal isolates display obligate mixotrophy and wide ecotypic variation. *Proc Natl Acad Sci U S A* **111**: 12504–12509.

Qin W, Meinhardt KA, Moffett JW, Devol AH, Virginia Armbrust E, Ingalls AE, *et al.* (2017). Influence of oxygen availability on the activities of ammonia-oxidizing archaea. *Environ Microbiol Rep* **9**: 250–256.

Reddy DA, Subrahmanyam G, Shivani Kallappa G, Karunasagar I, Karunasagar I. (2014). Detection of ammonia-oxidizing archaea in fish processing effluent treatment plants. *Indian J Microbiol* **54**: 434–438.

Richter M, Rosselló-Móra R, Oliver Glöckner F, Peplies J. (2016). JSpeciesWS: A web server for prokaryotic species circumscription based on pairwise genome comparison. *Bioinformatics* **32**: 929–931.

Rotthauwe JH, Witzel KP, Liesack W. (1997). The ammonia monooxygenase structural gene *amoA* as a functional marker: Molecular fine-scale analysis of natural ammonia-oxidizing populations. *Appl Environ Microbiol* **63**: 4704–4712.

Roy D, McEvoy J, Blonigen M, Amundson M, Khan E. (2017). Seasonal variation and ex-situ nitrification activity of ammonia oxidizing archaea in biofilm based wastewater treatment processes. *Bioresour Technol* **244**: 850–859.

Sauder LA, Albertsen M, Engel K, Schwarz J, Nielsen PH, Wagner M, *et al.* (2017). Cultivation and characterization of *Candidatus* Nitrosocosmicus exaquare, an ammonia-oxidizing archaeon from a municipal wastewater treatment system. *ISME J* **11**: 1142–1157.

Sauder LA, Peterse F, Schouten S, Neufeld JD. (2012). Low-ammonia niche of ammonia-oxidizing archaea in rotating biological contactors of a municipal wastewater treatment plant. *Environ Microbiol* **14**: 2589–600.

Sauder LA, Ross AA, Neufeld JD. (2016). Nitric oxide scavengers differentially inhibit ammonia oxidation in ammonia-oxidizing archaea and bacteria. *FEMS Microbiol Lett* **363**: fnw052.

Scarascia G, Cheng H, Harb M, Hong P-Y. (2017). Application of hierarchical oligonucleotide primer extension (HOPE) to assess relative abundances of ammonia- and

nitrite-oxidizing bacteria. *BMC Microbiol* **17**: 85.

Schubert M, Lindgreen S, Orlando L. (2016). AdapterRemoval v2: rapid adapter trimming, identification, and read merging. *BMC Res Notes* **9**: 88.

Sczyrba A, Hofmann P, Belmann P, Koslicki D, Janssen S, Dröge J, *et al.* (2017). Critical Assessment of Metagenome Interpretation - A benchmark of metagenomics software. *Nat Methods* **14**: 1063–1071.

Seemann T. (2014). Prokka: rapid prokaryotic genome annotation. *Bioinformatics* **30**: 2068–2069.

Shen T, Stieglmeier M, Dai J, Urich T, Schleper C. (2013). Responses of the terrestrial ammonia-oxidizing archaeon *Ca.* Nitrososphaera viennensis and the ammonia-oxidizing bacterium *Nitrosospira multiformis* to nitrification inhibitors. *FEMS Microbiol Lett* **344**: 121–129.

Sonthiphand P, Limpiyakorn T. (2011). Change in ammonia-oxidizing microorganisms in enriched nitrifying activated sludge. *Appl Microbiol Biotechnol* **89**: 843–853.

Spang A, Poehlein A, Offre P, Zumbrägel S, Haider S, Rychlik N, *et al.* (2012). The genome of the ammonia-oxidizing *Candidatus* Nitrososphaera gargensis: insights into metabolic versatility and environmental adaptations. *Environ Microbiol* **14**: 3122–3145.

Spieck E, Hartwig C, McCormack I, Maixner F, Wagner M, Lipski A, *et al.* (2006). Selective enrichment and molecular characterization of a previously uncultured *Nitrospira*-like bacterium from activated sludge. *Environ Microbiol* **8**: 405–415.

Srithep P, Pornkulwat P, Limpiyakorn T. (2018). Contribution of ammonia-oxidizing archaea and ammonia-oxidizing bacteria to ammonia oxidation in two nitrifying reactors. *Environ Sci Pollut Res* **25**: 8676–8687.

Stahl DA, de la Torre JR. (2012). Physiology and diversity of ammonia-oxidizing archaea. *Annu Rev Microbiol* **66**: 83–101.

Stein LY, Klotz MG. (2016). The nitrogen cycle. *Curr Biol* **26**: R94–R98.

Strous M, Fuerst JA, Kramer EH, Logemann S, Muyzer G, van de Pas-Schoonen KT, *et al.* (1999). Missing lithotroph identified as new planctomycete. *Nature* **400**: 446–449.

Tatari K, Gülay A, Thamdrup B, Albrechtsen H-J, Smets BF. (2017). Challenges in using allylthiourea and chlorate as specific nitrification inhibitors. *Chemosphere* **182**: 301–305.

Taylor AE, Vajrala N, Giguere AT, Gitelman AI, Arp DJ, Myrold DD, *et al.* (2013). Use of aliphatic n-alkynes to discriminate soil nitrification activities of ammonia-oxidizing thaumarchaea and bacteria. *Appl Environ Microbiol* **79**: 6544–6551.

Tourna M, Stieglmeier M, Spang A, Könneke M, Schintlmeister A, Urich T, *et al.* (2011). *Nitrososphaera viennensis*, an ammonia oxidizing archaeon from soil. *Proc Natl Acad Sci U S A* **108**: 8420–8425.

Treusch AH, Leininger S, Kletzin A, Schuster SC, Klenk H-P, Schleper C. (2005). Novel genes for nitrite reductase and Amo-related proteins indicate a role of uncultivated mesophilic crenarchaeota in nitrogen cycling. *Environ Microbiol* **7**: 1985–1995.

Ushiki N, Fujitani H, Aoi Y, Tsuneda S. (2013). Isolation of *Nitrospira* belonging to Sublineage II from a Wastewater Treatment Plant. *Microbes Environ* **28**: 346–353.

Vajrala N, Martens-Habbena W, Sayavedra-Soto LA, Schauer A, Bottomley PJ, Stahl DA, *et al.* (2013). Hydroxylamine as an intermediate in ammonia oxidation by globally abundant marine archaea. *Proc Natl Acad Sci U S A* **110**: 1006–1011.

Venter JC, Remington K, Heidelberg JF, Halpern AL, Rusch D, Eisen JA, *et al.* (2004). Environmental genome shotgun sequencing of the Sargasso Sea. *Science* **304**: 66–74.

Walker CB, de la Torre JR, Klotz MG, Urakawa H, Pinel N, Arp DJ, *et al.* (2010). *Nitrosopumilus maritimus* genome reveals unique mechanisms for nitrification and autotrophy in globally distributed marine crenarchaea. *Proc Natl Acad Sci U S A* **107**: 8818–8823.

Wang Y, Ma L, Mao Y, Jiang X, Xia Y, Yu K, *et al.* (2017). Comammox in drinking water systems. *Water Res* **116**: 332–341.

Wang Z, Zhang XX, Lu X, Liu B, Li Y, Long C, *et al.* (2014). Abundance and diversity of bacterial nitrifiers and denitrifiers and their functional genes in tannery wastewater treatment plants revealed by high-throughput sequencing. *PLoS One* **9**: e113603.

Watson SW, Bock E, Valois FW, Waterbury JB, Schlosser U. (1986). *Nitrospira marina* gen. nov. sp. nov.: a chemolithotrophic nitrite-oxidizing bacterium. *Arch Microbiol* **144**: 1–7.

Wells GF, Park H-D, Yeung C-H, Eggleston B, Francis CA, Criddle CS. (2009). Ammonia-oxidizing communities in a highly aerated full-scale activated sludge bioreactor: betaproteobacterial dynamics and low relative abundance of Crenarchaea. *Environ Microbiol* **11**: 2310–2328.

White RAI, Brown J, Colby S, Overall CC, Lee J-Y, Zucker J, *et al.* (2017). ATLAS (Automatic Tool for Local Assembly Structures) -a comprehensive infrastructure for assembly, annotation, and genomic binning of metagenomic and metatranscriptomic data. *PeerJ Prepr* 1–11.

Wu Y-W, Simmons BA, Singer SW. (2016). MaxBin 2.0: an automated binning algorithm to recover genomes from multiple metagenomic datasets. *Bioinformatics* **32**: 605–607.

Yarbrough JM, Rake JB, Eagon RG. (1980). Bacterial inhibitory effects of nitrite: inhibition of active transport, but not of group translocation, and of intracellular enzymes. *Appl Environ Microbiol* **39**: 831–834.

Zhalnina K V., Dias R, Leonard MT, Dorr de Quadros P, Camargo FAOF, Drew JC, *et al.* (2014). Genome sequence of *Candidatus* Nitrososphaera evergladensis from Group I.1b enriched from Everglades soil reveals novel genomic features of the ammonia-oxidizing archaea. *PLoS One* **9**: e101648.

Zhang T, Ye L, Tong AHY, Shao MF, Lok S. (2011). Ammonia-oxidizing archaea and ammonia-oxidizing bacteria in six full-scale wastewater treatment bioreactors. *Appl*

Microbiol Biotechnol **91**: 1215–1225.

Appendix A Dereplicated bins from all assemblies

Table A 1 All dereplicated bins from all assemblies.

Cluster	Cluster members	Closest cluster member	Furthest cluster member	Genome	Length	N50	Completeness	Contamination	Strain heterogeneity	Taxonomy contained
159_1	16	99.99	99.95	CA-NE8-2010.39	2716530	49217	99.03	2.91	0	k__Archaea;p__Thaumarchaeota;c__Nitrosopumilales;o__Nitrosopumilales
14_0	1	NA	NA	CA-NE8-2010.132	5445672	8163	85.76	2.54	0	k__Bacteria
16_0	1	NA	NA	CA-NE8-2010.55	3357787	12002	88.06	1.5	0	k__Bacteria
58_1	2	99.92	99.92	Upper-2016.32	5426382	26678	94.03	10.4	7.14	k__Bacteria
79_0	1	NA	NA	Upper-2016.249	4017003	6583	76.32	3.42	0	k__Bacteria
98_1	2	99.96	99.96	CA-NE8-2010.51	5766854	39427	93.49	2.43	0	k__Bacteria
98_2	3	99.74	99.65	SW.152	3721269	4310	75.55	0.81	0	k__Bacteria
101_0	1	NA	NA	CA-NE1-2010.212	3978538	71127	92.62	2.2	0	k__Bacteria
118_1	2	99.76	99.76	Upper-2016.135	4807119	6252	88.25	2.74	0	k__Bacteria
120_0	1	NA	NA	Upper-2016.225	9074009	3726	80.56	18.01	1.37	k__Bacteria
121_1	2	99.84	99.84	CA-NE1-2010.217	3950617	7031	90.11	1.1	0	k__Bacteria
121_2	1	NA	NA	NW.93	3478764	5285	75.32	1.1	0	k__Bacteria
122_1	3	99.83	99.07	SW.84	5282057	14918	84	2.56	0	k__Bacteria
123_0	1	NA	NA	CA-NE8-2010.227	5287771	5393	86.68	5.66	0	k__Bacteria
125_1	13	99.99	99.95	NW.122	5528595	142926	98.9	2.2	0	k__Bacteria

68_1	3	99.93	99.68	Upper-2016.246	5397273	12118	91.44	6.43	0	k__Bacteria;p__Acidobacteria
99_1	3	99.69	99.58	CA-NE8-2010.143	4897839	8158	88.41	5.77	0	k__Bacteria;p__Acidobacteria
100_0	1	NA	NA	Upper-2016.104	5614918	200928	95.3	10.43	21.43	k__Bacteria;p__Acidobacteria
104_1	2	99.93	99.93	NE1.006	9147490	28613	95.25	9.07	6.25	k__Bacteria;p__Acidobacteria
105_1	4	99.96	99.91	Upper-2016.215	5173988	64628	97.01	6.15	0	k__Bacteria;p__Acidobacteria
106_1	4	99.82	99.75	CA-NE1-2010.215	5288839	14096	89.74	5.13	0	k__Bacteria;p__Acidobacteria
107_1	4	99.53	99.47	Upper-2016.118	4756598	5517	78.78	7.03	27.78	k__Bacteria;p__Acidobacteria
108_0	1	NA	NA	Upper-2016.88	5534199	8526	78.22	3.38	26.32	k__Bacteria;p__Acidobacteria
109_1	2	99.63	99.63	FNE8.001	5407743	16829	88.39	4.49	0	k__Bacteria;p__Acidobacteria
110_1	10	99.76	99.59	NE.10	5126679	9365	83.96	2.56	0	k__Bacteria;p__Acidobacteria
111_1	7	99.82	99.78	NE.42	5623629	14143	96.72	3.42	0	k__Bacteria;p__Acidobacteria
112_1	2	99.89	99.89	Upper-2016.270	5671090	17837	89.67	6.84	12.5	k__Bacteria;p__Acidobacteria
113_0	1	NA	NA	CA-NE8-2010.12	6243844	194845	99.53	4.27	20	k__Bacteria;p__Acidobacteria
124_0	1	NA	NA	CA-NE8-2010.141	3516534	5785	77.28	7.69	0	k__Bacteria;p__Acidobacteria
128_1	2	99.64	99.64	Upper-2016.76	4872091	9647	98.12	10.34	0	k__Bacteria;p__Acidobacteria
130_0	1	NA	NA	CA-NE8-2010.38	4715704	6920	87.77	5.8	0	k__Bacteria;p__Acidobacteria
161_1	10	100	99.91	SW.4	4186568	273109	97.44	2.56	0	k__Bacteria;p__Acidobacteria
162_1	4	99.94	99.91	SW.112	6495333	11329	93.56	6.72	0	k__Bacteria;p__Acidobacteria
163_1	3	99.79	99.36	NW.118	4894602	4324	76.86	0.81	0	k__Bacteria;p__Acidobacteria
164_1	2	99.87	99.87	CA-NE8-2010.122	4126492	21866	94.02	3.42	0	k__Bacteria;p__Acidobacteria
165_1	12	99.99	99.9	SNE8.012	7256144	101273	93.96	0.85	0	k__Bacteria;p__Acidobacteria
5_1	9	100	99.96	CA-NE1-2010.200	7272536	163148	99.12	1.75	0	k__Bacteria;p__Acidobacteria;c__Acidobacteriia;o__Acidobacteriales
37_0	1	NA	NA	CA-NE8-2010.18	4399130	4203	82.76	15.42	0	k__Bacteria;p__Acidobacteria;c__Acidobacteriia;o__Acidobacteriales
88_1	9	99.79	99.51	SW.32	8159520	11670	93.62	1.79	0	k__Bacteria;p__Acidobacteria;c__Acidobacteriia;o__Acidobacteriales

89_0	1	NA	NA	SE.70	5749341	3878	76.51	7.9	0	k__Bacteria;p__Acidobacteria;c__Acidobacteriia;o__Acidobacteriales
90_0	1	NA	NA	Upper-2016.37	8290213	6377	89.89	20.71	7.14	k__Bacteria;p__Acidobacteria;c__Acidobacteriia;o__Acidobacteriales
151_1	13	99.99	99.92	SNE8.003	4415429	188599	98.26	1.74	0	k__Bacteria;p__Acidobacteria;c__Acidobacteriia;o__Acidobacteriales
94_0	1	NA	NA	Upper-2016.91	5481414	42847	96.67	6.03	0	k__Bacteria;p__Actinobacteria;c__Actinobacteria
96_0	1	NA	NA	CA-NE1-2010.145	5148969	5702	85.47	1.28	0	k__Bacteria;p__Actinobacteria;c__Actinobacteria
126_1	2	99.74	99.74	NE1.012	6568268	18473	86.87	2.14	0	k__Bacteria;p__Actinobacteria;c__Actinobacteria
126_2	4	99.3	99.02	SE8.004	6748042	23869	96.11	2.14	0	k__Bacteria;p__Actinobacteria;c__Actinobacteria
127_0	1	NA	NA	SE.60	6945775	5200	77.2	15.56	60.87	k__Bacteria;p__Actinobacteria;c__Actinobacteria
92_1	10	99.97	99.89	NE.46	6726814	28714	98.06	1.59	0	k__Bacteria;p__Actinobacteria;c__Actinobacteria;o__Actinomycetales;f__Mycobacteriaceae;g__Mycobacterium
93_0	1	NA	NA	CA-NE1-2010.52	7193923	5581	77.74	3.37	16.67	k__Bacteria;p__Actinobacteria;c__Actinobacteria;o__Actinomycetales;f__Mycobacteriaceae;g__Mycobacterium
85_1	1	NA	NA	CA-NE1-2010.37	3864605	11953	92.61	0.99	0	k__Bacteria;p__Bacteroidetes;c__Cytophagia;o__Cytophagales
85_2	1	NA	NA	CA-NE8-2010.201	3416491	6691	84.43	1.49	12.5	k__Bacteria;p__Bacteroidetes;c__Cytophagia;o__Cytophagales
152_1	2	99.87	99.87	CA-NE8-2010.37	4139492	91877	98.92	0.54	0	k__Bacteria;p__Bacteroidetes;c__Flavobacteriia;o__Flavobacteriales
153_1	2	99.92	99.92	SNE8.021	3940847	19400	97.38	0	0	k__Bacteria;p__Bacteroidetes;c__Flavobacteriia;o__Flavobacteriales
154_0	1	NA	NA	CA-NE1-2010.53	3981579	44198	96.77	0	0	k__Bacteria;p__Bacteroidetes;c__Flavobacteriia;o__Flavobacteriales
167_0	1	NA	NA	Upper-2016.85	3734684	7316	85.94	1.26	0	k__Bacteria;p__Bacteroidetes;c__Flavobacteriia;o__Flavobacteriales;f__Cryomorphaceae
155_1	3	99.76	99.74	JNE1.013	4431903	25483	95.71	0.03	0	k__Bacteria;p__Bacteroidetes;c__Sphingobacteriia;o__Sphingobacteriales;f__Chitinophagaceae
91_1	2	99.6	99.6	CA-NE8-2010.96	4443797	5601	79.81	1.02	16.67	k__Bacteria;p__Bacteroidetes;c__Sphingobacteriia;o__Sphingobacteriales;f__Saprospiraceae
150_0	1	NA	NA	Upper-2016.273	4442934	6717	76.31	2.97	0	k__Bacteria;p__Bacteroidetes;c__Sphingobacteriia;o__Sphingobacteriales;f__Saprospiraceae
156_1	4	99.95	99.73	CA-NE8-2010.165	4537368	29357	94.81	0.62	0	k__Bacteria;p__Bacteroidetes;c__Sphingobacteriia;o__Sphingobacteriales;f__Saprospiraceae
160_0	1	NA	NA	Upper-2016.243	6396764	6867	89.59	1.55	0	k__Bacteria;p__Bacteroidetes;c__Sphingobacteriia;o__Sphingobacteriales;f__Saprospiraceae
17_0	1	NA	NA	Upper-2016.234	1669733	10515	83.42	0	0	k__Bacteria;p__Chlamydiae;c__Chlamydiia;o__Chlamydiales
166_0	1	NA	NA	CA-NE8-2010.102	2764855	6344	76.64	0.91	0	k__Bacteria;p__Chloroflexi
95_1	3	99.88	99.84	Upper-2016.240	8785729	15124	96.7	4.68	11.11	k__Bacteria;p__Chloroflexi;c__Dehalococcoidetes

114_1	3	99.39	99.34	CA-NE8-2010.155	2115328	4897	78.38	0	0	k__Bacteria;p__Chloroflexi;c__Dehalococcoidetes
115_0	1	NA	NA	NW.81	2694648	15739	88.98	1.98	50	k__Bacteria;p__Chloroflexi;c__Dehalococcoidetes
131_1	8	99.64	99.21	SW1.007	4081924	24075	94.03	1.87	0	k__Bacteria;p__Nitrospirae;c__Nitrospira;o__Nitrospirales;f__Nitrospiraceae
132_1	4	100	99.95	CA-NE8-2010.42	3985495	125286	92.22	0.91	0	k__Bacteria;p__Nitrospirae;c__Nitrospira;o__Nitrospirales;f__Nitrospiraceae
133_1	9	99.84	99.74	Upper-2016.254	2985695	8041	86.82	1.09	0	k__Bacteria;p__Nitrospirae;c__Nitrospira;o__Nitrospirales;f__Nitrospiraceae
134_0	1	NA	NA	JNE1.001	2917856	8005	77.97	4.55	50	k__Bacteria;p__Nitrospirae;c__Nitrospira;o__Nitrospirales;f__Nitrospiraceae
135_0	1	NA	NA	CA-NE1-2010.95	3655795	9186	87.32	1.62	85.71	k__Bacteria;p__Nitrospirae;c__Nitrospira;o__Nitrospirales;f__Nitrospiraceae
138_1	2	99.36	99.36	CA-NE8-2010.148	2448680	5233	79.7	1.32	0	k__Bacteria;p__Nitrospirae;c__Nitrospira;o__Nitrospirales;f__Nitrospiraceae
139_0	1	NA	NA	Upper-2016.235	4708220	17866	75.61	4.39	0	k__Bacteria;p__Nitrospirae;c__Nitrospira;o__Nitrospirales;f__Nitrospiraceae
140_1	2	99.35	99.35	NW1.001	2982887	13033	89.94	2.78	25	k__Bacteria;p__Nitrospirae;c__Nitrospira;o__Nitrospirales;f__Nitrospiraceae
140_2	1	NA	NA	SNE8.002	2528397	8324	76.76	5.76	33.33	k__Bacteria;p__Nitrospirae;c__Nitrospira;o__Nitrospirales;f__Nitrospiraceae
140_3	1	NA	NA	SE8.002	5194310	23758	91.38	21.57	21.62	k__Bacteria;p__Nitrospirae;c__Nitrospira;o__Nitrospirales;f__Nitrospiraceae
141_1	3	99.65	99.61	SW.74	2627419	5942	78.07	2.26	61.54	k__Bacteria;p__Nitrospirae;c__Nitrospira;o__Nitrospirales;f__Nitrospiraceae
142_1	9	99.87	99.24	NE8.001	3985653	26973	92.22	2.73	0	k__Bacteria;p__Nitrospirae;c__Nitrospira;o__Nitrospirales;f__Nitrospiraceae
143_1	5	99.99	99.94	CA-NE8-2010.156	4369666	48920	96.76	2.73	0	k__Bacteria;p__Nitrospirae;c__Nitrospira;o__Nitrospirales;f__Nitrospiraceae
144_1	2	99.39	99.39	CA-NE8-2010.193	4145647	18888	87.01	5.76	12.5	k__Bacteria;p__Nitrospirae;c__Nitrospira;o__Nitrospirales;f__Nitrospiraceae
145_1	2	100	100	CA-NE8-2010.35	3868201	117006	95.85	3.84	0	k__Bacteria;p__Nitrospirae;c__Nitrospira;o__Nitrospirales;f__Nitrospiraceae
146_1	2	99.18	99.18	SW1.001	3393548	12389	87.82	4	46.15	k__Bacteria;p__Nitrospirae;c__Nitrospira;o__Nitrospirales;f__Nitrospiraceae
11_1	6	99.73	99.6	NW.1	5003303	6396	88.33	0.21	50	k__Bacteria;p__Planctomycetes;c__Planctomycetia;o__Planctomycetales;f__Planctomycetaceae
12_0	1	NA	NA	CA-NE8-2010.194	4262534	5945	86.26	1.7	0	k__Bacteria;p__Planctomycetes;c__Planctomycetia;o__Planctomycetales;f__Planctomycetaceae
13_0	1	NA	NA	Upper-2016.27	4857134	13525	85.23	1.47	0	k__Bacteria;p__Planctomycetes;c__Planctomycetia;o__Planctomycetales;f__Planctomycetaceae
15_0	1	NA	NA	CA-NE1-2010.55	3227670	6845	79.34	0.57	0	k__Bacteria;p__Planctomycetes;c__Planctomycetia;o__Planctomycetales;f__Planctomycetaceae
57_0	1	NA	NA	CA-NE1-2010.210	4450583	6573	88.26	6.46	0	k__Bacteria;p__Planctomycetes;c__Planctomycetia;o__Planctomycetales;f__Planctomycetaceae
61_0	1	NA	NA	Upper-2016.188	3828793	9318	91.95	4.47	0	k__Bacteria;p__Planctomycetes;c__Planctomycetia;o__Planctomycetales;f__Planctomycetaceae

18_1	3	99.33	99.25	Upper-2016.168	4173528	4227	78.19	1.83	0	k__Bacteria;p__Proteobacteria
168_0	1	NA	NA	SNE8.022	2572742	10062	92.86	2.73	42.86	k__Bacteria;p__Proteobacteria
10_0	1	NA	NA	CA-NE1-2010.144	1463116	7588	75.51	1.45	0	k__Bacteria;p__Proteobacteria;c__Alphaproteobacteria
21_1	1	NA	NA	CA-NE8-2010.82	3539585	5788	80.46	6.94	2.7	k__Bacteria;p__Proteobacteria;c__Alphaproteobacteria
21_2	1	NA	NA	SW.27	3895403	5899	82.83	8.88	0	k__Bacteria;p__Proteobacteria;c__Alphaproteobacteria
26_1	3	99.96	99.83	Upper-2016.115	3703325	26100	91.13	2.54	27.27	k__Bacteria;p__Proteobacteria;c__Alphaproteobacteria
27_0	1	NA	NA	Upper-2016.218	3669325	17309	84.22	8.51	52.63	k__Bacteria;p__Proteobacteria;c__Alphaproteobacteria
28_0	1	NA	NA	CA-NE8-2010.110	3076673	7051	82.08	5.19	24	k__Bacteria;p__Proteobacteria;c__Alphaproteobacteria
29_1	6	99.95	99.9	SNE1.006	2953509	61421	96.81	1.16	0	k__Bacteria;p__Proteobacteria;c__Alphaproteobacteria
30_0	1	NA	NA	Upper-2016.59	2268020	6984	78.57	7.03	2.08	k__Bacteria;p__Proteobacteria;c__Alphaproteobacteria
31_1	2	99.85	99.85	SE8.007	2674636	22345	83.72	1.14	0	k__Bacteria;p__Proteobacteria;c__Alphaproteobacteria
32_1	3	99.9	99.87	Upper-2016.51	3078838	10805	87.6	6.01	15.38	k__Bacteria;p__Proteobacteria;c__Alphaproteobacteria
33_0	1	NA	NA	Upper-2016.182	2753090	66840	88.29	3.04	6.25	k__Bacteria;p__Proteobacteria;c__Alphaproteobacteria
49_0	1	NA	NA	CA-NE1-2010.96	4692120	19640	94.95	5.66	14.29	k__Bacteria;p__Proteobacteria;c__Alphaproteobacteria
55_1	10	100	99.12	NW8.001	3729636	131888	97.84	0	0	k__Bacteria;p__Proteobacteria;c__Alphaproteobacteria
137_0	1	NA	NA	CA-NE1-2010.109	2629982	10413	91.17	6.09	0	k__Bacteria;p__Proteobacteria;c__Alphaproteobacteria
40_1	3	99.97	99.97	Upper-2016.230	3563019	126634	99.54	1.73	0	k__Bacteria;p__Proteobacteria;c__Alphaproteobacteria;o__Caulobacterales;f__Caulobacteraceae
41_1	2	99.7	99.7	CA-NE1-2010.18	4174833	5377	75.18	2.79	10	k__Bacteria;p__Proteobacteria;c__Alphaproteobacteria;o__Caulobacterales;f__Caulobacteraceae
42_0	1	NA	NA	CA-NE8-2010.167	4184146	5893	89.6	12.84	10.13	k__Bacteria;p__Proteobacteria;c__Alphaproteobacteria;o__Caulobacterales;f__Caulobacteraceae
36_1	10	100	99.81	SE.98	4199294	108152	96.3	0.58	0	k__Bacteria;p__Proteobacteria;c__Alphaproteobacteria;o__Rhizobiales
54_0	1	NA	NA	Upper-2016.105	3538219	16827	86.5	3.06	0	k__Bacteria;p__Proteobacteria;c__Alphaproteobacteria;o__Rhizobiales
82_0	1	NA	NA	CA-NE1-2010.222	3151944	23725	92.22	3.71	4.55	k__Bacteria;p__Proteobacteria;c__Alphaproteobacteria;o__Rhizobiales
147_1	4	99.41	99.07	CA-NE8-2010.30	2847426	6008	76.73	2.75	30	k__Bacteria;p__Proteobacteria;c__Alphaproteobacteria;o__Rhizobiales
147_2	1	NA	NA	FNE1.017	2758379	6960	75.81	6.97	0	k__Bacteria;p__Proteobacteria;c__Alphaproteobacteria;o__Rhizobiales

149_1	3	99.93	99.91	CA-NE8-2010.64	3574084	12769	91.6	0.43	0	k__Bacteria;p__Proteobacteria;c__Alphaproteobacteria;o__Rhizobiales
20_1	2	99.84	99.84	SW.135	8116582	21073	95.12	4.85	11.25	k__Bacteria;p__Proteobacteria;c__Alphaproteobacteria;o__Rhizobiales;f__Bradyrhizobiaceae;g__Bradyrhizobium
35_1	7	99.98	99.9	NE.35	4976723	58292	97.94	2.42	14.29	k__Bacteria;p__Proteobacteria;c__Alphaproteobacteria;o__Rhizobiales;f__Hyphomicrobiaceae
44_0	1	NA	NA	CA-NE1-2010.134	5123939	5785	82.68	3.23	3.03	k__Bacteria;p__Proteobacteria;c__Alphaproteobacteria;o__Rhizobiales;f__Hyphomicrobiaceae
45_0	1	NA	NA	Upper-2016.190	5535916	7581	83.45	12.52	27.42	k__Bacteria;p__Proteobacteria;c__Alphaproteobacteria;o__Rhizobiales;f__Hyphomicrobiaceae
47_1	2	99.87	99.87	Upper-2016.7	4823617	5886	79.47	5.44	25	k__Bacteria;p__Proteobacteria;c__Alphaproteobacteria;o__Rhizobiales;f__Hyphomicrobiaceae
48_0	1	NA	NA	CA-NE1-2010.104	3694433	5474	77.95	11.56	2.17	k__Bacteria;p__Proteobacteria;c__Alphaproteobacteria;o__Rhizobiales;f__Hyphomicrobiaceae
50_0	1	NA	NA	Upper-2016.108	5959393	64672	96.48	12.59	9.62	k__Bacteria;p__Proteobacteria;c__Alphaproteobacteria;o__Rhizobiales;f__Hyphomicrobiaceae
34_1	9	99.75	99.67	CA-NE8-2010.157	3278520	9956	92.57	0.03	0	k__Bacteria;p__Proteobacteria;c__Alphaproteobacteria;o__Rhizobiales;f__Hyphomicrobiaceae;g__Hyphomicrobium
56_1	5	99.92	99.76	Upper-2016.8	3509564	37981	99.13	2.73	0	k__Bacteria;p__Proteobacteria;c__Alphaproteobacteria;o__Rhizobiales;f__Hyphomicrobiaceae;g__Hyphomicrobium
46_1	4	99.62	99.49	NE.65	5941069	5588	87.3	6.17	0	k__Bacteria;p__Proteobacteria;c__Alphaproteobacteria;o__Rhodospirillales
51_1	2	99.73	99.73	CA-NE8-2010.36	3516971	9777	88.02	3.6	0	k__Bacteria;p__Proteobacteria;c__Alphaproteobacteria;o__Rhodospirillales
86_1	2	99.06	99.06	NW8.003	4541621	12916	90.82	1	0	k__Bacteria;p__Proteobacteria;c__Alphaproteobacteria;o__Rhodospirillales
86_2	6	99.26	99.03	SE8.005	4336132	12660	91.91	1.24	0	k__Bacteria;p__Proteobacteria;c__Alphaproteobacteria;o__Rhodospirillales
86_3	1	NA	NA	NE1.017	4302419	11323	87.26	2.04	0	k__Bacteria;p__Proteobacteria;c__Alphaproteobacteria;o__Rhodospirillales
86_4	1	NA	NA	SNE1.030	3394683	4471	77.78	2.78	0	k__Bacteria;p__Proteobacteria;c__Alphaproteobacteria;o__Rhodospirillales
86_5	1	NA	NA	SW8.007	4168898	8632	88.35	2.24	71.43	k__Bacteria;p__Proteobacteria;c__Alphaproteobacteria;o__Rhodospirillales
87_0	1	NA	NA	CA-NE8-2010.16	5735189	7062	91.03	3.83	57.14	k__Bacteria;p__Proteobacteria;c__Alphaproteobacteria;o__Rhodospirillales;f__Acetobacteraceae
52_1	5	99.67	99.35	SW.130	3295224	4687	77.97	0.44	0	k__Bacteria;p__Proteobacteria;c__Alphaproteobacteria;o__Rhodospirillales;f__Rhodospirillaceae
53_0	1	NA	NA	CA-NE8-2010.196	5150275	7414	86.61	9.99	10.42	k__Bacteria;p__Proteobacteria;c__Alphaproteobacteria;o__Rhodospirillales;f__Rhodospirillaceae
84_1	4	99.87	99.72	Upper-2016.70	3940398	15956	90.91	3.17	0	k__Bacteria;p__Proteobacteria;c__Alphaproteobacteria;o__Rhodospirillales;f__Rhodospirillaceae
136_1	5	99.64	99.52	SNE8.007	3118409	26313	77.5	1.3	33.33	k__Bacteria;p__Proteobacteria;c__Alphaproteobacteria;o__Rhodospirillales;f__Rhodospirillaceae
148_0	1	NA	NA	CA-NE1-2010.125	2275386	22691	97.8	1.1	0	k__Bacteria;p__Proteobacteria;c__Alphaproteobacteria;o__Rickettsiales
22_1	5	99.78	99.52	SE8.016	2254588	11288	87.59	0.64	0	k__Bacteria;p__Proteobacteria;c__Alphaproteobacteria;o__Sphingomonadales

22_2	1	NA	NA	SW8.015	2018209	5460	77.77	0.68	25	k__Bacteria;p__Proteobacteria;c__Alphaproteobacteria;o__Sphingomonadales
25_0	1	NA	NA	CA-NE8-2010.52	3592337	13510	89.52	6.77	45.24	k__Bacteria;p__Proteobacteria;c__Alphaproteobacteria;o__Sphingomonadales
43_1	2	99.91	99.91	CA-NE8-2010.28	3734122	10918	86.71	4.7	0	k__Bacteria;p__Proteobacteria;c__Alphaproteobacteria;o__Sphingomonadales;f__Sphingomonadaceae;g__Novosphingobium
23_1	2	99.98	99.98	CA-NE1-2010.136	4246273	51217	98.01	3.04	0	k__Bacteria;p__Proteobacteria;c__Alphaproteobacteria;o__Sphingomonadales;f__Sphingomonadaceae_3;g__Sphingobium
24_1	2	99.9	99.9	FNE1.013	3500839	67582	99.01	1.42	0	k__Bacteria;p__Proteobacteria;c__Alphaproteobacteria;o__Sphingomonadales;f__Sphingomonadaceae_3;g__Sphingobium
6_1	8	99.77	99.63	SW.102	5095127	8959	90.88	0.7	0	k__Bacteria;p__Proteobacteria;c__Betaproteobacteria
7_1	18	100	98.94	NE8.002	5372281	193545	97.99	1.18	0	k__Bacteria;p__Proteobacteria;c__Betaproteobacteria
8_1	1	NA	NA	CA-NE1-2010.101	4037830	7382	85.2	0.66	0	k__Bacteria;p__Proteobacteria;c__Betaproteobacteria
8_2	1	NA	NA	SW.122	4109277	7510	84.07	1.94	0	k__Bacteria;p__Proteobacteria;c__Betaproteobacteria
103_0	1	NA	NA	Upper-2016.169	3024630	5484	76.91	4.65	0	k__Bacteria;p__Proteobacteria;c__Betaproteobacteria
71_1	2	99.73	99.73	CA-NE1-2010.202	5122976	14933	95.53	4.57	21.43	k__Bacteria;p__Proteobacteria;c__Betaproteobacteria;o__Burkholderiales
72_0	1	NA	NA	CA-NE1-2010.12	5348816	109214	94.77	0.64	0	k__Bacteria;p__Proteobacteria;c__Betaproteobacteria;o__Burkholderiales
73_0	1	NA	NA	CA-NE1-2010.149	2993789	23658	95.47	0.12	0	k__Bacteria;p__Proteobacteria;c__Betaproteobacteria;o__Burkholderiales;f__Comamonadaceae
74_0	1	NA	NA	Upper-2016.219	4491662	8480	84.47	7.36	15	k__Bacteria;p__Proteobacteria;c__Betaproteobacteria;o__Burkholderiales;f__Comamonadaceae
75_1	3	99.92	99.92	Upper-2016.75	6049554	55442	92.69	0.9	0	k__Bacteria;p__Proteobacteria;c__Betaproteobacteria;o__Burkholderiales;f__Rubrivivax
76_1	6	99.99	99.88	CA-NE8-2010.216	3560721	68236	96.83	0.16	0	k__Bacteria;p__Proteobacteria;c__Betaproteobacteria;o__Burkholderiales;f__Rubrivivax
77_1	9	100	99.82	NW.99	2811580	48405	98.85	0	0	k__Bacteria;p__Proteobacteria;c__Betaproteobacteria;o__Burkholderiales;f__Rubrivivax
78_0	1	NA	NA	CA-NE1-2010.142	4925080	26934	97.97	1.91	0	k__Bacteria;p__Proteobacteria;c__Betaproteobacteria;o__Burkholderiales;f__Rubrivivax
1_1	3	99.9	99.87	SNE1.007	2786407	36428	93.81	0	0	k__Bacteria;p__Proteobacteria;c__Betaproteobacteria;o__Nitrosomonadales;f__Nitrosomonadaceae;g__Nitrosomonas
2_1	2	99.89	99.89	CA-NE8-2010.137	2847475	17081	93.68	1.67	16.67	k__Bacteria;p__Proteobacteria;c__Betaproteobacteria;o__Nitrosomonadales;f__Nitrosomonadaceae;g__Nitrosomonas
3_1	9	100	99.9	CA-NE1-2010.204	2679665	30421	99.4	0	0	k__Bacteria;p__Proteobacteria;c__Betaproteobacteria;o__Nitrosomonadales;f__Nitrosomonadaceae;g__Nitrosomonas
83_0	1	NA	NA	CA-NE1-2010.172	2646754	13788	84.88	1.34	0	k__Bacteria;p__Proteobacteria;c__Betaproteobacteria;o__Nitrosomonadales;f__Nitrosomonadaceae;g__Nitrosomonas
4_1	3	99.88	99.84	CA-NE8-2010.142	1881489	16614	82.03	0.55	0	k__Bacteria;p__Proteobacteria;c__Betaproteobacteria;o__Rhodocyclales;f__Rhodocyclaceae
9_1	3	99.58	99.44	SE.96	5980282	10429	92.47	3.23	0	k__Bacteria;p__Proteobacteria;c__Deltaproteobacteria

97_0	1	NA	NA	CA-NE8-2010.81	5117451	9337	75.15	2.8	0	k__Bacteria;p__Proteobacteria;c__Deltaproteobacteria
117_0	1	NA	NA	CA-NE8-2010.211	5266666	12365	90.13	7.78	11.76	k__Bacteria;p__Proteobacteria;c__Deltaproteobacteria
119_0	1	NA	NA	CA-NE1-2010.112	5659930	6292	78.71	7.2	0	k__Bacteria;p__Proteobacteria;c__Deltaproteobacteria
59_0	1	NA	NA	CA-NE8-2010.173	7651322	7903	84.08	6	0	k__Bacteria;p__Proteobacteria;c__Deltaproteobacteria;o__Myxococcales
60_0	1	NA	NA	CA-NE8-2010.199	9246992	9264	88.58	5.99	0	k__Bacteria;p__Proteobacteria;c__Deltaproteobacteria;o__Myxococcales
62_1	3	99.98	99.97	Upper-2016.202	8794007	48742	94.03	2.1	0	k__Bacteria;p__Proteobacteria;c__Deltaproteobacteria;o__Myxococcales
63_0	1	NA	NA	CA-NE8-2010.149	5323644	8325	81.44	2.05	0	k__Bacteria;p__Proteobacteria;c__Deltaproteobacteria;o__Myxococcales
116_0	1	NA	NA	Upper-2016.16	9635693	24762	96.02	3.39	0	k__Bacteria;p__Proteobacteria;c__Deltaproteobacteria;o__Myxococcales
39_0	1	NA	NA	CA-NE8-2010.88	2932135	7182	79.81	5.68	0	k__Bacteria;p__Proteobacteria;c__Gammaproteobacteria
80_0	1	NA	NA	Upper-2016.60	4761135	13567	82.68	16.27	7.5	k__Bacteria;p__Proteobacteria;c__Gammaproteobacteria
157_1	4	99.95	99.94	CA-NE1-2010.103	2584096	166059	97.38	1.94	0	k__Bacteria;p__Proteobacteria;c__Gammaproteobacteria;o__Legionellales
158_0	1	NA	NA	CA-NE8-2010.53	2219883	12135	84.27	3.34	0	k__Bacteria;p__Proteobacteria;c__Gammaproteobacteria;o__Legionellales
19_0	1	NA	NA	Upper-2016.191	4132717	45800	96.88	4.18	0	k__Bacteria;p__Proteobacteria;c__Gammaproteobacteria;o__Xanthomonadales
64_1	2	99.32	99.32	Upper-2016.100	4390843	4700	76.95	2.96	7.14	k__Bacteria;p__Proteobacteria;c__Gammaproteobacteria;o__Xanthomonadales
65_0	1	NA	NA	SW.148	5896559	6690	88.09	4.59	8.33	k__Bacteria;p__Proteobacteria;c__Gammaproteobacteria;o__Xanthomonadales
66_1	7	99.99	99.91	Upper-2016.2	4348934	249107	97.5	3.31	0	k__Bacteria;p__Proteobacteria;c__Gammaproteobacteria;o__Xanthomonadales
67_0	1	NA	NA	Upper-2016.242	4998318	42293	91.56	7.85	5.13	k__Bacteria;p__Proteobacteria;c__Gammaproteobacteria;o__Xanthomonadales
69_1	2	99.87	99.87	NW.77	2844401	14257	88.41	2.23	17.65	k__Bacteria;p__Proteobacteria;c__Gammaproteobacteria;o__Xanthomonadales
70_1	7	99.93	99.17	SNE1.003	3108323	41975	94.25	1.39	0	k__Bacteria;p__Proteobacteria;c__Gammaproteobacteria;o__Xanthomonadales
102_0	1	NA	NA	CA-NE8-2010.136	2523669	6316	77.31	1.87	0	k__Bacteria;p__Proteobacteria;c__Gammaproteobacteria;o__Xanthomonadales
129_1	3	99.92	99.84	Upper-2016.33	4314916	30680	96.94	3.16	6.67	k__Bacteria;p__Proteobacteria;c__Gammaproteobacteria;o__Xanthomonadales
81_1	12	99.99	99.88	SW.136	3721083	153912	99.63	1.03	0	k__Bacteria;p__Proteobacteria;c__Gammaproteobacteria;o__Xanthomonadales;f__Xanthomonadaceae;g__Luteimonas
38_0	1	NA	NA	Upper-2016.54	9649650	5073	83.83	13.95	0	k__Bacteria;p__Verrucomicrobia;c__Verrucomicrobiae;o__Verrucomicrobiales